COTRANSLATIONAL FOLDING OF CFTR

APPROVED BY SUPERVISORY COMMITTEE

Philip J. Thomas, Ph.D.

Joseph P. Albanesi, Ph.D.

Kevin H. Gardner, Ph.D.

Youxing Jiang, Ph.D.

To my husband David

Acknowledgements

I am grateful to everyone who has played a role in my training to become a physician scientist. First and foremost, to my graduate mentor Philip Thomas who has directed my research efforts and enabled me to pursue CFTR misfolding as a basic mechanism of disease. My work with cystic fibrosis has given me valuable insight into how basic science advances can translate to the clinic to change human disease. Through attendance at conferences, my views of research and of approaches to understand basic disease mechanisms have been broadened. I am also grateful for guidance and recommendations received for a pre-doctoral Fellowship and PEO Scholarship, which would not have otherwise been possible. My thesis committee members have also been a valuable resource for input and guidance over the course of my doctoral studies.

I would like to thank the members of the Thomas laboratory, both past and present, for their constant scientific discourse and aide in pursuing different experimental techniques. In particular, I would like to thank Andrey Karamyshev for his essential role in the *in vitro* translation studies and for experimental guidance. I would also like to acknowledge Arthur E. Johnson at Texas A&M from whom these protocols and the original materials originated, and Dr. Connie Hsia who provided us with the opportunity to obtain canine pancreas. I would like to recognize and thank Linda Millen for all of her help expressing and analyzing CFTR constructs for studies presented in Chapter 3, and for her day to day expertise. Additionally, I would like to recognize two rotation students, Heath Pascoe and Ali Vetter, who participated in CFTR studies involving protein interactions, and in particular, Ali, who is continuing this work. I would also like to express gratitude to the administrative staff, Jocelyn Wrighting and Leah Taylor, who have repeatedly helped me.

Without the core facilities at UT Southwestern, my work could not have been performed. I would like to thank Chris Gilpin for his help performing the electron microscopic examination of the prepared microsomes. I also thank George DeMartino and his laboratory for sharing technical expertise regarding all things proteasome.

I would like to acknowledge the Medical Scientist Training Program at UT Southwestern, which has given me multiple opportunities to present and discuss my work. None of the work I have done could have been completed without the aid of the administrative staff in the MSTP, Robin Downing and Stephanie Robertson.

I would like to thank my undergraduate mentor at the University of Pennsylvania, A. Joshua Wand, for exposing me to membrane proteins and concepts in protein folding. I also thank Dr. Rodger McEver at the Oklahoma Medical Research Foundation for time spent in his laboratory and discussions relating to pursuit of training as a physician scientist.

Finally, I thank my family for their never ending support; none of my work would have been possible without them. Most importantly, I would like to thank my husband David, who has given me his love and support unconditionally.

COTRANSLATIONAL FOLDING OF CFTR

by

Anna E. Patrick

DISSERTATION

Presented to the Faculty of the Graduate School of Biomedical Sciences

The University of Texas Southwestern Medical Center at Dallas

In Partial Fulfillment of the Requirements

For the Degree of

DOCTOR OF PHILOSOPHY

The University of Texas Southwestern Medical Center at Dallas

Dallas, Texas

May, 2011

COTRANSLATIONAL FOLDING OF CFTR

Anna E. Patrick

The University of Texas Southwestern Medical Center at Dallas, 2011

Mentor: Philip J. Thomas, Ph.D.

The life of the cystic fibrosis transmembrane conductance regulator (CFTR) protein in the cell is dictated by its biogenesis, cellular trafficking, regulated function, and destruction. Cystic fibrosis (CF) is the direct result of perturbations in these processes. Treatment of CF mandates the understanding of the molecular events leading to CFTR loss-of-function. The mechanisms by which different mutations throughout the CFTR protein result in misfolding are unclear. The correction of these processes and ultimately the treatment of CF require elucidation of these mechanisms.

In this report, CF-causing mutations in the first transmembrane (TM) spanning domain (TMD1) that result in CFTR misfolding are examined. First, the G85E and G91R mutations in TM1 are shown to have different molecular pathologies. For G85E, TM1 is destabilized in the membrane by the ionizable side chain, which correlates with temperature insensitive ER accumulation. By contrast, G91R does not destabilize TM1, which correlates with temperature sensitive ER accumulation. Both mutants were then identified to perturb TMD1 in a manner recognizable by the cell. Finally, consistent with propagation of these defects, all multidomain CFTR constructs were recognized and degraded in the cell. Other mutations in the interdomain interface between TMD1 and the cytosolic nucleotide binding domains (NBDs) did not perturb TMD1, but affected multidomain constructs containing four domains, which can traffic from the

ER. Notably, the interface mutants that change a hydrophobic residue to a basic residue increased levels of early multidomain constructs, suggesting a tradeoff between transient stability and later formation of interdomain interactions. The major cellular monitoring of most mutants occurs after TMD2 is present. In most current models, CF-causing mutations like ΔF508 are shown to perturb interdomain interactions before TMD2 is produced. However, evidence presented here suggests these interactions are not important until after TMD2 production. The comparison of TM1 mutants and other mutants supports specific domain interactions in the hierarchical folding model.

Taken together, the data herein generate a model of CFTR folding that begins with TMD1. Interdomain interactions then become important in a four domain construct, and the final domain confers additional stability and increases cellular trafficking. Multidomain misfolding clearly plays a role in the molecular pathology of CF, thus, a more detailed understanding of this process as globally outlined above is required to generate novel ways to rescue mutant CFTR.

Table of Contents

List of Publications

Patrick A.E., Karamyshev A.L., Thomas P.J., “Alteration of CFTR Transmembrane Span Integration by Disease-Causing Mutations" manuscript submitted

Patrick A.E., Millen L., Thomas P.J., "Perturbations in CFTR TMD1 Disrupt Disparate Folding Steps" manuscript in preparation

Karamyshev A.L., **Patrick A.E.**, Karamysheva Z.N., Griesemer D.S., Tjon-Kon-Sang S., Nilsson I., Otto H., Liu Q., Rospert S., von Heijne G., Johnson A.E., Thomas P.J., "Inefficient SRP Nascent Chain Interactions Recruit Ago2 and Enhance mRNA Degradation" manuscript in preparation

Karamyshev A.L., **Patrick A.E.**, Johnson A.E., Thomas P.J., “The First Steps in CFTR Biogenesis: Cotranslational Interactions with Nascent CFTR as It Exits the Ribosome.” manuscript in preparation

List of Figures

List of Abbreviations

CF	cystic fibrosis
CFTR	cystic fibrosis transmembrane conductance regulator
CFF	Cystic Fibrosis Foundation
CFAD	cystic fibrosis-associated diabetes
DNA	deoxyribonucleic acid
IRT	immunoreactive trypsinogen
ΔF508	deletion of phenylalanine at position 508
mmol	millimole
L	liter
kb	kilo-base pair
CFTR2	Clinical and Functional Translation of CFTR
cAMP	cyclic adenosine monophosphate
PKA	protein kinase A
PKC	protein kinase C
SLC	solute carrier family
ENaC	epithelial sodium channel
VX	Vertex Pharmaceuticals
ABC	ATP binding cassette
ATP	adenosine triphosphate
TMD	transmembrane spanning domain
NBD	nucleotide binding domain
ICL	intracellular loop
TM	transmembrane
Å	angstrom
Sav1866	*Staphylococcus aureus* 1866
P-glycoprotein	permeability glycoprotein
R	regulatory
mRNA	messenger ribonucleic acid
RI	regulatory insert
RE	regulatory extension
ER	endoplasmic reticulum
SRP	signal recognition particle
TRAM	translocating chain associating membrane protein
Hsc	heat shock cognate
Hsp	heat shock protein
CHIP	c-terminal Hsc70-interacting protein
Aha1	activator of Hsp90 ATPase
OST	oligosaccharyl transferase
WT	wild type
ECL	extracellular loop
EndoH	endoglycosidase H
PNGaseF	peptide-N4-(N-acetyl-beta-glucosaminyl)asparagines amidase
AE1	anion exchanger 1

CMV	cytomegalovirus
PCR	polymerase chain reaction
DMEM	Dulbecco's Modified Eagle Medium
FCS	Fetal Calf Serum
PVDF	polyvinylidene fluoride
SDS-PAGE	sodium dodecyl sulfate polyacrylamide gel electrophoresis
PBS	phosphate buffered saline
HEK293	human embryonic kidney 293
SEM	standard error of the mean
PEI	polyetheylenimine
RRL	rabbit reticulocyte lysate
WG	wheat germ
RM	rough microsome
CRM	column washed microsome
ATA	aurin tricarboxylic acid
pPL	preprolactin
LMW	low molecular weight
IP	immunoprecipitation

Chapter I

Introduction

Cystic fibrosis

Cystic fibrosis (CF) is an autosomal recessive disease affecting more than 70,000 people world-wide. CF is caused by mutations in the gene encoding the cystic fibrosis transmembrane conductance regulator (CFTR) protein (Kerem et al. 1989; Riordan et al. 1989; Rommens et al. 1989). CFTR functions as a regulated chloride channel in the apical membrane of epithelia, where it plays a critical role in maintaining the surface liquid layer. Lack of functional CFTR results in thick secretions that cause gastrointestinal, reproductive, and respiratory system defects. While most CF patients are diagnosed early in life, patients with mild disease are often undiagnosed for many years. Early recognition and treatment of CF has been shown to positively impact disease prognosis, and advances in palliative care have increased the average patient lifespan into the third decade (CFFRegistry 2011). More than 90% of mutant CFTR alleles result in a misfolded protein that is recognized, mistrafficked, and degraded in the cell. The current major clinical strategy for the treatment of CF is correction of the basic defect in the CFTR protein. Therefore, an understanding of CFTR protein folding is essential for development of therapeutic compounds that target this process.

In general, early in life characteristic CF symptoms are related to intestinal obstruction at birth, exocrine pancreas dysfunction, failure to thrive, and respiratory related illness (O'Sullivan and Freedman 2009). As the patient ages, respiratory dysfunction becomes severe, malnutrition persists, and reproductive, endocrine pancreas, and liver problems can become apparent (O'Sullivan and Freedman 2009). The multisystem effects reduce quality of life, however most patients die of respiratory-related problems (Rowe et al. 2005; O'Sullivan and Freedman 2009).

Respiratory dysfunction occurs as the mucus secreting airways in the lung are unable to clear the characteristic thick mucus of CF, leading to an infection prone environment (Fahy and

Dickey ; Rowe et al. 2005). This, in combination with altered inflammatory responses and disrupted immune responses are directly and indirectly caused by the lack of CFTR (Fahy and Dickey ; Rowe et al. 2005; Quinton 2007). CF lungs are colonized by pathogens early and remain in a persistent state of infection and inflammation, leading to loss of normal lung morphology and pulmonary insufficiency (O'Sullivan and Freedman 2009). Whether the pro-inflammatory lung status is present at birth or if it develops after exposure to environmental stimuli has not been resolved. The cycles of infection and scarring make CF lungs increasingly vulnerable to infections.

CF lungs are susceptible to many pathogens, with an increased susceptibility to *Pseudomonas aeruginosa*, *Staphylococcus aureus*, and the *Burkholderia cepacia* complex. These specific bacteria commonly colonize CF patient lungs and have a negative impact on disease prognosis (Rowe et al. 2005; O'Sullivan and Freedman 2009; CFFRegistry 2011). Additionally, *Pseudomonas aeruginosa* produces biofilms that make its eradication difficult to nearly impossible (Campodonico et al. 2008). Accordingly, patients benefit from aggressive treatments to prevent or delay colonization by *Pseudomonas aeruginosa* and other pathogens (O'Sullivan and Freedman 2009). As lung disease progresses, patients require lung transplantation or succumb during a pulmonary exacerbation.

Other CF-related pathologies are significant sources of morbidity. Gastrointestinal problems include obstruction, proteolytic enzyme insufficiency, and hepatic cirrhosis. At birth, 10% CF patients present with meconium ileus, wherein inspissated material in the intestines causes bowel obstruction (Rowe et al. 2005). Then, early in life the pancreatic exocrine glands are plugged by thick secretions, resulting in their replacement by fatty material. These processes result in a deficiency in proteolytic enzyme secretion into the intestines, with consequent

malabsorption and nutritional deficits throughout the patient's life (Borowitz et al. 2002). Malnutrition frequently presents as failure to thrive in infants and dramatically alters a CF patient's ability to respond to infection (Borowitz et al. 2002). In approximately 10% CF patients, the thick secretions damage the liver, resulting in hepatic biliary cirrhosis (Wilschanski and Durie 2007). In the male reproductive system, the vas deferens is commonly damaged by the thick secretions, resulting in infertility.

In all patients, the endocrine glands of the pancreas can become damaged, resulting in CF-associated diabetes (CFAD) (Moran et al. 2010; Stecenko and Moran 2010). CFAD is a growing problem in the now aging CF population, with half of CF patients affected by the third decade of life (CFFRegistry 2011). CFAD is associated with increased morbidity and mortality, particularly in female CF patients (Stecenko and Moran 2010). The treatment of CFAD is complex, as nutritional status must be maintained with simultaneous glucose control (Stecenko and Moran 2010). Finally, a major diagnostic tool for CF is based on the sweat glands in the skin, which do not appropriately remove sodium chloride and produce a very salty sweat (Rowe et al. 2005).

Cystic fibrosis diagnosis and treatment

CF patients are diagnosed by a combination of genetic, diagnostic, and clinical approaches (Farrell et al. 2008). It is very clear that the early detection and treatment of CF results in better disease outcomes (Farrell et al. 1997; Farrell et al. 2001; Farrell et al. 2005; Lai et al. 2005). Currently, in the United States, all states implement early diagnostic and genetic screening for CF based on recommendations from the Centers for Disease Control and Prevention (www.cff.org)(Grosse et al. 2005). In general, newborn screening programs are

based on a measure of pancreatic dysfunction and DNA sequencing. After birth or soon thereafter, pancreatic injury is identified by the measurement of immunoreactive trypsinogen (IRT) in the blood, which is not specific to CF (O'Sullivan and Freedman 2009). Positive results are followed by a second IRT 1-3 weeks later, or by analysis of DNA for specific CFTR mutations (O'Sullivan and Freedman 2009). DNA analysis relies on knowledge of the CFTR gene to identify common mutations.

Thousands of CF-causing CFTR alleles have been sequenced, generating a rich database of CF-causing and CF-associated mutations (www.genet.sickkids.on.ca). However, almost all CF patients have at least one and often two common mutations. The most frequent mutation, the deletion of phenylalanine 508 (ΔF508), represents more than 70% of CF alleles in Northern European populations (Riordan et al. 1989; Lao et al. 2003). Moreover, by screening for the most common 40 mutations, more than 90% of patient mutations can be identified (O'Sullivan and Freedman 2009). Yet, failure to detect a DNA mutation does not preclude diagnosis of CF by other diagnostic measures (Farrell et al. 2008). The sweat chloride test monitors the amount of chloride present in sweat to diagnose CF. A sweat chloride level equal to or greater than 60 mmol/L is likely to result in a diagnosis of CF for all people. Levels lower than 29 mmol/L for infants ≤ 6 months or 39 mmol/L for children older than 6 months are unlikely to result in a CF diagnosis (www.cff.org)(Farrell et al. 2008). Notably, there is a range wherein CF diagnosis is possible and other factors must be examined (Farrell et al. 2008).

Even after a diagnosis of CF, the clinical course may be unpredictable, especially for respiratory disease. Certain mutations manifest with a severe clinical presentation, and others tend to cause a more mild disease. However many mutations are associated with both presentations, and mutation combinations or unidentified mutations can lead to unpredictable

clinical symptoms, with some patients being very sick and others experiencing few symptoms (Zielenski 2000). Genetic modifiers also play a role in the clinical variance of CF-associated morbidities, and identification and characterization of the modifiers is ongoing (Cutting 2010). The understanding of CF is expanding, and continuing progress is required to generate the best approach to CF diagnosis and treatment.

Treatment strategies for CF have dramatically altered quality of life and lifespan for CF patients. In the 1950s, patients that survived birth died of malnutrition in the first few years of life. Yet today, on average, patients live into their third decade (CFFRegistry 2011). These developments are due to improved diagnosis, better preventive care, aggressive infection treatment, and recognition of milder CF. However, in clinically severe CF, death can still occur at a young age. CF patients have multiple system effects that are best addressed through regular patient care from a team of health-care practitioners experienced with the disease (O'Sullivan and Freedman 2009; CFFRegistry 2011).

A CF patient has extensive nutritional needs due to malabsorption, chronic inflammation, and infection. In order to maintain nutritional balance, patients consume high calorie nutrition, supplement with pancreatic enzymes and fat-soluble vitamins, and keep a regular dietary schedule with regular monitoring of body mass index (Borowitz et al. 2002). CFAD represents a growing challenge for clinicians and patients since it does not present with classic diabetes symptoms. Therefore, young patients must be screened, and all diagnosed patients treated while maintaining nutritional balance (Stecenko and Moran 2010).

Chronic respiratory therapies to maintain the lung include removing obstructive mucus, preventive antibiotics, and anti-inflammatory medications (Fahy and Dickey ; O'Sullivan and Flume 2009). Mucus clearance can be promoted by physical airway clearance techniques,

decreasing mucus viscosity with inhaled hypertonic saline and DNA hydrolase, and therapeutics in development to increase the airway liquid level (Fahy and Dickey). Regular inhaled antibiotics prevent and remove pathogens, and acute infection is aggressively combatted by inhaled, oral, and/or intravenous antibiotics (Fahy and Dickey ; O'Sullivan and Freedman 2009). Lung colonization by pathogens is monitored regularly to determine an individualized prognosis and therapeutic approach. All of these treatments target CF symptoms and are time consuming. The most effective therapeutic will correct the basic defect in CF by rescuing or replacing defective CFTR. Identifying therapeutics to achieve this goal requires an understanding of the effects of individual CF-causing mutations on CFTR.

CF-causing mutations in the CFTR gene

The CFTR gene is located on chromosome 7, spanning approximately 190kb of genomic DNA with 27 exons (Kerem et al. 1989; Riordan et al. 1989; Rommens et al. 1989; Ellsworth et al. 2000). Sequencing of CF patient and non-patient CFTR genes has been extensive, and hundreds of mutations have been identified (www.genet.sickkids.on.ca). Many of these mutations have been validated as CF-causing, while others are CF-associated but unstudied. Other sequence polymorphisms and non-CF associated mutations have also been identified during this extensive sequencing (www.genet.sickkids.on.ca). The validated CF-causing mutations are located throughout the CFTR gene, and are inherited in almost all cases (Riordan et al. 1989; Riordan 2008).

Mutant effects have been categorized into classes based on the resulting effect on CFTR (Welsh and Smith 1993; Zielenski and Tsui 1995). The alterations include lack of protein production (class I), defective protein maturation and early degradation (class II), defective

regulation of ATP interactions (class III), reduced chloride transport (class IV), reduced transcripts though splicing or promoter defects (class V), and increased cell surface turnover (class VI) (Welsh and Smith 1993; Zielenski and Tsui 1995). The ΔF508 mutation accounts for 70% of CF-causing mutant CFTR alleles (Riordan et al. 1989), making class II defects the most common cause of CF. Targeting this class of mutant is the highest priority for correcting the basic defect in CF.

The CF genotype-phenotype correlation is complex, with a classic presentation occurring for only some mutations (Zielenski 2000). Furthermore, the genotype-phenotype correlation is different for each morbidity, with pancreatic disease correlating most strongly and respiratory disease correlating weakly with different mutations (Zielenski 2000; Durno et al. 2002; Moskowitz et al. 2008). The weak genotype-phenotype correlation for respiratory outcomes suggests environmental effects and genetic modifiers are important for disease prognosis (Moskowitz et al. 2008; Cutting 2010). The range of CFTR mutant phenotypes, from classic CF to monosymptomatic presentations, makes diagnostic decisions complex for non-classic presentations (Moskowitz et al. 2008). For example, the R117H mutation is generally correlated with mild CF symptoms, and greatly varies depending on the presence of other CFTR mutations (Zielenski 2000). The R117H phenotype is likely due to residual function of the CFTR protein (Sheppard et al. 1993). It is suggested that only 10-35% of CFTR function is needed to positively impact pulmonary disease (Kerem 2004), therefore the production and residual activity of mutant CFTR is relevant for clinical outcomes. To clarify the effects of different mutants, a multi-institutional, collaborative approach called the **C**linical and **F**unctional **TR**anslation of CFTR, CFTR2, is in progress to characterize validated CF mutant effects on the CFTR protein (www.genet.sickkids.on.ca).

The highest frequency of CF is in the Caucasian population, affecting approximately 1 in 3,000 babies. The frequency of CF is lower in the Mediterranean population, and rare in African and Asian populations. For example, in America the non-Caucasian CF frequencies are 1 in 9200 Hispanic Americans, 1 in 10900 Native Americans, 1 in 15000 African Americans, and 1 in 31000 Asian Americans (Hamosh et al. 1998). The ΔF508 mutation accounts for 50% to almost 100% of the CF-mutant alleles in most populations, with other mutations sometimes having a high frequency within a distinct group of people (Riordan et al. 1989; Lao et al. 2003). For instance, the CF frequency in the Ashkenazi Jewish population is 1 in 3300, however 75% of the disease-causing alleles result in premature truncation of CFTR (Kerem and Kerem 1996).

A heterozygote advantage is strongly suggested by the prevalence of deleterious CFTR genes, specifically ΔF508, that confer no fertility advantage in a geographically identifiable pattern (Jorde and Lathrop 1988; Romeo et al. 1989). Increased heterozygote resistances to specific diseases including diarrheal illness, cholera, typhoid fever, bubonic plague, and tuberculosis have been explored (Poolman and Galvani 2007). Yet, most lack support or have not been rigorously tested. A better understanding of the roles of CFTR in the cell and in specific immune responses may help clarify the origins of ΔF508 and other mutations.

CFTR cellular function

CFTR is a regulated chloride channel at the apical surface of epithelial cells (Anderson et al. 1991; Bear et al. 1992) that plays an important role in maintaining the epithelial surface liquid (Quinton 1990; Rowe et al. 2005). Loss of CFTR results in abnormal chloride transport, which is coupled to defects in sodium and bicarbonate transport. These abnormalities ultimately result in a reduction in the epithelial surface liquid and thick mucus (Quinton 2010). CFTR channel

function is regulated in a cAMP dependant process, in which protein kinase A (PKA) phosphorylation of the regulatory domain is a prerequisite for channel gating and can be augmented by protein kinase C (PKC) phosphorylation of this region (Gadsby et al. 2006). ATP binding and hydrolysis cycles then result in opening and closing of the chloride channel (Gadsby et al. 2006). This opening and closing results in current that can be monitored by electrophysiological methods to study CFTR function (Gadsby et al. 2006). The chloride channel function of CFTR is required for normal epithelial physiology (Rowe et al. 2005), which is supported by mutations that solely disrupt this function and cause CF (Welsh and Smith 1993).

CFTR has other functions relating both to its interactions with proteins at the apical surface of epithelia and to its role in immune responses (Riordan 2008; O'Sullivan and Freedman 2009). These functions are thought to contribute to the increased susceptibility of CF patients to specific pathogens. For instance, *Pseudomonas aeruginosa* infection results in a reduced immune response if epithelial cells lack CFTR (Pier et al. 1996; Campodonico et al. 2008). Moreover, CF pathophysiology is impacted by the relationship of CFTR with other transporters, including the bicarbonate transporters of the SLC26 family (Ko et al. 2002). In the cell, CFTR simulates chloride bicarbonate exchangers. Thus, loss of CFTR reduces bicarbonate transport and the pH in the epithelial surface liquid, consequently increasing mucus viscosity (Fahy and Dickey ; Quinton 2008; Quinton 2010). Consistent with this, mutations in CFTR that leave chloride channel activity intact and alter bicarbonate transport result in CF (Choi et al. 2001).

Another important cell surface interaction occurs with the epithelial sodium channel, ENaC, that transports sodium into the cell and decreases the epithelial surface liquid (Donaldson and Boucher 2007). CFTR normally inhibits ENaC; therefore the loss of CFTR results in increased activity of ENaC and reduced surface liquid (Stutts et al. 1995). Highlighting the

importance of ENaC for CF pathophysiology, a mouse model over expressing ENaC results in CF-like lung disease (Mall et al. 2004). CFTR interactions with other transporters have been suggested, and studies are ongoing to characterize these interactions along with other transport machinery responsible for maintaining the epithelial liquid (Riordan 2008).

Models of CFTR function: cell culture to animal models

CFTR function can be studied from a reconstituted system, isolated cells, tissue samples, or whole organisms. The complex folding of CFTR has made it impossible to produce in bacterial expression systems to date, limiting recombinant protein expression to eukaryotic systems (Bear et al. 1992; O'Riordan et al. 1995; Rosenberg et al. 2004). Most studies that characterize the function or folding of full length CFTR have been performed in a eukaryotic system. The function of CFTR can be studied at the single-channel level, whole cell level, and as transepithelial current across a cell monolayer. Each functional measurement is based on ionic current, membrane potential, or chloride flux (Moran and Zegarra-Moran 2008). At the single-channel and whole cell levels, isolated primary cells, secondary cells, or cell cultures heterologously expressing CFTR are used to study function (Moran and Zegarra-Moran 2008). In heterologous expression systems, both transient and stably expressing CFTR cell lines can be utilized. Transepithelial current measurements require polarized epithelia that forms tight junctions, which is present in primary tissue samples and in some commercially available cell lines (Moran and Zegarra-Moran 2008). Reconstituted CFTR can also be studied in planar membranes and proteoliposomes (Bear et al. 1992; O'Riordan et al. 1995).

The advantages of each of these systems include the availability of material, ease of maintenance, available mutations, and desired technique to study CFTR function (Moran and

Zegarra-Moran 2008). The available samples and technical expertise are significant constraints in determining the utilized technique. In many cases, an experiment is designed to study the effects of compounds and treatments intended to rescue mutant CFTR trafficking and/or function at the cell surface. This approach has been used for screens to identify novel therapeutics for rescuing the basic defects in mutant CFTR (Ma et al. 2002; Yang et al. 2003; Van Goor et al. 2006; Sloane and Rowe 2010). These cell culture screens have successfully identified novel compounds that are now in clinical trials (Kerem et al. 2008; Accurso et al. 2010; Sloane and Rowe 2010; Wilschanski et al. 2011), validating the cell culture approach.

Development of a CF animal model that reproduces the human CF phenotype has been difficult. The major barriers stem from differences in animal lung morphology and species-specific differences in CFTR protein expression (Ostedgaard et al. 2007; Widdicombe 2010). Mice, the most common mammalian model organism, have few mucus glands in the airways and do not typically display the thick mucus and gland hyperplasia observed in CF patients (Guilbault et al. 2007; Widdicombe 2010). The ferret and pig have a similar quantity of airway mucus glands to humans, and were therefore thought to be more likely to recapitulate the human CF respiratory phenotype (Aigner et al. 2010; Widdicombe 2010). Another hurdle is that small changes in the CFTR sequence alter its folding and trafficking in the cell. Compared to human CFTR, the mouse and pig proteins have sequence identities of 78% and 93%, which result in different cellular processing and function of the ΔF508 protein (Ostedgaard et al. 2007). In addition, the ΔF508 and some CF-causing mutations are sensitive to temperature, the cellular environment, and chemical chaperones, making human-like recapitulation of ΔF508 difficult in other species (Denning et al. 1992; Brown et al. 1996; Sato et al. 1996; Wang et al. 2008b).

Regardless, multiple animal models with varying phenotypes exist and have been employed to study CF.

The CF mouse models have been generated in different genetic backgrounds by knocking out the CFTR protein (-/-), destroying CFTR function or expression, introducing the ΔF508 mutation (ΔF508/ΔF508), and over expressing ENaC (Guilbault et al. 2007). In the mouse models, various phenotypes are observed, with a dominant intestinal phenotype, mild pancreatic phenotype, and some resistance or susceptibility to different pulmonary pathogens (Guilbault et al. 2007). Unfortunately, due to the aforementioned pulmonary physiology of mice and species specific CFTR trafficking, the mouse models do not have CF-like pulmonary disease. Therefore, the mouse models are most useful for studying facets of CF relating to intestinal disease, pathogens, and genetic modifiers (Guilbault et al. 2007).

A ferret model of CF was generated due to their more human-like lung morphology (Sun et al. 2008). The ferret knockout has a severe gastrointestinal phenotype with obstruction, poor nutrient absorption, and post-natal lethality (Sun et al. 2010). If lethality is rescued in these animals by a special diet, a CF-like pulmonary phenotype develops (Sun et al. 2010). However, ferret mucus gland development and airway size also differ from humans, and ferrets are therefore not an ideal model (Widdicombe 2010). These limitations led to the development of a large animal model for CF.

The most promising CF animal model has been developed in the pig. Pig lung morphology and development is like humans with similar gland numbers and size (Aigner et al. 2010; Widdicombe 2010). The CFTR knockout (-/-) pig displays pathologic CF gastrointestinal manifestations and a 100% penetrant severe obstructive intestinal phenotype at birth that causes death (Rogers et al. 2008; Meyerholz et al. 2010). After surgical correction of this obstruction,

the animals spontaneously develop pulmonary disease and defective bacterial eradication similar to CF patients (Stoltz et al. 2010). Recently, a pig harboring two ΔF508 alleles (ΔF508/ΔF508) was reported to have misprocessed CFTR with a CF-like lung phenotype (Ostedgaard et al. 2011). Notably, the ΔF508-CFTR porcine airway epithelia retained 6% maximal wild-type CFTR function, indicating that, as commonly proposed, this level of CFTR function correlates with the development of CF lung disease (Ostedgaard et al. 2011). This provides further rationale for using cell culture models to identify compounds to increase mutant CFTR trafficking and function. The ΔF508/ΔF508 pig is an exciting new tool to study CF pathophysiology and to better elucidate the basic mechanisms underlying this disease.

Targeting the basic defect of CF

Identification of the CFTR gene and CF-causing mutations therein resulted in a focus on rescuing the defective CFTR protein. Current CF therapies focus on treating one aspect of this multisystem disease, and no therapy has been able to eradicate the associated morbidities and mortality (O'Sullivan and Flume 2009; O'Sullivan and Freedman 2009). Rescuing the basic defect with one therapeutic could impact multiple organ systems and prevent many aspects of CF that develop with time. Two main methods are being pursued to achieve this goal: gene replacement therapy and correction of the existent mutant protein. In both cases, the level of CFTR function required to prevent significant pulmonary morbidity is as little as 10-35% (Kerem 2004). Gene therapy to replace CFTR has met little success, and major hurdles are associated with vector development, appropriate delivery in the lung, and CFTR expression (Sinn et al. ; Griesenbach and Alton 2009). By contrast, therapeutic correction of the existent mutant CFTR protein has recently had success both experimentally and in clinical trials.

Many CF-causing mutations have been identified that have different effects on the CFTR protein (www.genet.sickkids.on.ca). Ongoing therapeutic developments are aimed at targeting mutations that introduce premature termination codons, decrease chloride channel function, and alter cellular trafficking. Premature termination codons result in truncated, nonfunctional CFTR protein, and are found at very high frequency in specific CF populations (Zielenski 2000). Some aminoglycoside antibiotics reduce the fidelity of ribosomal proofreading, and allow low frequency introduction of an amino acid at the position of a stop codon, resulting in full-length protein production (Hermann 2007). This approach has been applied to CFTR in cell culture (Howard et al. 1996), and ongoing clinical trials for a therapeutic utilizing this approach are showing promise (Kerem et al. 2008; Wilschanski et al. 2011).

Other mutations in CFTR disrupt chloride channel function at the cell surface. Cell culture approaches were used to discover molecules that potentiate chloride channel activity for this type of mutant (Riordan 2008; Sloane and Rowe 2010). The G551D mutant in CFTR has normal cell surface expression and half-life, but confers a severe defect in channel gating (Welsh and Smith 1993). Clinical trials of the potentiator, VX-770, in CF patients having at least one G551D mutation are ongoing. Early published results from these studies show that upon treatment with VX-770, both adult and pediatric CF participants have improved measures of biological CFTR function and lung function (Accurso et al. 2010; PressRelease [Accessed 4 April 2011]). These results are promising for CF patients as adults, who already have lung scarring and dysfunction, and for children, who may be able to avoid lung dysfunction with this therapeutic. This work is an important proof of principle that an orally active compound can distribute through the body to affect CFTR function and alter the CF disease (Accurso et al. 2010).

The last category of therapeutically targeted CF mutants includes ΔF508 and other mutants that cause CFTR misfolding, and thereby mistrafficking and disrupted channel function (Riordan 2008). These mutants are being targeted by strategies aimed at correcting the trafficking defect and potentiating channel function. The combination of two drugs, one to correct trafficking and one to potentiate function may be therapeutically beneficial. In this regard the compound VX-809, which has shown some efficacy for the correction of CFTR trafficking, has been combined with the potentiator VX-770 in ongoing clinical trials (Sloane and Rowe 2010). However, combination therapy may be more likely to produce undesired side effects. Ideally, a single compound to both correct and potentiate mutant CFTR will be identified (Sheppard 2011). CFTR misfolding underlies the majority of CF, therefore identifying and rescuing the relevant folding deficiency may rectify channel function. Extensive work has gone into describing CF mutant CFTR misfolding in order to identify the most pertinent misfolding step(s), especially for ΔF508 (Riordan 2008). A better understanding of CFTR protein biogenesis, structure, and function is essential for identifying these steps and developing therapeutics to correct them and treat the majority of CF patients.

CFTR is an ATP-binding cassette transporter

CFTR is a member of the ABC transporter superfamily of proteins, which includes membrane spanning proteins that use nucleotide hydrolysis to transport substrates across the membrane bilayer (Holland 2003). ABC transporters function to move substrates either into the cytoplasm (importers) or out of the cytoplasm (exporters). Exporters are found in both eukaryotes and prokaryotes, while importers have only been found in prokaryotes (Rees et al. 2009). The importance of prokaryotic ABC transporters for cellular functions, such as import of

nutrients and export of toxins, is highlighted by their representation as 5% of the *Escherichia coli* genome (Linton and Higgins 1998). In humans, 48 or 49 distinct ABC transporters have been identified, many of which are implicated in disease (Dean et al. 2001; Gottesman and Ambudkar 2001; Borst and Elferink 2002). The core ABC transporter architecture is comprised of two transmembrane spanning domains (TMDs) and two nucleotide binding domains (NBDs). Many transporters also have accessory domains with regulatory functions (Biemans-Oldehinkel et al. 2006). In general, the TMDs are organized as two wings that open and close in response to NBD movements resulting from ATP binding and hydrolysis (Figure 1.1) (Moody et al. 2002; Locher 2009; Rees et al. 2009). Additionally, at the external surface, prokaryotic importers interact with an accessory protein that plays a role in substrate transport (Biemans-Oldehinkel et al. 2006). The domains are often modular, and are found expressed individually, in combinations, or as a single full length transporter to form the functional protein (Locher 2009).

ABC transporters have a conserved coupling mechanism, whereby signals from the NBDs are transmitted to the intracellular loops (ICLs) of TMDs to cause substrate transport (Locher 2009). The conserved NBDs form a sandwich around two ATPs, with each site for ATP binding and hydrolysis requiring both domains. Two subdomains are present in each NBD. The catalytic subdomain contains the conserved Walker A and B motifs, a Q-loop, and an H-motif, and the alpha-helical subdomain contains the ABC signature motif, LSGGQ (Figure 1.1C) (Rees et al. 2009). Each active site is composed of components from the catalytic subunit of one NBD and the alpha-helical components of the other NBD in a head-to-tail arrangement (Rees et al. 2009). The binding of ATP in these sites drives the association of the NBDs (Moody et al. 2002; Smith et al. 2002).

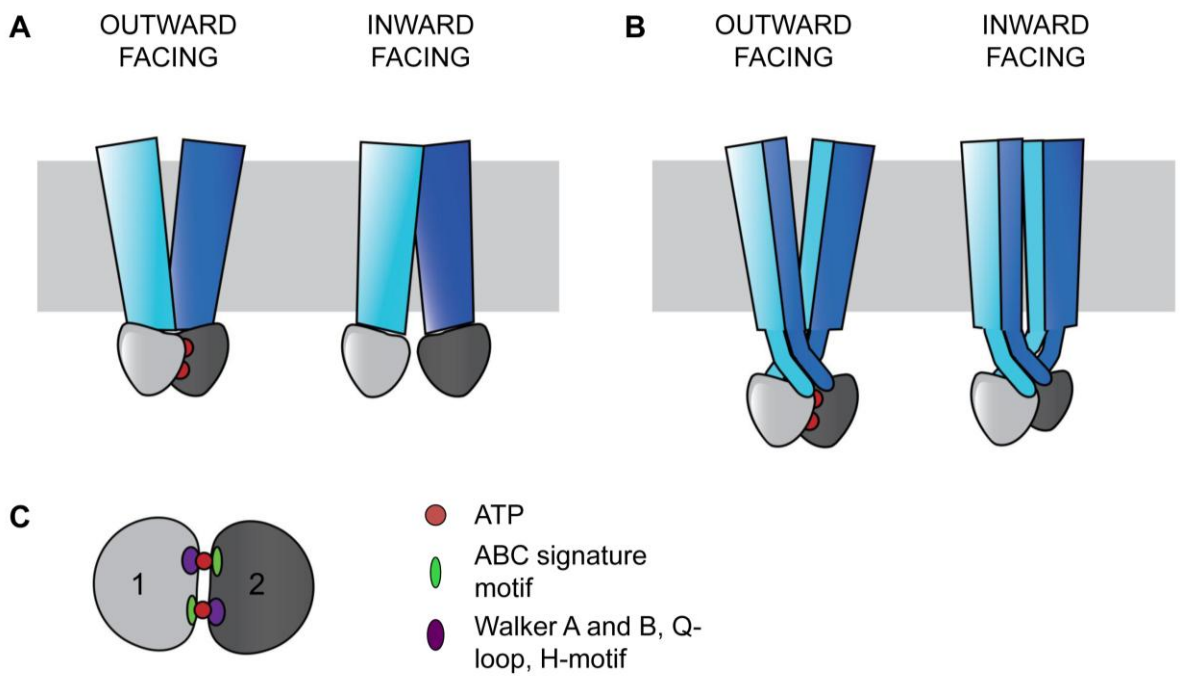

Figure 1.1 ABC transporters contain a core architecture of two TMDs (blue and cyan) and two NBDs (light and dark gray). Signals from the NBDs relating to ATP binding and hydrolysis result in wing-like TMD movements that transport substrates across the membrane (grey rectangle). In the outward facing configuration, the two NBDs bind ATP (red circles) and are close together, with the TMDs open to the non-cytosolic side. In the inward facing configuration, the NBDs are more distant without ATP bound, and the TMDs are open to the cytosol (Rees et al. 2009). **A.** In ABC importers, each TMD interacts with a single NBD. (Examples include BtuCD and MalFGK) **B.** In ABC exporters, the TMDs wrap around each other in a domain-swapped fashion, with each TMD interacting with both NBDs. (Examples include Sav1866 and MsbA) **C.** The two NBDs sandwich two ATPs in a head-to-tail fashion (Smith et al. 2002, Moody et al. 2002). Each ATP binding and hydrolysis site is comprised of both NBDs, containing the conserved structural motifs in the catalytic subdomain including the Walker A and B, Q-loop, and H-motif (purple oval), and the ABC signature motif in the alpha-helical subdomain (green oval).

The TMDs are proposed to function in an alternating access model of transport and are the most variable between different ABC transporters (Dawson et al. 2007). ABC transporters can be divided into three classes based on the TMD fold (Locher 2009). Type I and II ABC importers contain different core transmembrane (TM) span topologies of 10 and 20 TM helices respectively, with the latter tending to facilitate transport of larger substrates (Locher et al. 2002; Hollenstein et al. 2007; Locher 2009). In both importer types, one TMD interacts with one NBD to form two TMD-NBD units that together form a functional transporter (Figure 1.1A)(Locher 2009). ABC exporters contain a core of 12 TM helices, with each wing of the transporter made of both TMDs and each TMD interacting with both NBDs in a domain-swapped fashion (Figure 1.1B)(Dawson and Locher 2006; Locher 2009). In this arrangement, the ICLs extend into the cytoplasm, positioning the NBDs approximately 25Å from the membrane (Figure 1.1C) (Locher 2009). In exporters, the TMDs and NBDs are expressed as TMD-NBD units, and eukaryotic exporters are most frequently found as full length transporters (Nikles and Tampe 2007).

CFTR structural models

CFTR is a member of the ABC C subfamily, and is structurally homologous to the domain-swapped exporters. Structures of the homologous ABC exporters such as bacterial Sav1866 (Dawson and Locher 2006; Dawson and Locher 2007), bacterial MsbA (Ward et al. 2007), and mammalian P-glycoprotein (Aller et al. 2009) have been solved. The available structural data in combination with sequence alignments form the basis for homology models of full length CFTR that provide insight into its structure, mechanisms of regulation, and signal transduction (Mendoza and Thomas 2007; Mornon et al. 2008; Serohijos et al. 2008; Mornon et al. 2009). The exporter structures are in both open and closed forms, giving insight into

movements within the CFTR protein during a transport cycle (Figure 1.2, open form)(Ward et al. 2007; Locher 2009; Mornon et al. 2009; Rees et al. 2009). The similarity of CFTR movements to other ABC transporters is supported by electron microscopy data in combination with a low resolution crystal structure (Rosenberg et al. 2004; Zhang et al. 2009; Zhang et al. 2011). The only high resolution structures of CFTR domains are of NBD1 (Lewis et al. 2004; Thibodeau et al. 2005) and NBD2 (pdb 3GD7). As an ABC transporter, CFTR contains two TMDs, two NBDs, and a unique regulatory R region translated from an mRNA transcript as a single polypeptide chain (Riordan et al. 1989). Sav1866 based CFTR models have extensive interdomain interactions between the TMDs and NBDs, but lack regions without sequence homology, like the R domain (Figure 1.2) (Dawson and Locher 2006; Mendoza and Thomas 2007).

The NBDs of CFTR, like other ABC transporters (Moody et al. 2002; Smith et al. 2002), interact in a head-to-tail fashion forming two sandwiched ATP binding pockets made of both domains (Mense et al. 2006). Each NBD has a catalytic subdomain that contains the Walker A and B motifs and an alpha helical subdomain that contains the conserved ABC signature motif (Lewis et al. 2004; Thibodeau et al. 2005). However, like several other members of the ABC C subfamily, one ATP binding site is non-hydrolytic (Muallem and Vergani 2009). In this site, non-conservative mutations, which are located in the NBD1 Walker B and switch motifs and in the NBD2 signature sequence, result in tight binding and inefficient ATP hydrolysis (Aleksandrov et al. 2002; Basso et al. 2003; Gadsby et al. 2006). In general, CFTR ATP driven conformational changes include ATP binding, which results in an NBD dimer that signals the TMDs to open. Then, hydrolysis of one ATP disrupts the NBD interface, the NBDs separate,

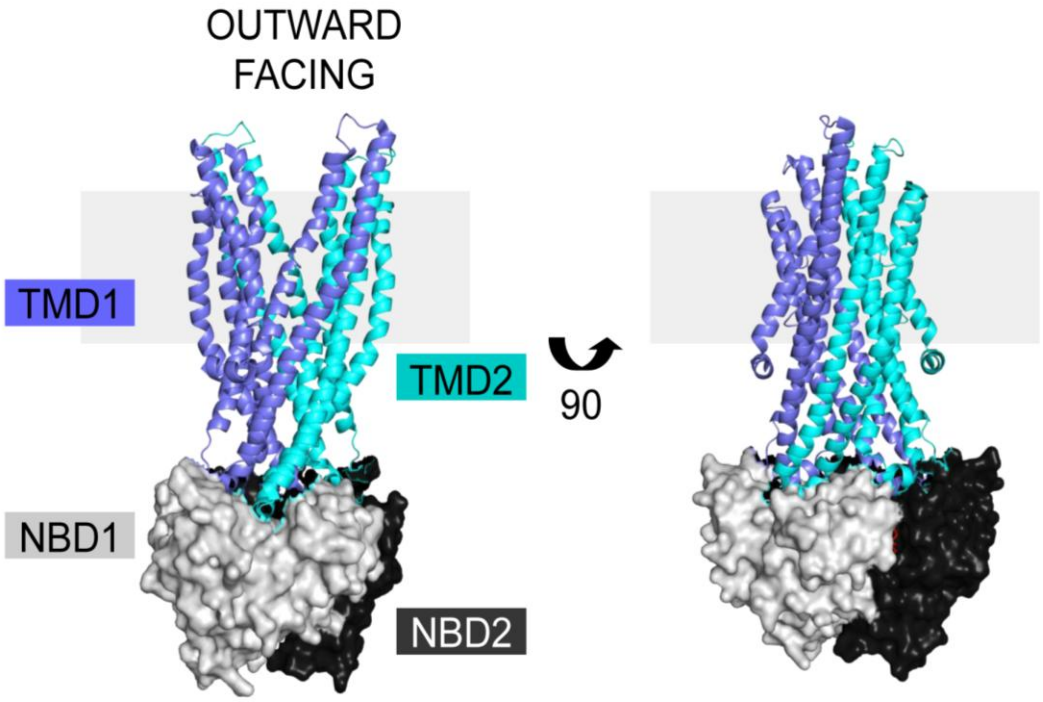

Figure 1.2 CFTR homology models are based on the ABC exporter structures. The Sav1866 (pdb 2HYD) exporter is shown with domains colored based on representative CFTR domains, with TMD1 (blue), NBD1 (light gray), TMD2 (cyan), and NBD2 (black). There is no homologous structure for the CFTR R domain. The structure is in the outward facing configuration, which for CFTR is the open channel. The view is shown in the plane of the membrane (gray rectangle).

and the channel closes (Gadsby et al. 2006; Aleksandrov et al. 2007; Muallem and Vergani 2009). However, the driving forces that control the gating transitions and the signals transmitted by ATP binding and hydrolysis are a matter of debate (Gadsby et al. 2006; Aleksandrov et al. 2007; Muallem and Vergani 2009). NBD1 also contains two non-conserved regions, a regulatory insert (RI) near the N-terminus and a regulatory extension (RE) near the C-terminus. Of these two regions, studies have focused on the RI. The RI is disordered in the NBD1 crystal structures and plays a role in regulation of CFTR channel gating, but is not required for trafficking in the cell (Lewis et al. 2004; Thibodeau et al. 2005; Aleksandrov et al. 2010). Furthermore, a mechanism wherein RI movements alter ICL1-NBD1 interactions to affect phosphorylation-dependent CFTR gating has been proposed (Kanelis et al. 2010).

Like other domain-swapped exporters, the TMDs form two wings containing TMs from both TMD1 and TMD2, such that the first two TMs and last four TMs of each domain make a wing (Figure 1.2) (Dawson and Locher 2006; Mendoza and Thomas 2007). Based on the exporter structures, the wings move to open and close the chloride channel for ion transport (Dawson et al. 2007; Mornon et al. 2009). In each TMD, two alpha-helical ICLs extend into the cytoplasm, with each having a distal coupling helix that interacts with the NBDs (Mendoza and Thomas 2007; Mornon et al. 2008; Serohijos et al. 2008). In combination, the four ICLs form four helix inner and outer bundles that end in the coupling helices (Figure 1.2)(Mornon et al. 2008; Mornon et al. 2009). Each coupling helix is parallel to the NBD surface, and forms a largely hydrophobic interface (Mendoza and Thomas 2007). In CFTR, ICL2 interacts with NBD2, ICL4 interacts with NBD1, and ICLs 1 and 3 interact with both. Importantly, the F508 position in NBD1 is predicted to lie near the interface between NBD1 and ICL4 (Mendoza and Thomas 2007). Many of the predicted interdomain interactions are also experimentally validated

by crosslinking studies (Chen et al. 2004; Mense et al. 2006; He et al. 2008; Loo and Clarke 2008; Serohijos et al. 2008). Additionally, crosslinks between an ICL and the opposing NBD disrupt channel opening, supporting the essential roles of these components for channel function (He et al. 2008).

CFTR is the only known channel among the ABC transporters. In the alternating access model, ABC transporters are open to one side of the membrane bilayer at a time (Dawson et al. 2007). In CFTR, channel formation abrogates this model, as one of the gates that would normally block substrate transport must be atrophied or gone to allow chloride flux (Gadsby 2009). With regard to this, CFTR has been called a broken ABC transporter (Jordan et al. 2008; Muallem and Vergani 2009). Similar to other chloride channels, CFTR is not very selective among small monovalent anions and has a relatively featureless pore (Gadsby et al. 2006; Gadsby 2009). Putative residues that make the chloride channel have been identified in TMs and in extracellular loops, with a focus on TM1 and TM6 (Linsdell 2006). However, it is difficult to validate these residues without better characterizing the TM span positions and TMD structures. Further complicating the TMD structures is a TMD1 N-terminal cytosolic region that regulates CFTR channel activity through interactions with the R domain, neither of which have homologous structures (Naren et al. 1999; Chappe et al. 2005).

The chloride channel activity of CFTR is regulated by the R domain (Riordan 2008). The R domain is largely unstructured and has multiple sites that are phosphorylated by PKA, resulting in CFTR channel activation (Gadsby et al. 2006; Baker et al. 2007). Consistent with this, the unphosphorylated R domain has an inhibitory effect on the CFTR channel (Rich et al. 1991; Csanady et al. 2000). The R domain interacts with multiple other regions of CFTR, including NBD1 and the N-terminus of TMD1 (Naren et al. 1999; Baker et al. 2007; Kanelis et

al. 2010). This evidence suggests the R domain may act as a signal integrator to regulate channel function via interactions with different regions of CFTR. However, due to its lack of homology and disordered nature, the R domain location within CFTR models is unknown (Mendoza and Thomas 2007).

In summary, the combination of experimental and modeling studies provide significant insight into the CFTR structure and form a model within which CF-causing mutations can be framed. However, since many CF-causing mutations, including ΔF508, result in misfolding of the CFTR protein, the folded full length structure does not adequately describe the relevant defects.

CFTR folding as a multispanning membrane protein

ABC transporters contain extensive interdomain surfaces (Rees et al. 2009) that, in the case of CFTR, likely form during translation (Zhang et al. 1998; Du et al. 2005; Kleizen et al. 2005; Thibodeau et al. 2005). During protein translation, secondary structure can begin to form early, even while the nascent chain is in the tunnel of the ribosome (Kramer et al. 2001; Woolhead et al. 2004). For CFTR, as translation continues, each domain folds and can then interact with previously translated domains to form multidomain folding intermediates (Lukacs et al. 1994; Du et al. 2005; Kleizen et al. 2005; Thibodeau et al. 2005; Cui et al. 2007; Cheung and Deber 2008; Du and Lukacs 2009). The current model of CFTR folding holds that individual domain structures form cotranslationally (Kleizen et al. 2005). Then, intermediate structures form that eventually make a TMD1-NBD1-R-TMD2 structure required for cellular trafficking (Meacham et al. 1999; Du et al. 2005; Cui et al. 2007; Du and Lukacs 2009). Finally, NBD2 posttranslationally incorporates into the CFTR structure (Du et al. 2005). Much of this

model is based on individual CFTR domains forming protease-resistant structures during translation (Zhang et al. 1998; Kleizen et al. 2005). The critical role of the protein primary sequence in this folding process is highlighted by the multitude of CF-associated folding mutations in the CFTR protein (www.genet.sickkids.on.ca). Focused studies to identify both normal and CF mutant translational interdomain interactions are needed to understand the CFTR (mis)folding path. Chapters 2 and 3 of this work focus on better understanding this process as it relates to TMD1.

CFTR folding occurs during translation as a linear polypeptide (Riordan et al. 1989). However, many ABC transporter domains are expressed separately, and later associate to form the functional transporter (Locher 2009). To some extent, this has been shown for CFTR. CFTR can be expressed as a split construct, which forms structure that traffics to the cell surface and functions as a chloride channel (Ostedgaard et al. 1997; Chan et al. 2000; Csanady et al. 2000; Du and Lukacs 2009). Additionally, expression of constructs containing TMD1-NBD1-R or R-TMD2-NBD2 formed chloride channels, likely as multimers (Sheppard et al. 1994; Devidas et al. 1998). Finally, in the cell the minimal construct that traffics from the ER contains TMD1-NBD1-R-TMD2, which forms a chloride channel (Cui et al. 2007). These studies suggest that the domains of CFTR, to a certain extent, can associate to form a functional chloride channel. Yet, CFTR is a linear chain, such that folding requires that each domain attain structure in a more spatially confined manner.

CFTR cotranslational folding requires protein interactions

Membrane protein folding is a complex, cotranslational process that involves both inter-protein and intra-protein interactions. For CFTR, before, during, and after integration,

interactions with other proteins in the endoplasmic reticulum (ER) membrane, ER lumen, and cytosol are involved in structure formation in a poorly understood process. For example, the TM spans of membrane proteins are recognized by the signal recognition particle (SRP), which brings them to the translocon protein complex in the ER membrane. The translocon, primarily the Sec61α and TRAM protein components, then integrates the TM spans into the membrane (McCormick et al. 2003). Studies to identify and characterize the earliest protein interactions during mutant CFTR translation and folding are lacking. Recently, a powerful technique has been developed that utilizes the incorporation of a photocrosslinkable amino acid at specific sites in the nascent polypeptide chain to identify early cotranslational interactions with membrane proteins during their translation and integration (Do et al. 1996; Liao et al. 1997; McCormick et al. 2003). This technology has been used to study cotranslational protein interactions during CFTR biogenesis, elucidating that, as the N-terminus of CFTR is translated, it interacts with many proteins (Karamyshev et al. manuscript in preparation). Furthermore, these studies reveal that TM1 interacts with SRP54, but forms alternate interactions when SRP is not present or the TM span is perturbed (Karamyshev et al. manuscript in preparation).

CFTR folding involves many proteins that act at different stages to aid folding or recognize misfolding. This misfolded CFTR is retained in the ER, and eventually degraded (Lukacs et al. 1994) by the proteasome (Jensen et al. 1995; Ward et al. 1995). These proteins interact with CFTR in the ER lumen, ER membrane, and cytoplasm, suggesting that the domains of CFTR are differentially monitored during the biosynthetic process. Among these identified interacting partners are the cytoplasmic proteins Hsc/p 40, 70, 90 and associated co-chaperones CHIP (Meacham et al. 1999; Meacham et al. 2001; Younger et al. 2006) and Aha1 (Wang et al. 2006), the ER membrane associated protein RMA1 (Younger et al. 2006; Grove et al. 2011), the

ER integral membrane proteins Derlin (Sun et al. 2006; Younger et al. 2006; Wang et al. 2008a) and BAP31 (Wang et al. 2008a), and the ER luminal-interacting protein calnexin (Pind et al. 1994). After trafficking to the cell surface, CFTR interactions with cytoskeletal proteins are important for its maintenance at this cellular location (Okiyoneda and Lukacs 2007). Also at the plasma membrane, peripheral protein quality control is involved in the ubiquitination, internalization, and degradation of misfolded CFTR (Okiyoneda et al. 2010). Moreover, a protein interactome for CFTR includes potential interactions far beyond those that have been studied (Wang et al. 2006). However, it is not clear which proteins interact at the earliest stages of folding/maturation and are responsible for initial and irreversible recognition of mutant CFTR. These interactions paint a picture of CFTR biogenesis whereby normal interactions are formed with cellular folding and quality control machinery, providing multiple points to monitor CFTR folding.

Folding of NBD1 and ΔF508-NBD1

Particular focus has been given to *in vitro* folding of NBD1, wherein F508 resides. High resolution crystal structures of both NBD1 and ΔF508-NBD1 have been solved (Lewis et al. 2004; Lewis et al. 2005; Thibodeau et al. 2005). Surprisingly, these structures place F508 on the domain surface, and ΔF508 does not cause significant perturbations in the crystal structure (Lewis et al. 2005). However, ΔF508-NBD1 has an increased tendency to aggregate and is destabilized, indicating a disruption during folding that is not represented in these structures (Qu and Thomas 1996; Lewis et al. 2005; Thibodeau et al. 2005). Consistent with this, a non-native conformation of NBD1 has been identified that is promoted by ΔF508 and linked to increased aggregation (Hoelen et al. 2010)(J. Richardson, unpublished data). The NBD1 structure is

obtained cotranslationally (Kleizen et al. 2005; Hoelen et al. 2010; Khushoo et al. 2011). During translation, a ligand-dependent N-terminal compact structure forms, and upon completion of NBD1 translation another compact structure forms (Khushoo et al. 2011). The compact N-terminal structure is not affected by ΔF508, suggesting that the folding error likely occurs at a later step of NBD1 folding (Khushoo et al. 2011). Additionally, NBD1 becomes translationally paused in certain *in vitro* translation systems, suggesting an additional complexity that is discussed in the Appendix. The ΔF508 misfolding begins in NBD1, making this an attractive target for correcting ΔF508-CFTR. Importantly, the ΔF508 effects on NBD1 also manifest during translation of the full length CFTR (Kleizen et al. 2005).

In full length CFTR, ΔF508 also effects multidomain stability and interdomain interactions. In mammalian cells, the ΔF508-CFTR misfolds, resulting in cellular mistrafficking via its accumulation in the ER (Cheng et al. 1990). ΔF508-CFTR that is induced to fold/traffic by low temperature or chemical modifier treatments has disrupted chloride channel function (Dalemans et al. 1991) and shorter residence times at the cellular surface (Lukacs et al. 1993), indicating the native structure is not achieved. As shown by limited proteolysis and pulse chase analysis, the ΔF508 mutation destabilizes NBD1 and multidomain folding intermediates, implying a more global destabilization of the entire ΔF508-CFTR (Zhang et al. 1998; Meacham et al. 1999; Du et al. 2005; Cui et al. 2007; Rosser et al. 2008; Du and Lukacs 2009). The homology model of CFTR places the F508 position at an interface between NBD1 and ICL4 of TMD2 (Mendoza and Thomas 2007). Consistent with this, ΔF508 disrupts crosslinks between ICL4 and NBD1 and within the TMDs (Chen et al. 2004; Serohijos et al. 2008). Additionally, mutations in ICL4 can suppress the effect of ΔF508, further supporting a disruption of this interface (Thibodeau et al. 2010). This strongly supports a multidomain assembly step in

ΔF508-mediated misfolding. However, these experiments do not identify the timing or mechanism(s) of interaction disruption. More details regarding the early CFTR folding steps where CF-mutant folding errors initiate are needed to rationally devise new therapeutic interventions.

CF-mutants perturb CFTR cotranslational folding

CF-associated mutations have been found in every domain of CFTR (www.genet.sickkids.on.ca). Misfolded CFTR, specifically the ΔF508 mutant protein, is recognized by cellular quality control machinery, accumulates in the ER (Cheng et al. 1990), and is eventually degraded (Lukacs et al. 1994) by the proteasome (Jensen et al. 1995; Ward et al. 1995). Many studies have identified CF-causing mutants that result in accumulation of CFTR in the ER. Some mutants likely perturb domain structure, while others are surface exposed and likely perturb interactions with other domains or proteins. For instance, in the NBD-ICL4 interface, mutants in ICL4 including L1065P, R1066C, and A1067T alter trafficking and chloride channel function (Cotten et al. 1996; Seibert et al. 1996a).

Mutants in different domains also alter biogenic intermediates of CFTR, suggesting that misfolding does not require full length CFTR (Du and Lukacs 2009). Furthermore, in full length CFTR, the proteolytic stability of all domains was reduced for spatially separate mutations, suggesting propagation of one mutant to other domains (Rosser et al. 2008; Du and Lukacs 2009). The propagation of mutants could occur through a rearrangement step involving multiple domains (Du and Lukacs 2009), or through coupled folding of the domains. As discussed, various components of cell quality control recognize CFTR as it is created, such that domain and multidomain states are likely differentially monitored (Younger et al. 2006). For each mutation,

the effect on individual domain folding and multidomain units plays a fundamental role in determining the mechanisms by which that mutation is recognized and managed within the cell. In the following chapters, work is presented to examine how CF-causing mutants perturb CFTR and what domains are required for mutant cellular recognition and degradation. A better understanding of these processes is essential for generating the knowledge required for mutant specific CF therapeutics.

Chapter II

Alteration of CFTR Transmembrane Span Integration by Disease-Causing Mutations

ABSTRACT

Many missense mutations in the cystic fibrosis transmembrane conductance regulator protein (CFTR) result in its misfolding, endoplasmic reticulum (ER) accumulation, and, thus, cystic fibrosis. A number of these mutations are located in the predicted CFTR transmembrane (TM) spans and have been projected to alter span integration. However the boundaries of the spans have not been precisely defined experimentally. In this study, the ER luminal boundaries of TM1 and TM2 were determined using the ER glycosylation machinery, and the effects of the CF-causing mutations G85E and G91R thereon were assessed. The mutations either destabilize the integrated conformation or alter the TM1 ER luminal boundary. G85E misfolding is based in TM1 destabilization by glutamic acid and loss of glycine, and correlates with the temperature insensitive ER-accumulation of immature full length CFTR harboring the mutation. By contrast, temperature-dependent misfolding owing to the G91R mutation depends on the introduction of the basic side chain rather than the loss of the glycine. This work demonstrates that CF-causing mutations predicted to have similar effects on CFTR structure actually result in disparate molecular perturbations that underlie ER accumulation and the pathology of CF.

INTRODUCTION

Cystic fibrosis (CF) is a lethal genetic disease caused by a lack of functional cystic fibrosis transmembrane conductance regulator protein (CFTR) (Riordan et al. 1989; Cheng et al. 1990). In the cell, the CFTR protein is translated and integrated into the ER membrane. It then traffics through the secretory pathway to the cell surface, where it functions as a chloride channel (Anderson et al. 1991; Bear et al. 1992). More than 70% of CF patients have at least one allele with a deletion of phenylalanine at position 508 (ΔF508) (Kerem et al. 1989). ΔF508 (Cheng et al. 1990) and many other CF mutations (Gregory et al. 1991) result in mutant CFTR that does not properly fold and is retained in the ER by cell protein quality control. Thus, loss of function due to cellular mistrafficking is the major molecular pathology leading to CF. CFTR contains five domains: two transmembrane spanning domains (TMDs), two nucleotide binding domains (NBDs), and a regulatory region (R). Missense mutations in all domains have been identified that result in mutant CFTR accumulation in the ER (www.genet.sickkids.on.ca). For the bulk of these mutations, neither the CFTR structural perturbation(s) nor the cellular mechanisms for recognizing the perturbation(s) are well characterized. A detailed understanding of CF-causing mutant effects on the CFTR protein is required to decipher the cellular machinery responsible for recognition and retention of the mutants, and for individualizing CF therapeutic strategies.

During translation, each CFTR domains folds and can then associate with previously folded domains to form the final, functional CFTR structure (Du et al. 2005; Kleizen et al. 2005; Thibodeau et al. 2005; Hoelen et al. 2010; Thibodeau et al. 2010). The first domain of CFTR translated is TMD1, which contains 6 TM spans. The first TM span of TMD1 is translated near

the beginning of CFTR production, when a CF-causing mutation could disrupt local protein secondary structure or intradomain structure. Conversely, a mutation could modestly affect TMD1 domain structure, but dramatically alter interdomain interactions and global CFTR folding. The roles of intradomain and interdomain defects in CFTR global misfolding or recognition and retention in the ER have not been clearly elucidated.

Mutations that introduce charge into the hydrophobic interior of a TM span are predicted to disrupt that span in a position dependent manner (Monne et al. 1998; Partridge et al. 2002). Within TMD1, more than thirty mutations introduce or alter a charged amino acid residue in the predicted TM spans, and many are near TM1 (Therien et al. 2001). The first transmembrane span of a multispanning integral membrane protein is important for targeting, integration into, and ultimate topology within the ER membrane (Hartmann et al. 1989). Therefore, TM1 mutant cellular mistrafficking could be caused by disrupted ER targeting, integration, topology formation, or TM span stability. The defect(s) could then augment further CFTR misfolding by disrupting intradomain, interdomain, and/or interprotein interactions. One or more of these misfolding event(s) is ultimately recognized by cellular quality control machinery, resulting in mistrafficking. Much of the current knowledge about recognition of aberrant proteins is based on studies of soluble proteins or the extramembrane domains of integral membrane proteins. Understanding the details of the misfolding caused by TM mutations is required for addressing subsequent questions about the identity of the proteins involved in recognizing aberrant transmembrane structures.

The CF-causing mutants G91R and G85E are in the original predicted TM1 span, (residues 81 to 102) (Riordan et al. 1989). Both mutations were predicted to perturb the TM1 due to introduction of a charged amino acid residue into the putative TM1 span (Xiong et al. 1997). Even though TM1 signal sequence activity *in vitro* was reduced by both mutations, TM2 appropriately oriented both TMs due to its ability to also act as a signal sequence (Lu et al. 1998). Indeed, TM1 and TM2 have both been implicated in determining CFTR TM span topology (Lu et al. 1998; Chen and Zhang 1999). The mutant TM1 topologies were indistinguishable from wild type CFTR, but multidomain constructs containing these mutants have decreased stability in *Xenopus laevis* oocytes (Xiong et al. 1997). Consistent with reduced stability, full length G91R CFTR accumulates in the ER and multiple domains exhibit increased proteolytic susceptibility in mammalian cells (Du and Lukacs 2009). However, the structural defect(s) that underlie mutant protein destabilization, recognition and accumulation in the ER remains obscure. The locations of the 85 and 91 positions with respect to various predictions of the TM1 and TM2 spans are shown (Figure 2.1). These positions are within or peripheral to TM1 depending on the utilized algorithm. The energy associated with the cost of placing a charged residue into a TM span is position dependent (Hessa et al. 2005), and the topology and integration profile of a TM span are dependent on the placement of positive and negative charge (von Heijne 1992; Monne et al. 1998). Therefore, precise, experimental knowledge of the boundaries of TM1 is required for understanding the role of the glycine at positions 85 and 91 on CFTR folding and of the alterations caused by the disease associated missense mutations at these positions.

Although the topology of CFTR has been assessed experimentally (Chang et al. 1994), the TM span boundaries have not been experimentally determined, and predicted span boundaries for TM1 and TM2 vary significantly (Figure 2.1). Further complicating TM span prediction, the initial integrated span and the span placement in the final protein structure may not be equivalent for many TM spans (Lu et al. 2000; Kauko et al. 2010). In the present work, TM1 and TM2 ER luminal boundaries were determined utilizing fitness as a substrate for N-linked core glycosylation. As a membrane protein is integrated into the ER membrane, prior to trafficking through the secretory pathway, core glycosylation of appropriate consensus sequences, NXS/T (X≠P), occurs in the ER lumen. This core glycosylation is then modified in the Golgi to produce complex glycosylated proteins (Helenius and Aebi 2001). For CFTR, two natural glycosylation sites are present that can be used to monitor CFTR integration and cellular trafficking by changes in electrophoretic mobility upon core glycosylation, producing Band B at approximately 150 kDa, and complex glycosylation, producing a diffuse Band C above 170 kDa.

In the ER, the oligosaccharyl transferase (OST) protein complex catalyzes the *en bloc* covalent attachment of a 14-saccharide unit to the consensus sequence asparagine residue (Helenius and Aebi 2001). The OST complex resides in the ER membrane associated with the translocation machinery, and, thus, core glycosylation likely occurs cotranslationally (Nilsson et al. 2003; Chavan and Lennarz 2006). Access to the active site of OST and efficient core glycosylation requires that the asparagine residue is a minimum of twelve residues from the luminal surface of the ER membrane (Nilsson and von Heijne 1993). This distance dependence can be utilized as a molecular ruler to examine the distance from the boundaries of a TM span to the active site of OST (Nilsson et al. 1998). This type of analysis has been used *in vitro* to

characterize the effects of single amino acid residues on TM helix integration profiles (Monne et al. 1998; Nilsson et al. 1998), and in cell culture to characterize ER luminal TM span boundaries (Popov et al. 1997; Cheung and Reithmeier 2005; Cheung and Reithmeier 2007). N-linked glycosylation has also been utilized more generally to identify the ER luminal portions of transmembrane proteins, thus determining protein topology (Chang et al. 1994; Cheung and Reithmeier 2007). Recently, core glycosylation has been developed as a technique to characterize the TM span properties required for recognition and integration by the translocon (Hessa et al. 2005; Hessa et al. 2007; Lundin et al. 2008). Utilizing this method, ten of the twelve CFTR TMs, including TM1 and TM2, could insert independently into the ER membrane (Enquist et al. 2009).

In this study, the span boundaries or integration profiles of TM1 and TM2 were determined and the effects of the CF-causing mutations G85E and G91R assessed. The G91R and G85E mutations were previously predicted to have similar effects on CFTR folding, yet are shown here to cause disparate perturbations in the protein. This work further elucidates CFTR membrane spanning structures and provides mechanistic insight into the molecular pathology of the G85E and G91R CF-causing mutations.

RESULTS

CFTR TM1 and TM2 span predictions

The initial prediction of TM1 and TM2 included residues 81 to 102 (TM1) and 118 to 138 (TM2) (Riordan et al. 1989). Since then, additional prediction algorithms to identify span boundaries have been developed. Several of these algorithms were utilized to predict boundaries for TM1 and TM2 (Figure 2.1). All methods indicate the presence of a TM span between residues 73 and 102 (TM1) and between residues 117 to 145 (TM2), with the TM boundaries at different positions depending on the method employed. Moreover, when the CF causing mutations G85E and G91R were analyzed using these algorithms, variable effects of mutations including shortening, no affect, no TM, or shifting TM1 boundaries were predicted (Table 2.1). Taken together, the absence of relevant biochemical data regarding TM1 and 2 structural information, the dramatic differences in predicted TM boundaries, and the lack of consensus in the mutant predicted effects highlight the need for an experimental approach.

Natural glycosylation sites in CFTR are not required for its cellular trafficking

Glycosylation of CFTR occurs at two natural sites between TM7 and TM8 during its cellular trafficking, with core glycosylation occurring in the ER and complex glycosylation occurring subsequent to trafficking out of the ER (Figure 2.2A). The need of the natural sites for CFTR integration and subsequent trafficking from the ER was tested by their individual or combined removal. The sites, with asparagines at positions 894 and 900, were independently mutated (N to D) to remove the glycosylation consensus sequence. CFTR trafficking to the ER, Golgi, and cell surface of HeLa cells was monitored using glycosylation and cell surface

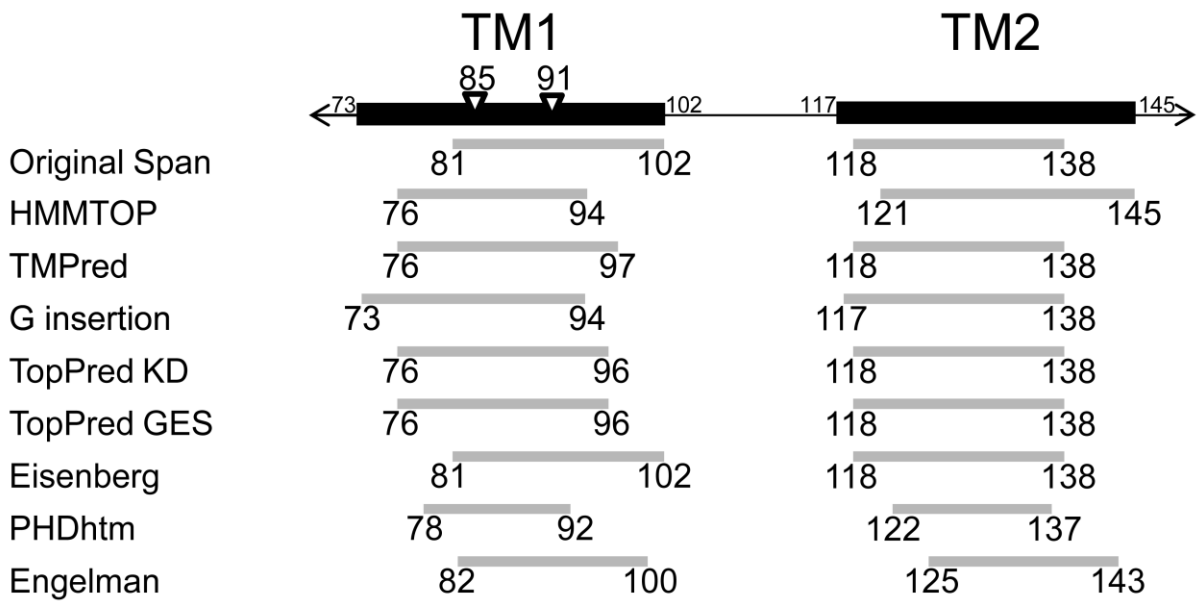

Figure 2.1. Predicted TM1 and TM2 spans. Black rectangles including all residues predicted to be in TM1 or TM2 are shown above gray rectangles representing the individual predictions from algorithms listed on the left. The positions of the CF-causing mutants G85E and G91R are indicated by triangles.

Table 2.1. Predicted TM1 spans for CF-causing and non-charged mutants.

Mutation / Prediction method	WT	G85E	G91R	G85A	G91A
HMMTOP	76-94	76-94	76-94	76-94	76-94
TMPred	76-97	69-90	69-90	76-97	76-97
G insertion	73-94	72-90	73-91	73-94	73-94
TopPred KD	76-96	86-106	73-93	76-96	76-96
TopPred GES	76-96	No TM	No TM	76-96	76-96
PHDhtm	75-92	76-93	75-92	75-93	76-93

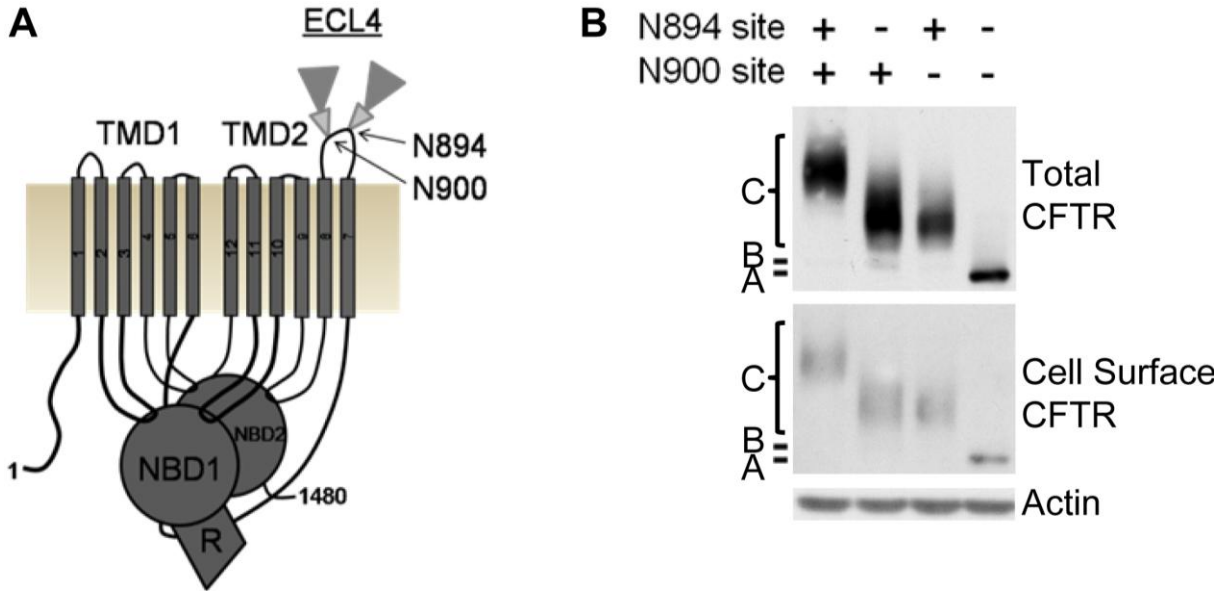

Figure 2.2. CFTR natural glycosylation sites are not required for cellular trafficking. (A) Schematic of the five CFTR domains: two transmembrane spanning domains (TMD1 and 2), two nucleotide binding domains (NBD1 and 2), and a regulatory region (R). Two natural N-linked glycosylation sites are in extracellular loop 4 (ECL4) between TM7 and TM8 with core glycosylated (small triangle) and complex glycosylation (large triangle) depicted. (B) Cellular trafficking of CFTR containing both, individual, or lacking natural glycosylation sites in HeLa cells was monitored by Western blot analysis. The positions of CFTR with no glycosylation (Band A), core glycosylation (Band B), and complex glycosylation (Band C) are marked. The top panel is total cell CFTR, the middle panel is cell surface CFTR identified by biotinylation, and actin is a control.

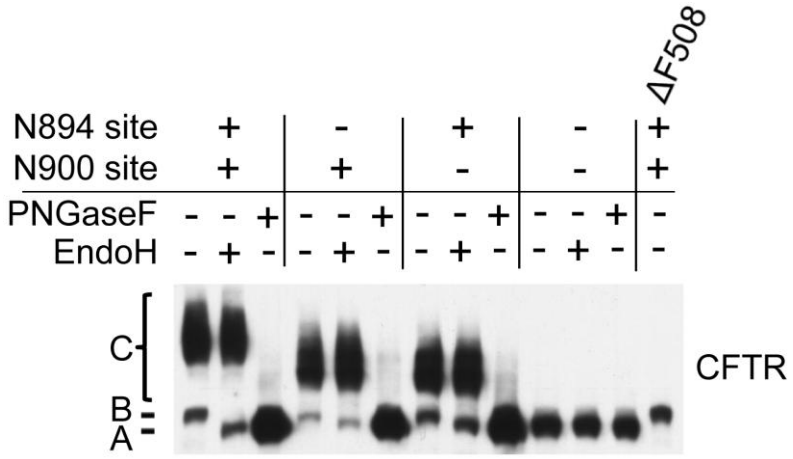

Figure 2.3. Glycosidase treatment of CFTR natural ECL4 (N894 and N900) glycosylation sites. HeLa cell trafficking of CFTR containing both, individual, or no natural glycosylation sites monitored by Western blot analysis. Core and complex glycosylation were verified by digestion with glycosidase selective for core and complex glycosylation (PNGaseF) or core glycosylation (Endo H). The positions of CFTR with no glycosylation (Band A), core (Band B) and complex (Band C) glycosylation, WT and ΔF508 CFTR are marked.

biotinylation. Each natural CFTR site can be core and complex glycosylated independently of the other site, and these proteins trafficked to the cell surface (Figure 2.2B). In order to verify core and complex glycosylation, samples were treated with specific glycosidases that result in electrophoretic mobility shifts of deglycosylated samples (Figure 2.3).

CFTR containing an artificial glycosylation site between TM1 and TM2 is trafficked in the cell

In order to utilize glycosylation to as a tool to monitor TM1 and TM2 ER luminal boundaries, the effect of introducing an artificial glycosylation site into extracellular loop 1 (ECL1) between TM1 and TM2 was determined. ER luminal core glycosylation depends on consensus site (NXS/T) placement more than 12 residues N- and C- terminal from the ER membrane (Nilsson and von Heijne 1993). TM1 and TM2 boundary predictions (Figure 2.1) were used to introduce additional residues both N- and C-terminal to the artificial site to bracket the appropriate distance (Figure 2.4A). This artificial glycosylation site is introduced between CFTR residues Y109 and D110, and includes five residues added N-terminal and four residues added C-terminal to the NST site, which in total is denoted the ECL1 site in this study. In HeLa cells, the ECL1 site is both core and complex glycosylated and trafficked to the cell surface in CFTR containing or lacking the natural ECL4 sites (Figure 2.4B), again indicating the natural ECL4 sites are not required for CFTR maturation. Mutation of the consensus sequence in the ECL1 site resulted in no glycosylation of the ECL1 loop, confirming glycosylation at the specific site (Figure 2.5A). Core and complex glycosylation were verified by electrophoretic mobility shifts after treatment with specific glycosidase (Figure 2.5B). Importantly, the introduced ECL1

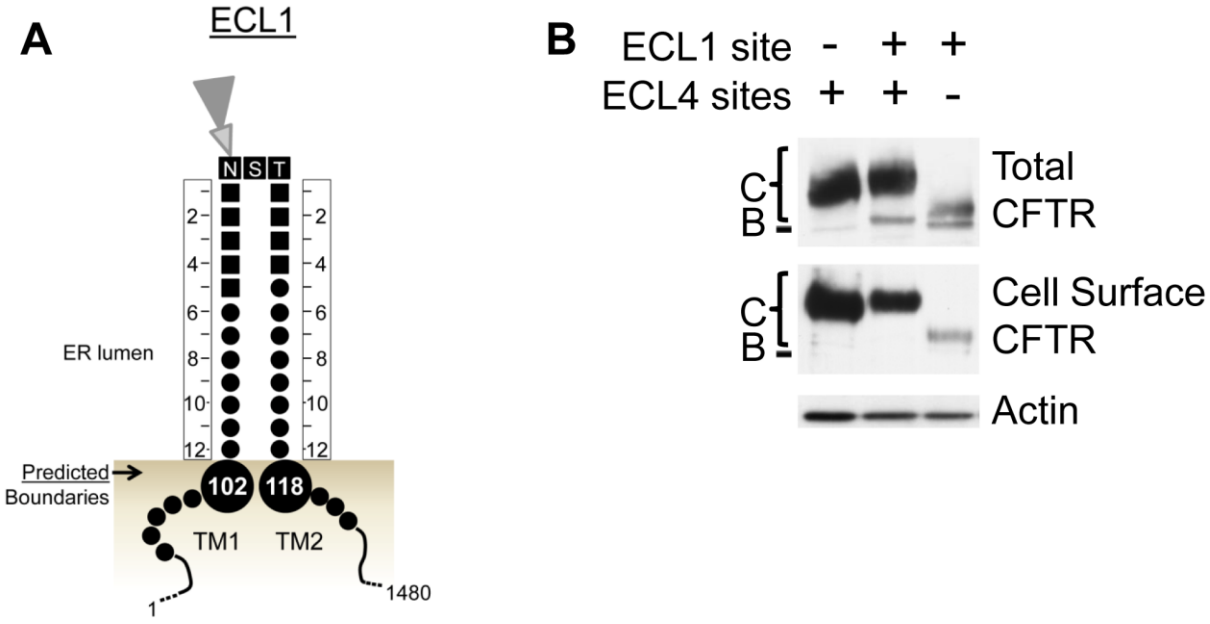

Figure 2.4. An artificial glycosylation site introduced in ECL1 between TM1 and TM2 is glycosylated and trafficked to the cell surface. (A) Schematic of the predicted TM1 and TM2 ER luminal boundaries (large circles) with the artificial glycosylation site with CFTR residues (small circles) and introduced residues (small squares) shown. Twelve residues are located between the core glycosylation site (NST) and the predicted TM boundaries. (B) Cellular trafficking of CFTR containing the natural ECL4 glycosylation sites and/or the artificial ECL1 site in HeLa cells was analyzed by Western blot analysis. The positions of core (Band B) and complex (Band C) glycosylated CFTR forms are marked. The top panel is total cell CFTR, the middle panel is cell surface CFTR identified by biotinylation, and actin is a control.

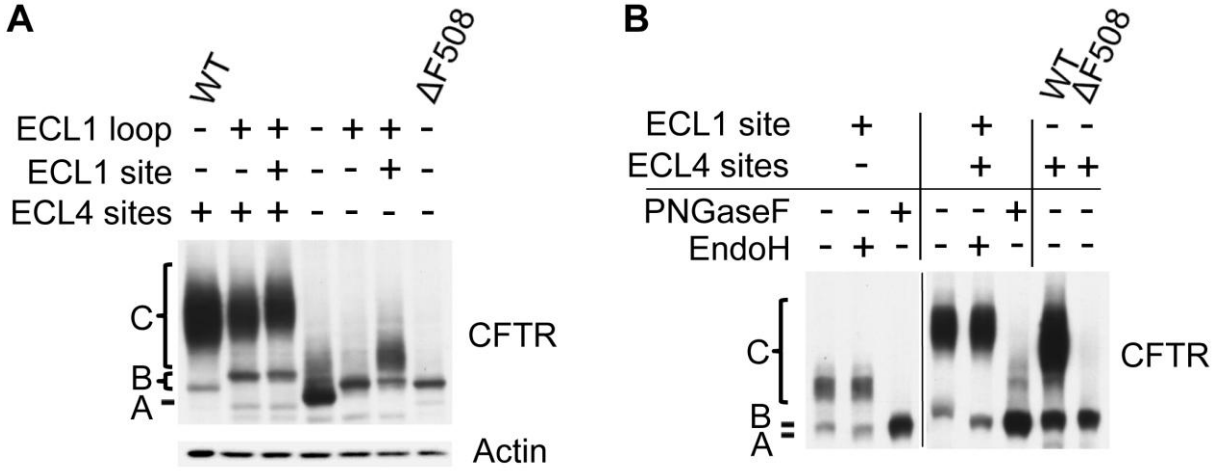

Figure 2.5. The artificial ECL1 glycosylation site is core and complex glycosylated. (A) HeLa cell trafficking of CFTR containing combinations of the natural ECL4 sites, the ECL1 loop without a site, and the ECL1 loop with a site were monitored by Western blot analysis. (B) Core and complex glycosylation of CFTR containing only the ECL1 site or all three sites were verified by digestion with glycosidase selective for core and complex glycosylation (PNGaseF) or core glycosylation (Endo H). The positions of CFTR with no glycosylation (Band A), core (Band B) and complex glycosylation (Band C), WT and ΔF508 CFTR are marked.

site is efficiently core glycosylated with no non-glycosylated band detected, suggesting this variant is efficiently integrated into the ER membrane (Figure 2.4B, Figure 2.6A, Figure 2.5).

Experimentally determined TM1 and TM2 ER luminal boundaries of WT CFTR

To examine the TM1 and TM2 ER luminal boundaries of WT CFTR, an assay was employed that utilizes core glycosylation of the artificial ECL1 site as a molecular ruler in HeLa cells. Using this assay, ER luminal boundaries for WT CFTR TM1 and TM2, as a basis for comparison to the boundaries for the mutant CFTRs, were determined. As previously described, at least a 12 residue distance from the surface of the ER membrane is needed for efficient core glycosylation. Deletion of residues proximal to the site reduces the distance between the ECL1 site and the ER membrane surface/TM span boundary. When the ECL1 site is too close to the ER membrane, it can no longer be core glycosylated in the OST active site. N- or C-terminal residue deletions reduce the distance from the ELC1 site to TM1 or TM2 respectively. Full length CFTR constructs containing the ECL1 site were expressed in HeLa cells and ECL1 site core glycosylation monitored. N-terminal deletion constructs from the ECL1 site were completely core glycosylated until a sixteen-residue deletion resulted in partial core glycosylation, and an eighteen-residue deletion was not glycosylated (Figure 2.6A). With a sixteen-residue deletion, I86 is twelve residues from the ECL1 site, positioning the TM1 ER luminal boundary near residues 85 and 86 (Figure 2.6C). By contrast, the original TM1 prediction used as a starting point in development of the ECL1 site indicated the ER luminal boundary was at residue 102 (Figure 2.4A). The experimentally identified TM1 boundary is shifted N-terminal to all of the TM1 predictions (Figure 2.1) with PHDhtm closest with a boundary of residue 92 predicted.

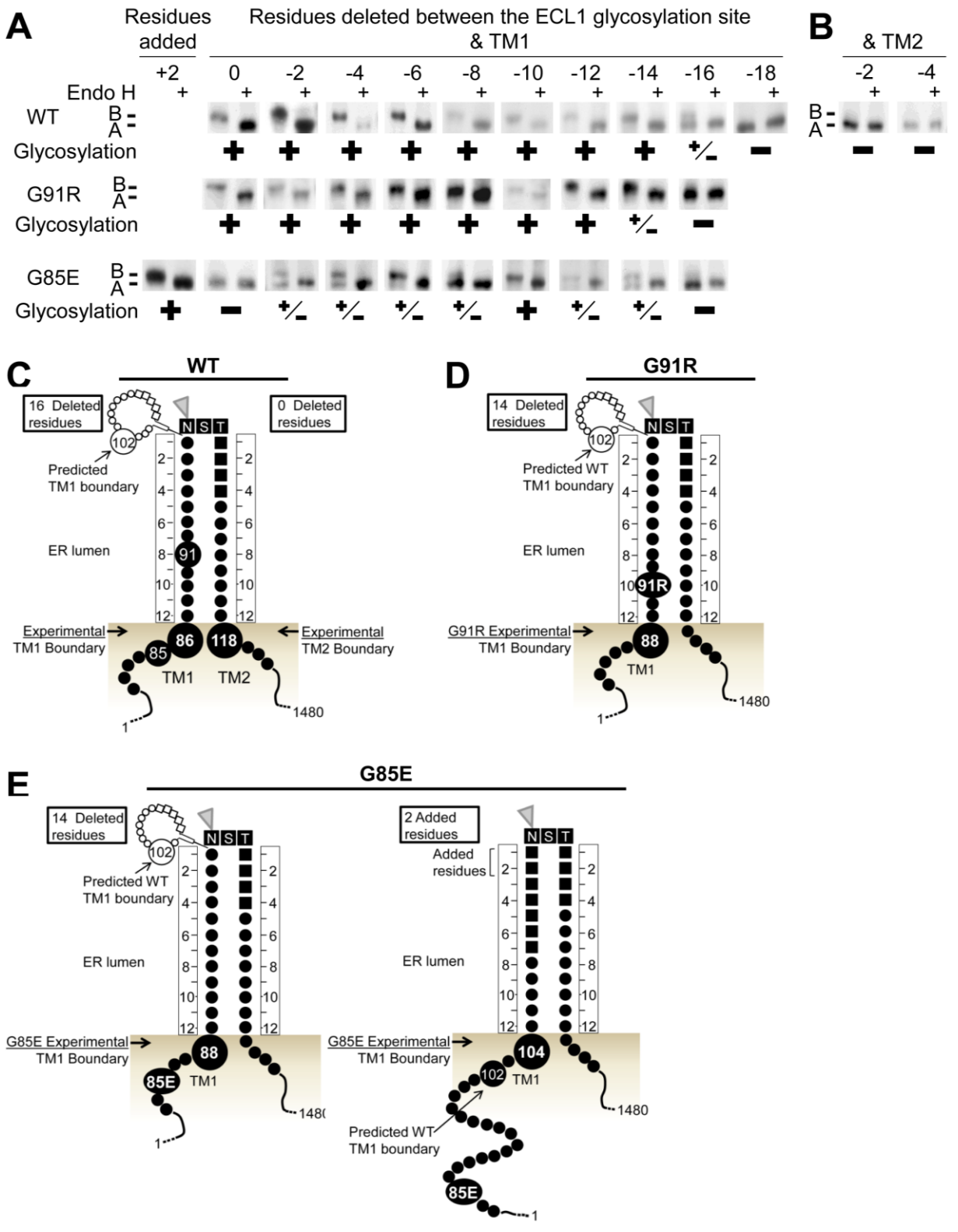

Figure 2.6. *(Figure legend continued on next page)*

Figure 2.6. Experimental TM1 ER luminal boundaries for WT and CF mutant CFTR. Core glycosylation requires a minimum of twelve residues between the artificial ECL1 site and the ER membrane. The distance between the ECL1 site and TM1 or TM2 was reduced by deleting residues proximal to the site. Core glycosylation analysis of wild-type (WT), G91R, and G85E CFTR containing the artificial ECL1 site was performed by deletion of residues between the glycosylation site and TM1 (A) or between the glycosylation site and TM2 (B). Core glycosylation was detected by gel shift after its removal with Endo H. The presence (cross) or absence (minus) of core glycosylation is noted below each sample. The positions of non-glycosylated (Band A) and core glycosylated (Band B) CFTR are marked. Schematics of the experimentally identified ER luminal boundaries in WT (C) or G91R (D) and G85E (E) mutants.

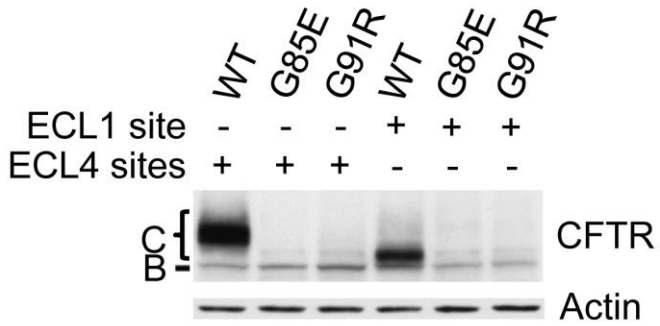

Figure 2.7. WT, G85E, or G91R CFTR containing the natural ECL4 sites or the artificial ECL1 site was monitored for cellular trafficking in HeLa cells using Western blot analysis. The positions of CFTR with no glycosylation (Band A) or core (Band B) and complex (Band C) glycosylation are marked.

The predictions are in closer agreement with experiment for the TM2 boundary. All C-terminal deletions to the ECL1 site tested abolished ECL1 glycosylation (Figure 2.6B). In the unmodified ECL1 construct, S118 is twelve residues from the ECL1 site, positioning it at the TM2 ER luminal boundary (Figure 2.6C). Thus, both the experimentally identified TM2 boundary and the original predicted TM2 boundary are at residue 118 (Figure 2.4A), as are many of the other predictions (Figure 2.1).

Determining the ER luminal boundaries of CF-causing mutants

To assess any effects of the CF-causing mutants G91R and G85E on the TM1 ER luminal boundary, these mutations were analyzed utilizing the ECL1 site core glycosylation assay. The G85E and G91R mutations introduce an ionizable group into or near the predicted TM1 span, and might be reasonably expected to alter its ER luminal boundary (Xiong et al. 1997). If the TM span positioning or integration is altered or destabilized, multiple TM span positions within the ER membrane will be detected as an aberrant or split pattern of core glycosylation (Mingarro et al. 2000). The G91R and G85E mutations in CFTR containing the natural ECL4 sites or the ECL1 site resulted in misfolding and accumulation in the ER (Figure 2.7). Since core glycosylation occurs in the ER prior to complete trafficking or functioning of CFTR, it can be used to characterize TM spans that are integrated into and retained in the ER despite their inability to traffic to the plasma membrane. Thus, as for WT ECL1, glycosylation analysis was used to characterize the boundaries of TM1 for the G91R and G85E mutants.

CF-causing mutant G91R shifts the ER luminal boundary of TM1

The effect of the G91R mutation on the TM1 ER luminal boundary was tested by its introduction into the ECL1 core glycosylation assay. The core glycosylation derived TM1 ER luminal boundary places residue 91 in the ER lumen for the wild type sequence (Figure 2.6C). By contrast, G91R N-terminal deletion constructs were completely core glycosylated until a fourteen-residue deletion resulted in partial core glycosylation, and a sixteen-residue deletion was completely non-glycosylated (Figure 2.6A), indicating the boundary of the mutant TM span shifted by two or three residues. Thus, instead of I86 as in the wild type, L88 is twelve residues from the ECL1 site in the mutant, positioning it at the G91R TM1 ER luminal boundary (Figure 2.6D).

The CF-causing mutant G85E dramatically alters TM1 in the ER membrane

The effect of the G85E mutation on the TM1 ER luminal boundary was examined by its introduction into the ECL1 core glycosylation assay. The core glycosylation derived TM1 ER luminal boundary (Figure 2.6C) and all prediction algorithms place position 85 within TM1 (Figure 2.1). In the presence of G85E, the unmodified ELC1 site is not glycosylated (Figure 2.6A). An additional two residues must be added N-terminal to the ECL1 site to observe its efficient glycosylation (Figure 2.6A). Unexpectedly, N-terminal deletions from zero to fourteen residues exhibited an aberrant pattern of core glycosylation, with a mixture of glycosylated and non-glycosylated forms (Figure 2.6A). This aberrant pattern is in stark contrast to WT TM1, and is consistent with multiple conformations and/or profiles of G85E TM1 in the ER membrane, with the two extreme positions defined by residues L88 or R104 at the ER luminal boundary (Figure 2.6E). As is the case for G91R, the L88 TM1 boundary conformation is slightly shifted

from the WT boundary. However, the R104 TM1 boundary conformation is dramatically shifted from the WT boundary, indicating a significant disruption in the G85E TM1. Comparison of this boundary to predicted TM1 boundaries reveals that it is surprisingly close to several of the original predicted WT TM1 boundaries (Figure 2.1) and the KD scale predicted G85E TM1 (Table 2.1).

Role of an ionizable side-chain in the altered G91R and G85E TM1 ER luminal boundaries

In the G91R and G85E mutants, an ionizable side-chain replaces the glycine Cα hydrogen. Glycine has many important roles in the stability of and interaction between transmembrane helices (Curran and Engelman 2003). In order to investigate if the mutant effects on folding and TM boundaries are caused by the loss of glycine or by the introduction of the ionizable group, the 85 and 91 positions were mutated to the neutral residue alanine (G91A and G85A). The alanine mutants were examined for cellular trafficking of CFTR, and for TM1 span boundaries using the ECL1 site core glycosylation assay. In the ECL-site assay, G91A and G85A N-terminal deletion constructs were completely glycosylated, a fourteen residue deletion partially glycosylated, and a sixteen residue deletion was not glycosylated (Figure 2.8A). L88 was at the TM1 ER luminal boundary for both G91A and G85A (Figure 2.8B), shifted by two or three residues from the WT TM1 ER luminal boundary. This boundary is the same as the G91R TM1 boundary and one of the boundaries for the two conformers of G85E TM1. The two residue boundary shifts are consistent with the substitution for glycine causing a small but consistent decreased distance between the ECL1 site and the ER membrane. Strikingly, the G85A TM1 glycosylation pattern does not indicate multiple conformations or profiles for TM1,

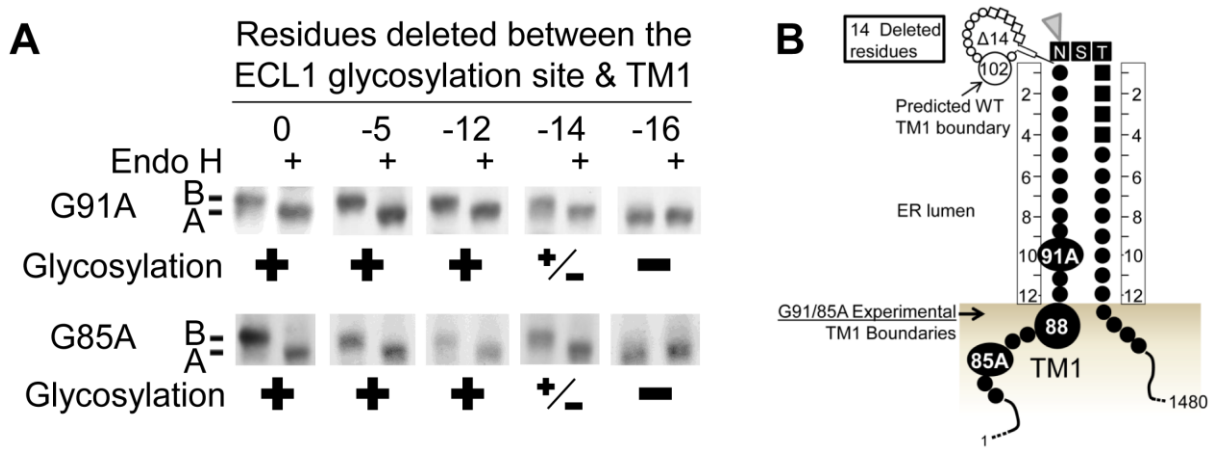

Figure 2.8. Experimental TM1 ER luminal boundaries for G91A and G85A mutant CFTR. (A) Core glycosylation analysis of G91A and G85A mutant CFTR containing the artificial ECL1 site by deletion of residues between the glycosylation site and TM1. The presence (cross) or absence (minus) of core glycosylation is noted below each sample. The positions of non-glycosylated (Band A) and core glycosylated (Band B) CFTR are marked. (B) A combined schematic of the experimentally identified TM1 ER luminal boundaries for the G91A and G85A mutants.

indicating that the aberrant pattern of G85E TM1 results from introduction of the glutamate side-chain (Figure 2.8A).

Role of side-chain polarizing in trafficking of G91R and G85E

The data from the glycosylation assay, demonstrate that the G85E mutant splits the integration profile of TM1, while the G91R, G85A, and G85E mutants do not. To examine how these mutants effect the cellular trafficking of CFTR, trafficking at physiologic (37°C) and reduced temperatures (30°C) was monitored. TM1 mutant CFTR with natural glycosylation sites were expressed in HeLa cells, with CFTR cellular trafficking observed by glycosylation and cell surface biotinylation (Figure 2.9A). G91A is both core and complex glycosylated and traffics to the cell surface, indicating that introduction of arginine, rather than loss of glycine causes G91R ER retention. Consistent with this, the G91A mutant has unaltered topology and wild type like degradation in *Xenopus laevis* oocytes (Xiong et al. 1997). However, G85E was not assessed in the *Xenopus* system. In stark contrast to G91A, G85A is retained in the ER, suggesting that both introduction of charge and loss of glycine at position 85 contribute to G85E ER retention.

The ΔF508 mutation exhibits a temperature sensitive trafficking from the ER, in which it is retained in the ER at 37°C, but partially traffics from the ER at lower temperatures (Denning et al. 1992). To test the effect of temperature on the TM1 mutants, they were grown at 30°C with ΔF508 monitored as a control (Figure 2.9B). At both temperatures, G91A traffics like WT CFTR. At the lower temperature, both G91R and G85A mutants partially traffic from the ER, and are thus temperature sensitive similar to ΔF508. Glycosylation patterns were confirmed by treatment with specific glycosidases (Figure 2.10). Strikingly, the G85E mutant exhibited temperature insensitive mistrafficking. This observation cannot be accounted for by lower

protein expression of G85E as Band B is not measurably altered. Importantly, G85E temperature insensitive mistrafficking correlates with the G85E conformer with a TM1 boundary of R104.

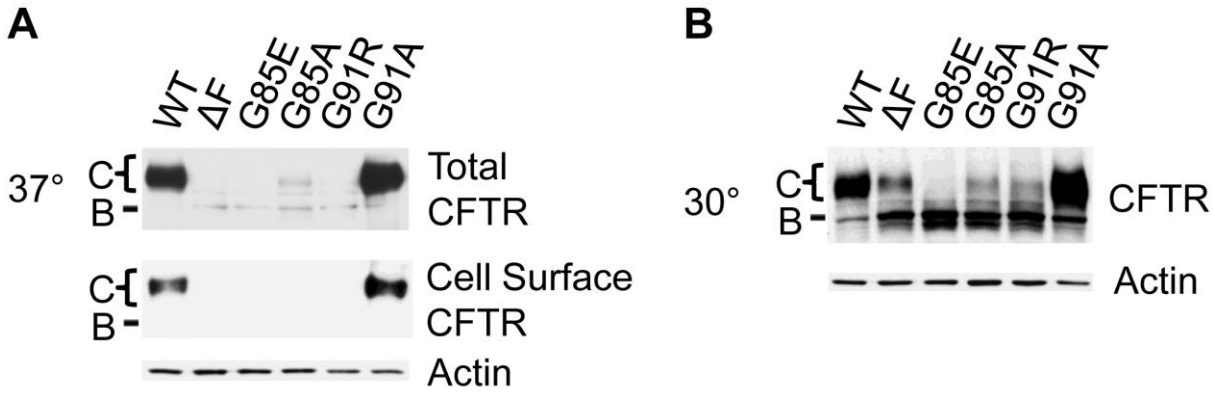

Figure 2.9. Cellular trafficking of CFTR constructs containing the natural glycosylation sites. HeLa cell trafficking of WT, ΔF508, G85E, G85A, G91R, and G91A mutant CFTR was monitored at 37°C as in Figure 1B (A). The top panel is total cell CFTR, the middle panel is cell surface CFTR identified by biotinylation, and actin is a control. Low temperature trafficking rescue at 30°C was performed and analyzed by Western blot analysis (B). The ΔF508 control is retained in the ER at 37°C and partially traffics from the ER at 30°C. The positions of core (Band B) and complex (Band C) glycosylated CFTR are marked.

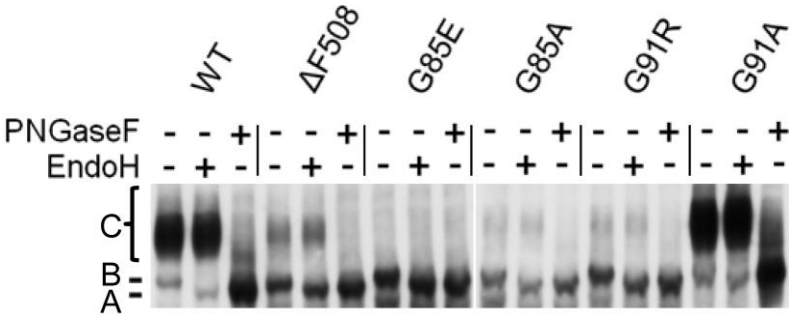

Figure 2.10. Glycosidase treatment of WT and mutant CFTR with natural ECL4 glycosylation sites grown at 30°C. Core and complex glycosylation were verified by digestion with glycosidase selective for core and complex glycosylation (PNGaseF) or core glycosylation (Endo H). The positions of CFTR with no glycosylation (Band A), core glycosylation (Band B), and complex glycosylation (Band C) are marked.

DISCUSSION

Many disease-causing mutations in CFTR are predicted to introduce ionizable side-chains into or near its hydrophobic TM spans (Cheung and Deber 2008). Prediction and testing of these mutant consequences is impeded by the lack of detailed CFTR structural data and difficulties in producing the full length protein. Thus, much present work relies on structural models derived from homologues and predictions of domain and transmembrane span boundaries. The predicted boundaries for TM1 and TM2 vary widely depending on the algorithm employed; therefore, experimentally determined TM span boundaries are needed to accurately characterize the native and CF-causing mutant TM spans. This study determined the TM1 and TM2 ER luminal boundaries, and CF-causing mutant G91R and G85E effects on TM1 using the mammalian ER luminal core glycosylation machinery.

Before identification of these boundaries, the two natural glycosylation sites in ECL4 were removed. The natural glycosylation sites were not required for cellular trafficking (Figure 2.2), consistent with their described nonessential roles for trafficking from the ER and chloride channel function (Howard et al. 1995; Chang et al. 2008; Glozman et al. 2009). Recently, these sites have been found to influence the efficiency of CFTR productive protein folding and early secretory trafficking (Glozman et al. 2009), and cell surface retention and turnover in post-ER cellular compartments (Chang et al. 2008; Glozman et al. 2009). While these effects likely alter overall CFTR levels in the cell, the effects on ER biogenesis do not contribute measurably to the integration process monitored in this study.

An artificial glycosylation site was introduced into ECL1 in CFTR devoid of natural glycosylation sites. This construct was specifically designed to include twelve residues between

the predicted TM spans and the consensus sequence, unlike other artificial ECL1 glycosylation sites previously utilized to monitor cellular localization (Chang et al. 1994; Cui et al. 2007). The studied ECL1 site herein can be core and complex glycosylated, indicating this region is tolerant of the glycosylation manipulation. However, the total protein quantity of the construct is slightly decreased and an altered channel function cannot be ruled out. Yet, Band B is not measurably decreased and, thus, the slight reduction in total CFTR may result from altered turnover during later steps in CFTR trafficking as observed for other non-natively glycosylated CFTR forms (Chang et al. 2008; Glozman et al. 2009).

The TM span topology and membrane boundaries for membrane spanning proteins have been studied using the ER core glycosylation machinery both *in vitro* and in cell culture (Cheung and Reithmeier 2005; Cheung and Reithmeier 2007). In one such study, the major disease causing mutation in the anion exchanger 1 (AE1) resulted in incorrect positioning of a TM span (Cheung and Reithmeier 2005). In the work presented here, CF-causing mutant effects on TM1 were identified by core glycosylation in mammalian cells. In both cases, this experimental approach provides insight into disease-causing TM span structural perturbations in the mammalian cell that are otherwise difficult to detect. The greatest challenge to core glycosylation analysis is monitoring the small produced electrophoretic differences, which were overcome here by a combination of glycosidase treatments and high resolution electrophoretic separation.

The core glycosylation machinery is associated with the ER translocon, and core glycosylation likely occurs cotranslationally (Chavan and Lennarz 2006). Yet, the timing of the reaction with respect to TM span integration and translation of other parts of the protein have not been determined in detail. Furthermore, in TM span predictions based on translocon integration

energy, the selected span can vary from the identified crystallographic TM span (Kauko et al. 2010). Hence, some TM spans may be able to shift and reposition during protein translation, folding, and as interacting TM spans are formed (Kauko et al. 2010). It is therefore reasonable to assume that core glycosylation may be indicative of a TM span ER luminal boundary that occurs prior to the final folded protein structure. A tilting or shift of TM1 subsequent to the glycosylation modification would therefore not be reflected, or perhaps allowed, in the glycosylation-based analysis. If so, the technique allows identification of a cotranslational TM span position.

In this study, core glycosylation was used to identify the WT TM1 and TM2 ER luminal boundaries, which are near but not overlapping with the previously predicted spans. The experimentally determined TM2 ER luminal boundary is most consistent with the predictions (Figure 2.1). Interestingly, it is more hydrophobic than TM1 (Wigley et al. 1998), an important parameter for TM span prediction by most methods. The TM1 ER luminal boundary is significantly N-terminal to the predicted span boundaries, placing C-terminal residues previously predicted to reside in TM1 within the ER lumen. These residues may form a structural extension, an amphipathic helix or reentrant loop, interact with parts of CFTR or cellular proteins, or shift into the membrane during a later folding step. Based on the criteria for span repositioning (Kauko et al. 2010), which uses transmembrane insertion efficiency predictions (Hessa et al. 2007), the TM1 span is within the range for potential repositioning (data not shown). The only experimentally determined CFTR TM1 boundary is that identified herein, and other studies in full length protein will be required to validate the final span position.

Thus, CF-mutations, such as G91R, in the C-terminal region may be within or exposed to the ER lumen during translation and integration. Consistent with this is the modest shift in the

G91R-CFTR TM1 ER luminal boundary. The data here and previous reports indicate that G91R, but not G91A, disrupts CFTR trafficking in the cell and has significant effects on the stability and assembly of full length CFTR (Xiong et al. 1997; Younger et al. 2006; Rosser et al. 2008; Du and Lukacs 2009). Arginine introduction likely propagates throughout the structure of CFTR, much as ΔF508 mediated alterations in NBD1 and ICL4 (Thibodeau et al. 2005; Hoelen et al. 2010; Thibodeau et al. 2010) are most evident in the proteolytic susceptibility of NBD2 (Du et al. 2005).

The core glycosylation experiments demonstrate that G85E is within TM1, and causes at least two TM1 positions with distinct ER luminal boundaries. Interestingly, the most C-terminal extreme G85E TM1 boundary is within several residues of the original predicted WT TM1 span boundary (Figure 2.1) and a boundary predicted by TopPred KD (Table 2.1). The introduction of the ionizable side chain thus causes nonnative TM1 span position(s), tilt, or structure during glycosylation. Since core glycosylation is likely cotranslational, these defects occur at an early step prior to formation of later domain and multidomain structures. Thus, G85E destabilization is an early folding defect potentially recognizable in the ER before translation is complete. Furthermore, the G85A non-polar mutation does not split the TM1 integration profile and continues to cause CFTR ER accumulation. Consequently, G85E misfolding results from both introduction of a polarizing group and glycine loss, which respectively correlate with temperature insensitive and sensitive accumulation in the ER. The specific mis-steps caused by the two mutants, which have different molecular pathologies, could be recognized individually, in combination, or as a consequent common misfolding domain or multidomain event. In this regard, a Derlin-1 containing complex mediates the retro translocation and ER-associated degradation of misfolded proteins (Lilley and Ploegh 2004; Ye et al. 2004). This complex has

been implicated in the recognition and removal of improperly folded CFTR, including G85E mutant CFTR (Sun et al. 2006; Younger et al. 2006; Wang et al. 2008a). Experiments designed to test the role of Derlin-1 in the recognition of the G85A mutant would be a reasonable future step toward distinguishing between these two models.

Previous work demonstrated that the G85E and G91R mutations also disrupt later steps in CFTR folding, particularly interdomain interactions, which were proposed to underlie mutant recognition by ER quality control machinery (Xiong et al. 1997). The results presented here demonstrate that G85E dramatically alters the conformation/integration profile of TM1. Such an alteration would occur at the earliest steps of translation and integration, and could be recognized as a very early misfolding event by ER quality control machinery. The G91R mutant was predicted to have a similar effect on CFTR (Xiong et al. 1997). Yet, the experimental evidence presented herein distinguishes G91R from G85E, both with respect to perturbations from the ionizable side-chain, the role of glycine, and temperature sensitivity. Strikingly, the corrector compound 4 also exhibited mutant specific effects, partially rescuing the G91R but not G85E CFTR (Grove et al. 2009). This suggests that the molecular pathologies identified in these studies may have significance for determining CF-mutants that can benefit from specific treatments to rescue defective CFTR. The detailed mechanistic study of these disease causing mutants is therefore important to augment the fundamental understanding of membrane protein misfolding and relevant for CF therapeutics.

MATERIALS AND METHODS

Plasmids, DNA techniques

An expression plasmid of full length, wild type CFTR (pCMV-CFTR-pBQ6.2) was a gift from J. Rommens (The Hospital for Sick Children, Toronto) and was mutagenized using standard protocols for site-directed mutagenesis (Sambrook 1989). Site-directed mutagenesis was performed by PCR techniques using PfuUltra high-fidelity DNA Polymerase (Stratagene). All mutations were confirmed by DNA sequencing. The sense primers are listed in Table 2.2. A glycosylated sequence, NEFDQNSTGQGF, was introduced between CFTR residues Y109 and D110. Residues immediately proximal to the consensus sequence, NST, were removed by site-directed mutagenesis on the CFTR construct containing the artificial ECL1 site. The mutations G91R, G91A, G85E, and G85A were introduced into CFTR constructs containing the natural, artificial, and deletion mutants on the artificial site.

Cell culture and transfection

HeLa Tet-On cells (Clonetech), referred to as HeLa cells, were routinely maintained in Dulbecco's Modified Eagle Medium (DMEM, Invitrogen) supplemented with 10% Fetal Calf Serum (Gemini Bio-Products), 50 μg mL^{-1} penicillin, and 50 units mL^{-1} streptomycin using standard culture techniques. Plasmids were transfected using Lipofectamine 2000 reagent (Invitrogen) and expressed for 16-24 hours. Cells were washed with phosphate buffered saline (pH7.4) (PBS), lysed in RIPA buffer (20mM tris pH7.6, 150mM NaCl, 0.1% SDS, 1% IGEPAL, 0.5% deoxycholic acid, 1mg EDTA-free protease inhibitor tablet (Roche)) at 4°C for 1 hour, and centrifuged at 13000g's. Sample buffer (60mM tris pH6.8, 5% glycerol, 2% SDS, bromophenol

Table 2.2. Sense primers for generation of DNA constructs.

Primer (5'-3' sense primers)	Mutations	Purpose
CCTCTTCAAGACAAAGGGGATAGTACTCATAGTAGAAATAACAG	N894D	Remove native glycosylation site
GGGATAGTACTCATAGTAGAGATAACAGCTATGCAGTGATTATC	N900D	Remove native glycosylation site
CCTCTTCAAGACAAAGGGGATAGTACTCATAGTAGAGATAACAGCTATGCAGTGATTATC	N894D, N900D	Remove both native glycosylation sites
CTCTTACTGGGAAGAATCATAGCTTCCTATAACGAATTTGATCAGAATAGTACTGGCCAAGGATTCGA CCCGGATAACAAGGAGGAACGC		Introduce artificial glycosylation site into ECL1
GGGAAGAATCATAGCTTCCTATAACGAATTTAATAGTACTGGCCAAGGATTCGACCCGG	-2N	Remove residues from CFTR containing the artificial glycosylation site in ECL1
GGGAAGAATCATAGCTTCCTATAACAATAGTACTGGCCAAGGATTCGACC	-4N	
GGGAAGAATCATAGCTTCCTATAATAGTACTGGCCAAGGATTCG	-5N	
CAGCCTCTCTTACTGGGAAGAATCATAGCTTCCAATAGTACTGGCCAAGGATTCGACCCGGATAAC	-6N	
CCTCTCTTACTGGGAAGAATCATAAATAGTACTGGCCAAGGATTCG	-8N	
CAGCCTCTCTTACTGGGAAGAAATAGTACTGGCCAAGGATTCG	-10N	
GCAGTACAGCCTCTCTTACTGAATAGTACTGGCCAAGGATTCG	-12N	
CCAAAGCAGTACAGCCTCTCAATAGTACTGGCCAAGGATTCG	-14N	
GGAAGTCACCAAAGCAGTACAGAATAGTACTGGCCAAGGATTCG	-16N	
GGGGAAGTCACCAAAGCAAATAGTACTGGCCAAGGATTCG	-18N	
CATAGCTTCCTATAACGAATTTGATCAGAATAGTACTGGATTCGACCCGGATAACAAGGAGGAACGC	-2C	
CATAGCTTCCTATAACGAATTTGATCAGAATAGTACTGACCCGGATAACAAGGAGGAACGCTCTA	-4C	
GCTTCCTATAACGAATTTGATCAGGCCGCCAATAGTACTGGCCAAGGATTCG	+2N	Add residues to CFTR containing the artificial glycosylation site in ECL1
TCTGGAGATTTATGTTCTATGAAATCTTTTTATATTTAGGGGAAG	G85E	G85E
GGAGATTTATGTTCTATGCCATCTTTTTATATTTAGGGG	G85A	G85A
CTATGGAATCTTTTTATATTTAAGGGAAGTCACCAAAGCAGTACAGC	G91R	G91R
GGAATCTTTTTATATTTAGCCGAAGTCACCAAAGC	G91A	G91A

blue, 280mM β-mercaptoethanol) was added to supernatant and incubated at 37°C for 20 minutes.

Temperature sensitive trafficking of CFTR mutants was performed as follows. HeLa Tet-On cells were transfected as above, expressed for 16 hours at 37°C, and then moved to 30°C for 16-24 hours. Lysis and protein analysis was performed as described.

Western blot analysis

Cell lysate proteins were separated by electrophoresis on 6% (w/v) polyacrylamide gels using a tris-glycine buffering system, and transferred to PVDF Immobilon membranes (Millipore). Western blot analysis was performed using primary CFTR antibodies M3A7 (Millipore) or 596 (UNC School of Medicine) and actin antibody (Millipore), secondary antibody peroxidase-AffiniPure goat anti-mouse IgG (Jackson ImmunoResearch Laboratories, Inc.), and developed with ELC Plus detection reagent (GE Healthcare) and film.

Glycosylation analysis

HeLa Tet-On cells were transfected and lysed as described. 500U of glycosidase, PNGaseF or Endoglycosidase H, was added to 40μL of lysis supernatant and incubated at 37° for 2 hours. Samples were analyzed by electrophoresis and Western blotting as described above.

High resolution SDS-PAGE analysis of full length CFTR core glycosylation samples was performed as described with the following differences. Samples were analyzed on a 13 cm separating gel (6% acrylamide, 375mM tris pH8.8, 0.1% SDS) with 1.5cm stacking gel (4% acrylamide, 125mM tris pH6.8, 0.1% SDS) at constant milliamperes (20-30mA) until the

150kDa molecular weight marker is 3-4cm from the gel bottom. Mock treated and glycosidase treated samples were loaded next to each other for comparison.

Cell surface biotinylation

HeLa Tet-On cells were transfected and CFTR expressed as above. Cells were washed with PBS and exposed to membrane impermeable EZ-link sulfo-NHS biotinylation reagent (ThermoScientific) for 30 minutes at 4°C. The reagent was quenched by 3 washes with 200mM glycine, 25mM tris pH8. Cells were washed with PBS and lysed in RIPA buffer as described. Lysate supernatant was incubated with ImmunoPure Immobilized Streptavadin (ThermoScientific) at 4°C for one hour. Beads were collected and washed vigorously three times with RIPA buffer. The biotinylated samples were eluted from beads with sample buffer and analyzed by SDS-PAGE and Western blot analysis as described.

TM spans predictions:

The full length CFTR sequence was used to identify predicted TM spans within the TM1 and TM2 regions by previous reports or online prediction algorithms. The original predicted span (Riordan et al. 1989) and Eisenberg and Engelman predictions (Wigley et al. 1998) were previously reported. Online predictions utilized are HMMTOP version 2.0 (www.enzim.hu/hmmtop/index.html) (Hoelen et al. 2010; Kanelis et al. 2010), TMPred (www.ch.embnet.org/software/TMPRED_form.html) (Hofmann 1993), ΔG insertion (http://dgpred.cbr.su.se/index.php?p=home) (Hessa et al. 2007), TopPred KD (Kyte and Doolittle) or GES (Goldman, Engelman, Steitz) scales (http://mobyle.pasteur.fr/cgi-bin/portal.py?#forms::toppred) (von Heijne 1992; Claros and von Heijne 1994), and PHDhtm

utilizing refined PHDRhtm TM span (http://npsa-pbil.ibcp.fr/cgi-bin/npsa_automat.pl?page=/NPSA/npsa_phd.html) (Rost and Sander 1993; Rost and Sander 1994; Combet et al. 2000).

Chapter III

Role of TMD1 in CFTR Folding

ABSTRACT

The cystic fibrosis transmembrane conductance regulator (CFTR) protein is comprised of two transmembrane spanning domains (TMDs), two nucleotide binding domains (NBDs) and a unique regulatory region (R). The domains obtain cotranslational structure that is required to interact with the other domains as they are produced and folded. The first domain translated, TMD1, forms extensive interdomain interactions with the other domains in CFTR homology models. In TMD1, long intracellular loops extend into the cytoplasm and interact with both NBDs via coupling helices and with TMD2 via transmembrane spans (TMs). In this study, mutations within this domain, either in a TM span or in the cytosolic ICLs, only become apparent in constructs containing different CFTR domains, suggesting they interfere with specific steps in the hierarchical folding of CFTR. TM1 CF-causing mutants, G85E and G91R, directly affect TMD1, whereas most ICL1 and ICL2 mutant effects were apparent only after TMD2 production. A single mutant in ICL2 altered levels only in the presence of NBD2, suggesting it causes a perturbation of the ICL2-NBD2 interface. Notably, mutation of hydrophobic residues in the ICL coupling helices increased levels of pre-TMD2 biogenic intermediates, but caused ER accumulation in the presence of TMD2. This suggests a tradeoff between transient stability during translation and final structure. NBD2 increased the efficiency of mutant trafficking from the ER, consistent with stabilization of the intact CFTR. While the G85E and G91R mutants in TM1 have immediately detectable effects, most of the studied mutant effects are apparent only after production of TMD2, suggesting this intermediate is a major point of recognition by protein quality control.

INTRODUCTION

Cystic fibrosis (CF) is a common, lethal monogenetic disease caused by mutations in the cystic fibrosis transmembrane conductance regulator protein (CFTR) (Kerem et al. 1989; Riordan et al. 1989; Rommens et al. 1989). CFTR acts as a chloride channel at the surface of secretory epithelia, in which loss of CFTR function results in a reduced liquid layer and thick mucus secretions (Rowe et al. 2005). Currently, CF patients experience respiratory, digestive, and reproductive system pathologies, with respiratory-associated illness as the most common cause of death (O'Sullivan and Freedman 2009). CF-causing mutations in CFTR have been identified throughout the entire protein. However, 90% CF patients have at least one allele containing a deletion of phenylalanine at position 508 (ΔF508) (Riordan et al. 1989). The ΔF508 and many other mutations result in misfolding of the CFTR protein, ER accumulation, and eventually degradation. Thereby, the majority of CF is caused by mutations that disrupt CFTR folding.

CFTR folding is a complex and incompletely described process. CFTR is a member of the ABC transporter superfamily that uses ATP binding and hydrolysis to move substrates across membranes (Holland 2003). Like other ABC transporters, CFTR contains two transmembrane spanning domains (TMDs) and two nucleotide binding domains (NBDs) that have homologous structures, and CFTR also has a unique regulatory region (R) with no well-ordered structure (Baker et al. 2007). In the structures of the homologous ABC transporters, Sav1866 (Dawson and Locher 2006; Dawson and Locher 2007), MsbA (Ward et al. 2007), and P-glycoprotein (Aller et al. 2009), the two TMDs wrap around each other in a domain-swapped fashion. For each TMD, two long intracellular loops (ICLs) extend into the cytoplasm and interact with the

NBDs. Based on these homologues, several homology models of CFTR have been constructed (Mendoza and Thomas 2007; Mornon et al. 2008; Serohijos et al. 2008; Mornon et al. 2009). Consistent with the models, and like other ABC transporters (Moody et al. 2002; Smith et al. 2002), in CFTR the two NBDs interact in a head-to-tail fashion forming two sandwiched ATP binding sites, each made of the two NBDs (Mense et al. 2006).

Interactions between the ICLs and NBDs occur through a coupling helix at the end of each ICL. In the CFTR models, the coupling helices of ICL1 and ICL3 interact with both NBDs, with primary interactions occurring between ICL1 and NBD1 or ICL3 and NBD2. The coupling helices of ICL2 and ICL4 interact with NBD2 and NBD1 respectively (Mendoza and Thomas 2007). Conformational signals generated in the NBDs in relation to ATP binding and hydrolysis are transmitted by the ICLs in the TMDs, resulting in chloride channel opening and closing (Gadsby et al. 2006; Riordan 2008). The interactions between CFTR ICLs and NBDs have been validated by crosslinking studies (He et al. 2008; Serohijos et al. 2008) and complementation of a mutant located in an NBD with a mutant in an ICL (Thibodeau et al. 2010). The importance of the ICL-NBD dynamics for signaling is emphasized by stable crosslink disruption of CFTR channel function (He et al. 2008). Thereby, interactions between ICLs and dynamics of these interactions are essential for channel function.

As CFTR is translated, each domain folds and can then interact with previously translated domains to form multidomain intermediates (Lukacs et al. 1994; Du et al. 2005; Kleizen et al. 2005; Thibodeau et al. 2005; Cui et al. 2007; Cheung and Deber 2008; Du and Lukacs 2009). The domains are translated in the order: TMD1-NBD1-R-TMD2-NBD2. When and which interdomain interactions form, and whether initial interactions are the same as those in the final CFTR structure remain unresolved questions. The current model of the CFTR folding path holds

that individual domain structures form cotranslationally (Kleizen et al. 2005). Then, intermediate structures form. A minimal construct of TMD1-NBD1-R-TMD2 is able to traffic from the ER (Pollet et al. 2000; Du et al. 2005; Cui et al. 2007; Du and Lukacs 2009). Finally, NBD2 posttranslationally incorporates into the CFTR structure (Du et al. 2005). Mutations within a domain can destabilize other domains in CFTR, consistent with domain folding being required for interactions, and the interactions stabilizing these structures (Rosser et al. 2008; Du and Lukacs 2009). The effects of specific CF-causing mutations provide a means of testing this broad model, but these mutants are currently poorly understood. Elucidating these details is critical for development of relevant therapeutics.

The best studied disease-causing mutation, ΔF508, alters multiple steps during CFTR folding. The crystal structure of ΔF508-NBD1 is not significantly perturbed (Lewis et al. 2005), however the mutant domain has an increased tendency to aggregate, is destabilized, and folds less efficiently, indicating a domain folding problem (Thomas et al. 1992; Qu and Thomas 1996; Lewis et al. 2005; Thibodeau et al. 2005; Hoelen et al. 2010). NBD1 structure begins to form cotranslationally (Kleizen et al. 2005) with ΔF508 effects already apparent during CFTR translation (Du et al. 2005; Hoelen et al. 2010). In addition, the full length ΔF508-CFTR lacks wild type-like crosslinks between the TMDs and NBDs (Chen et al. 2004; Serohijos et al. 2008), and ΔF508 destabilizes multidomain folding intermediates (Meacham et al. 1999; Du et al. 2005; Cui et al. 2007; Rosser et al. 2008; Du and Lukacs 2009). This is consistent with the known ΔF508 effects on NBD1 folding, which is a prerequisite for its interdomain interactions and formation of an NBD1 surface for ICL4 interactions. The ΔF508 mutant effects can be rescued independently by suppressor mutations within NBD1 (Teem et al. 1993; Qu et al. 1997; DeCarvalho et al. 2002; Hoelen et al. 2010) and by a suppressor mutation in ICL4 (Thibodeau et

al. 2010). The point at which ΔF508 effects are detectable, and the ability to target multiple steps to rescue the ΔF508 protein, emphasizes the multistep misfolding of ΔF508-CFTR.

The first domain, TMD1, contains extracellular loops, six transmembrane spans (TMs), and cytosolic regions including an N-terminal region, two ICLs, and a linker that connects to NBD1. In CFTR homology models, the TM spans and ICLs domain swap with TMD2, forming extensive contacts (Mendoza and Thomas 2007), consistent with observed crosslinking between the TMDs (Chen et al. 2004). The ICLs form a helical bundle extending into the cytoplasm with the coupling helix at the distal end (Mendoza and Thomas 2007). The surface formed between the NBD and ICL1 coupling helix is a mix of hydrophobic and hydrophilic interactions, whereas the surface formed by ICL2 is largely hydrophobic (Mendoza and Thomas 2007). During TMD1 translation, the TM and ICL regions that form later interdomain interactions are present for minutes until interaction partners are produced. These regions contain hydrophobicity that is unlikely to be stable without structure or other protein interactions in the cytosol. It is not known if ICL structure is formed in TMD1, or what happens to the coupling helices during this transient stage of CFTR biogenesis.

CF-associated mutations within the TMs and ICLs of TMD1 (www.genet.sickkids.on.ca) could provide further insight into this fundamental process. Many of these mutations introduce charge into the hydrophobic TM spans, and are thereby predicted to disrupt TMD1 structure (Cheung and Deber 2008). In TM1, the CF-causing G85E and G91R mutations result in accumulation of CFTR in the ER (Chapter 2). These mutants maintain normal CFTR TM1 topology and multidomain constructs containing the mutations have reduced stability (Xiong et al. 1997). Despite these similarities, it is clear their molecular pathologies are different which is reflected in the ability of the cell to distinguish these mutations. The G85E mutant destabilizes

the TM1 span in the ER membrane, producing an early defect for cellular recognition (Chapter 2). Whereas the G91R mutant did not measurably destabilize TM1 (Chapter 2), it causes disruption of multiple domains in the full-length CFTR (Du and Lukacs 2009). Whether G85E and G91R alter folding as reflected in recognition by the cellular machinery within TMD1 alone or only in multidomain constructs has not been determined.

In TMD1, several additional CF-associated mutations have been identified within ICL1 and ICL2, with most residing in the helical bundle that extends into the cytoplasm and a few near the coupling helices (www.genet.sickkids.on.ca)(Seibert et al. 1997). CF-associated mutations within ICL3 are similarly distributed (Seibert et al. 1996b). By comparison, ICL4 contains far more CF-mutations (Cotten et al. 1996; Seibert et al. 1996a). Whereas ICL4 interacts with NBD1 near the position of F508, this interface may be particularly sensitive to perturbation.

Based on a homology model, the predicted ICL1 and ICL2 contain residues 141 to 194 and 242 to 307 respectively (Mendoza and Thomas 2007). Within these sequences, four disease-causing mutations inhibit maturation of CFTR (H139R, G149R, D192G, and R258G) and two reduce CFTR function (G178R and E193K) (Seibert et al. 1997). Only the G178R mutation is near the coupling helix. The coupling helices are vital for membrane-cytoplasmic domain interfaces important for CFTR channel function and gating (He et al. 2008). In this regard, deletion of nineteen residues including the ICL2 coupling helix resulted in CFTR accumulation in the ER, and not surprisingly, altered channel function (Xie et al. 1995).

The homology models and crosslinking studies support that ICL2 interactions with NBD2 and ICL1 interactions with NBD1 and NBD2 occur (He et al. 2008). Phosphorylation-dependent interactions between NBD1 and an ICL1 peptide are also observed (Kanelis et al. 2010). Specific residues have been predicted to be critical for these interactions, including Y275

and W277 which form an interface with NBD2 (He et al. 2008; Mornon et al. 2008); D173,S169, and R170 which are predicted to contact nucleotide and NBD1 (Mornon et al. 2008); and S263 and E267 which stabilize ICL helical bundle structure (Mornon et al. 2009). Notably, the W277 position is equivalent to the R1070 position in ICL4 (Mornon et al. 2008) that when mutated, R1070W, suppresses the ΔF508 mutation (Thibodeau et al. 2010). However, the predicted requirement of these positions in the hierarchical folding and maturation of CFTR has not been experimentally tested.

In this study, full length CFTR containing CF-causing mutations in TM1 and basic residue mutations in the ICL1 and ICL2 coupling helices were examined. Biogenic intermediates were utilized to determine the domains required for the mutant effect elaboration.

RESULTS

Mutations in TMD1 alter CFTR cellular trafficking

TMD1 is an integral membrane domain and thus contains regions in the cytosol, ER membrane, and ER lumen during CFTR translation. Positions in TM1, ICL1, and ICL2 known to disrupt CFTR folding or with predicted locations near the ICL coupling helices were perturbed by introduction of charge. The positions selected are mapped onto the homologous Sav1866 structure (Figure 3.1A). The CF-causing mutations, G85E and G91R, are located in TM1. The G178K, M265R, and W277R CF-associated mutations are in ICL1 and ICL2, and predicted to introduce a basic residue close to the coupling helices (www.genet.sickkids.on.ca). The coupling helices for CFTR were modeled by aligning the sequences of the homologous exporter structures, and selecting residues in CFTR utilizing the Sav1866 structure (Figure 3.1B). The mutated positions within CFTR and respective positions in other transporters are highlighted (Figure 3.1B). Positions were mutated to a basic amino acid residue, lysine or arginine.

The TM1, ICL1, and ICL2 mutations were introduced into full length CFTR, transiently transfected in HEK293 cell culture, and CFTR maturation monitored by Western blot analysis (Figure 3.1C). The progression of CFTR as it traffics in the cell is reflected by the glycosylation status of two natural N-linked glycosylation sites in TMD2 that become core glycosylated in the ER (Band B), and are then modified by complex glycosylation in the Golgi (Band C). The ΔF508 mutation accumulates in the ER as Band B and is monitored as a control that does not efficiently mature. The CF-causing TM1 mutants, G85E and G91R, also accumulate in the ER, indicated by the presence of Band B. Mutations at the test positions are all integrated into the ER and mature at a variety of efficiencies as compared to WT. G85E, G91R, ΔF508, S168K,

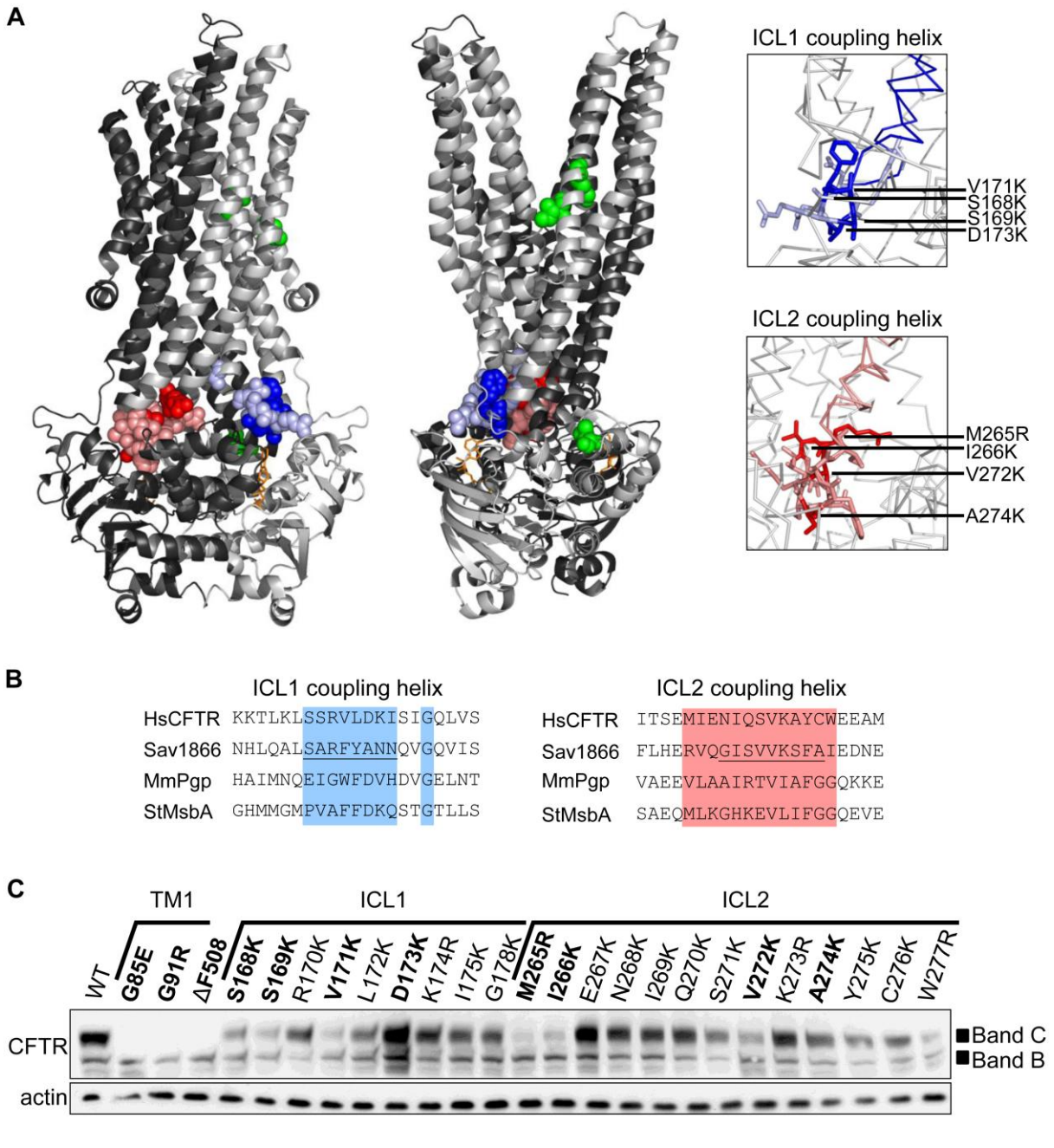

Figure 3.1. *(Figure legend continued on next page)*

Figure 3.1. TMD1 mutant effects on full length CFTR cellular trafficking. **A.** The selected mutations for study are mapped onto the Sav1866 structure (pdb 2HYD). Sav1866 is a homodimer, and each protein unit is colored with light gray representing CFTR TMD1 and NBD1 and dark grey representing CFTR TMD2 and NBD2. Respective CFTR mutation positions are shown as spheres for TM1 and ΔF508 (green), ICL1 (light blue), and ICL2 (light red). A view down the axis of the ICL1 and ICL2 coupling helices are shown with the protein backbone as a ribbon and mutated residues as sticks. Within ICL1 and ICL2, mutants selected for further study are more darkly colored blue or red. **B.** Alignments of human CFTR with ABC exporters with solved structures was performed using ClustalW software and sequences for *H. sapiens* CFTR, *S. aureus* Sav1866, *M. musculus* P-glycoprotein, and *S. typhimurium* MsbA (UniProt accession numbers: P13569, Q99T13, P21447, and P63359). The screened mutant positions in CFTR and respective positions in other transporters are highlighted blue for ICL1 and red for ICL2. The coupling helix for Sav1866 is underlined. **C.** TMD1 mutants were introduced into full length CFTR. CFTR expression and trafficking in HEK293 cell culture was monitored by Western blot analysis with antibody 596. Band B is core glycosylated CFTR in the ER and Band C has been complex glycosylated in the Golgi. The mutants selected for further studies are bolded. The ΔF508 mutation accumulates in the ER and was monitored as a control, as was actin.

S169K, V171K, M265R, I266K, V272K, D173K, and A274K were chosen for further study because they matured inefficiently or were predicted to be positioned directly in the ICL-NBD interfaces.

Generation of CFTR biogenic intermediates

TMD1 forms interactions with all other domains in CFTR homology models (Mendoza and Thomas 2007). CFTR structure forms cotranslationally (Kleizen et al. 2005), and multidomain biogenic intermediates of CFTR have been used as tools to examine potential interactions that occur during this process (Xiong et al. 1997; Meacham et al. 1999). Furthermore, in the ER misfolded CFTR can be recognized by cellular quality control, resulting in its eventual degradation by the proteasome (Jensen et al. 1995; Ward et al. 1995). Thereby, mutations that perturb CFTR structure within the ER and are degraded are reflected in the cellular steady-state levels. To generate biogenic intermediates, stop codons, designated by x, were introduced after different domains based on the structural model, resulting in constructs producing residues 1-414 (TMD1x), 1-670 (NBD1x), 1-836 (Rx), and 1-1174 (TMD2x) (Figure 3.2A).

Consistent with other studies (Cui et al. 2007; Du and Lukacs 2009), the full length and TMD2x constructs traffic from the ER and are complex glycosylated in the Golgi (Figure 3.2B). The TMD1x, NBD1x, and Rx constructs do not contain the natural N-linked glycosylation sites. Trafficking of these constructs was monitored using a previously described reporter glycosylation site introduced in extracellular loop 1 (Chapter 2). As expected, the TMD1x, NBD1x, and Rx constructs are core glycosylated, but not complex glycosylated, indicating integration into the ER membrane but inefficient trafficking to the Golgi and attendant

A

Construct	Residues	Domains
Full Length	1-1480	TMD1-NBD1-R-TMD2-NBD2
TMD2x	1-1174	TMD1-NBD1-R-TMD2
Rx	1-836	TMD1-NBD1-R
NBD1x	1-670	TMD1-NBD1
TMD1x	1-414	TMD1

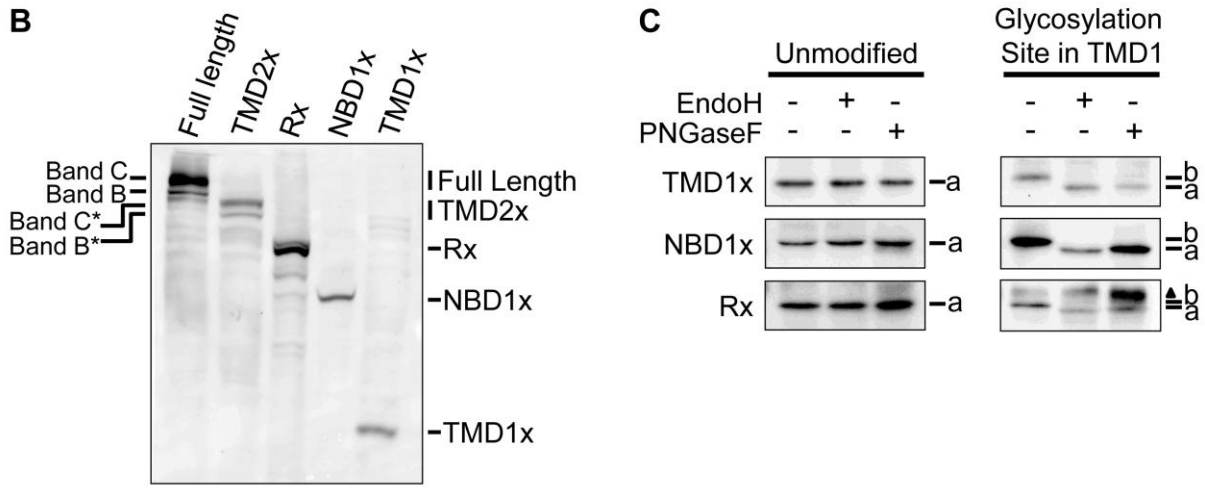

Figure 3.2. CFTR biogenic intermediates that would be generated during translation were produced by introducing stop codons after TMD1x (1-414), NBD1x (1-670), Rx (1-836), and TMD2x (1-1174). **A.** A table lists the biogenic intermediates and CFTR residues and domains therein. **B.** Full length CFTR (1-1480) and biogenic intermediates were transiently expressed in HEK293 cells and monitored by Western blot analysis with mixed CFTR antibodies 570 and MM13-4. TMD2 contains the two natural glycosylation sites for monitoring cellular trafficking of CFTR. Full length Bands B and C and 1174x core glycosylated Band B* and complex glycosylated Band C* are indicated. **C.** A core glycosylation site introduced into TMD1 was used to monitor the glycosylation pattern of TMD1x, NBD1x, and Rx. Unmodified biogenic intermediates or biogenic intermediates with the TMD1 glycosylation site were expressed in HEK293 cells and examined by treatment with glycosidase followed by Western blot analysis with MM13-4 antibody. Glycosidase treatment was performed with EndoH to remove core glycosylation and PNGaseF to remove both core and complex glycosylation. The positions of core glycosylated (b) and non-glycosylated (a) constructs are noted. Unrelated background in the TMD1 glycosylation site Rx sample is designated by a triangle.

accumulation in the ER (Figure 3.2B,C). Consistent with this result, similar biogenic intermediates co-localize with the ER resident protein calnexin (Du and Lukacs 2009).

Mutant specific effects in TMD1

TMD1 forms a protease resistant structure during translation (Kleizen et al. 2005). Mutations within TMD1 could alter this structure immediately or during later folding steps, or mutations can alter interactions with other domains or proteins. Constructs containing different C-terminal residues after TMD1 were generated by placing stop codons after residues 354 (354x), 388 (388x), and 414 (414x) to include all of TM6, an additional linker region, and the N-terminal residues of NBD1 respectively (Figure 3.3A). Steady state levels of transiently transfected constructs in HEK293 cells were examined by Western blot analysis for wild type and G85E mutant protein (Figure 3.3B). The wild type 388x and 414x constructs have higher steady-state levels than the 354x construct, suggesting the latter is less stable (Figure 3.3B). The G85E mutation reduces the levels of the 388x and 414x constructs, indicating the G85E mediated reduction in TMD1 does not require the additional NBD1 residues in the 414x construct (Figure 3.3B). The 354x construct expresses at low levels for both wild type and G85E, suggesting the C-terminus of this construct is too close to the membrane for efficient TMD1 folding (Figure 3.3B).

All of the selected mutations were examined in the TMD1x biogenic intermediate containing residues 1-414 (Figure 3.4A). Steady state levels of transiently transfected constructs in HEK293 cells were examined by Western blot analysis, quantified, and normalized to wild type TMD1 levels (N=4, SEM) (Figure 3.4B). Both CF-causing mutants, G85E and G91R, have reduced steady-state levels with respect to wild type. Only the mutant D173K, which replaces a

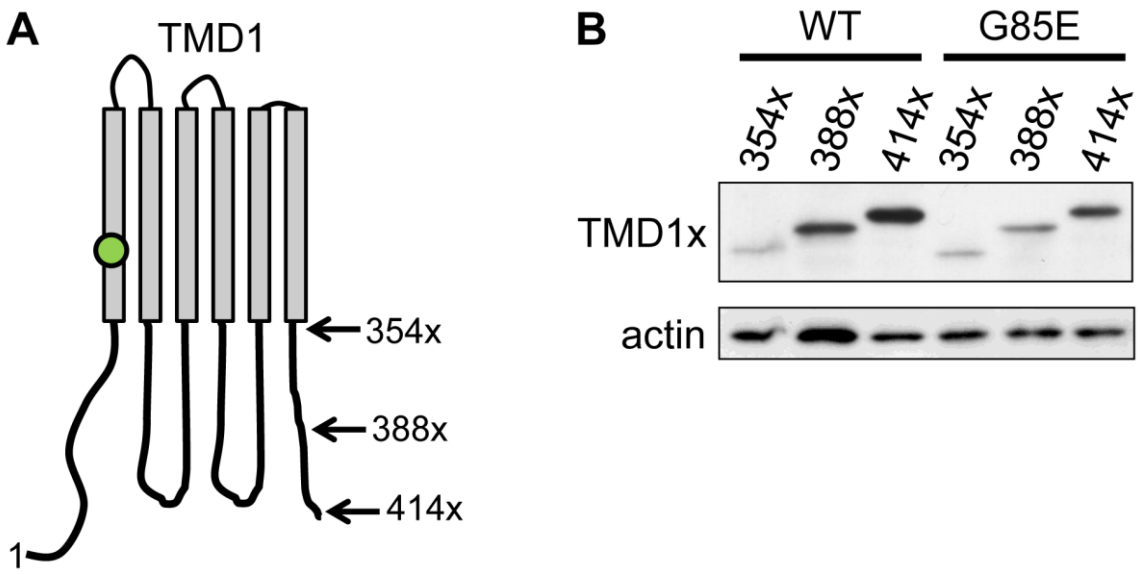

Figure 3.3. TMD1 C-terminal boundary mapping. **A.** A schematic of the TMD1 C-terminal stop codon placement after TM6 (354x), after the linker region (388x), or including N-terminal NBD1 residues (414x) is depicted with the position of G85E indicated (green circle). **B.** Wild type (WT) and G85E constructs were transiently transfected into HEK293 cells and monitored by Western blot analysis with the antibody MM13-4, with actin as a loading control.

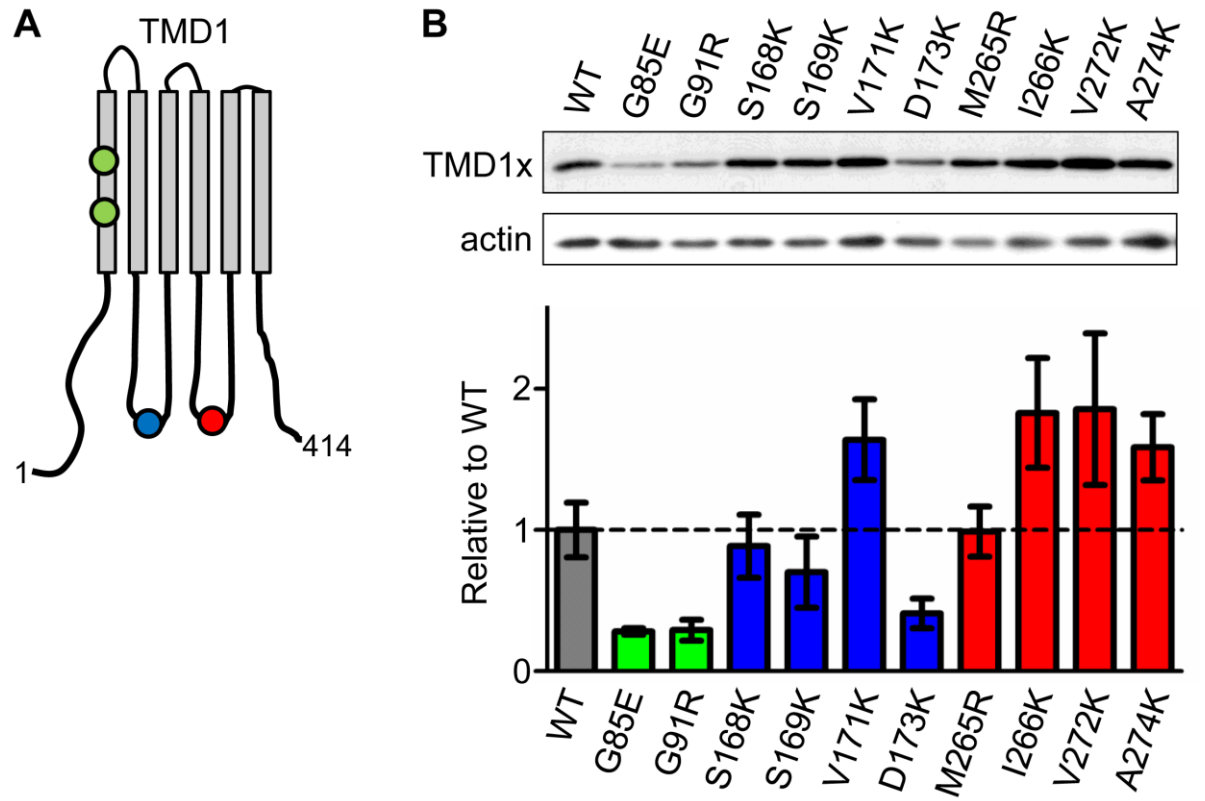

Figure 3.4. TMD1 mutant analysis in the TMD1x biogenic intermediate. **A.** A schematic of the residues in the TMD1x construct (1-414) depicts the six transmembrane spans, ER luminal, and cytosolic regions. The approximate locations of mutants in TM1 (green circles), ICL1 (blue circle), and ICL2 (red circle) are marked. **B.** TMD1x constructs containing the noted mutation were transiently transfected into HEK293 cells and monitored by Western blot analysis with the antibody MM13-4. CFTR steady-state levels were quantified and normalized to wild type with the average and the standard error of the mean plotted (N=4). TM1 mutants are green, ICL1 mutants are blue, and ICL2 mutants are red. Actin was monitored as a loading control.

negatively charged with a positively charged residue, decreases the steady-state TMD1x similar to the CF-causing mutations. Mutations that replace a polar residue with a positively charged residue had no effect on steady-state TMD1x. By contrast, mutants that replace a hydrophobic residue with a positively charged residue resulted in an increase in steady-state levels of TMD1x. This suggests that hydrophobicity in the ICL loops has an impact on the stability of TMD1 in the cell. Most strikingly, mutant effects on TMD1 do not match those observed in full length CFTR, suggesting other domains are required before structural perturbations caused by these mutants become apparent.

Mutant effects in the presence of NBD1 and the R domain suggest no stable interdomain intermediates

In CFTR, interdomain interactions between the ICLs and NBDs are essential for forming the fully functional structure. The first opportunity for predicted interdomain interactions to occur, and therefore to be perturbed by mutants, is after the first two domains, TMD1 and NBD1, have been translated and folded. If no interdomain interactions occur at this early state, ICL1 mutant effects in TMD1x should be the same as in NBD1x. The CF-causing and ICL mutants were examined in the NBD1x construct containing residues 1-670 of CFTR (Figure 3.5A). Steady-state levels of this construct were monitored after transient transfection in HEK293 cells by Western blot analysis (N=4, SEM) (Figure 3.5B). The CF-mutants G85E and G91R continue to be recognized by cellular quality control preferentially as compared to wild type, indicating NBD1 does not rescue nor amplify the defect. Similarly, V171K and I266K have increased levels as compared to wild type in NBD1x, suggesting that introduction of a basic residue at sites normally apolar continues to increase steady-state levels. All other mutants had NBD1x levels

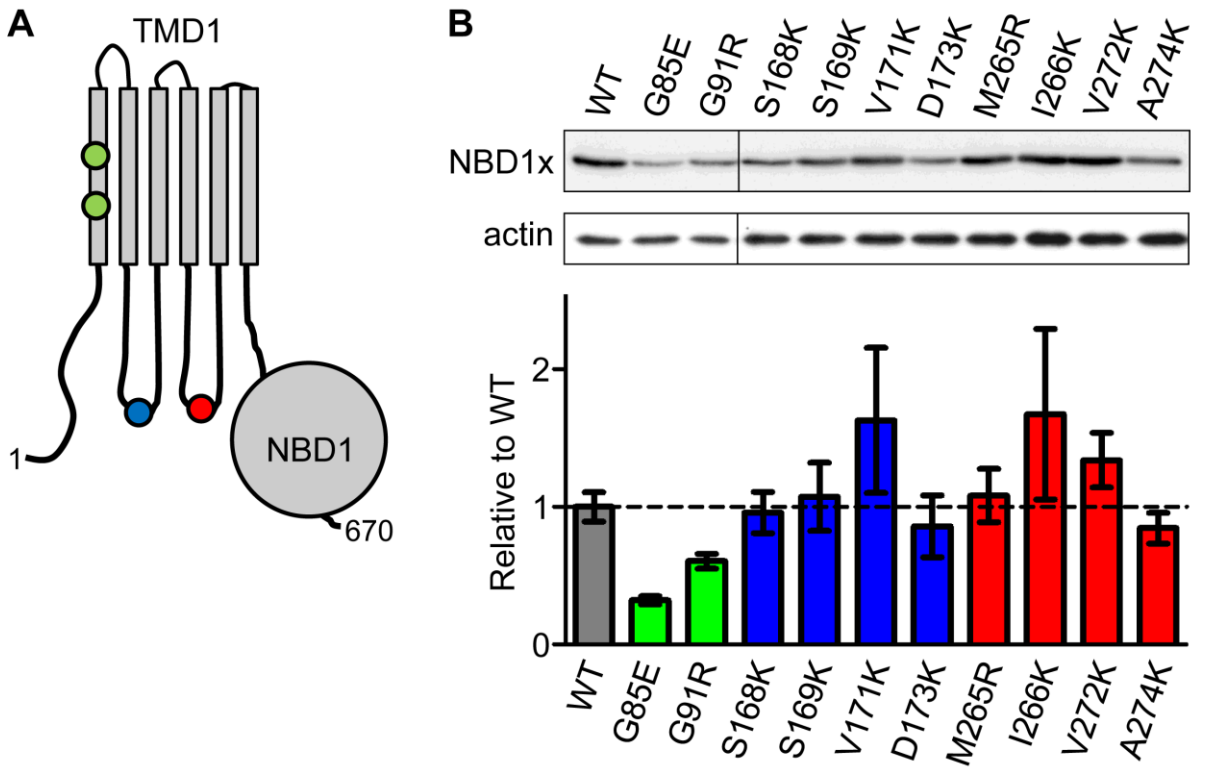

Figure 3.5. TMD1 mutant analysis in the NBD1x biogenic intermediate. **A.** A schematic of the residues in the NBD1x construct (1-670) depicts TMD1 and NBD1. The approximate locations of mutants in TM1 (green circles), ICL1 (blue circles), and ICL2 (red circles) are marked. **B.** NBD1x constructs were transiently transfected into HEK293 cells and monitored by Western blot analysis with the antibody MM13-4. CFTR steady-state levels were quantified and normalized to wild type with the average and the standard error of the mean plotted (N=4). TM1 mutants are green, ICL1 mutants are blue, and ICL2 mutants are red. Actin was monitored as a loading control.

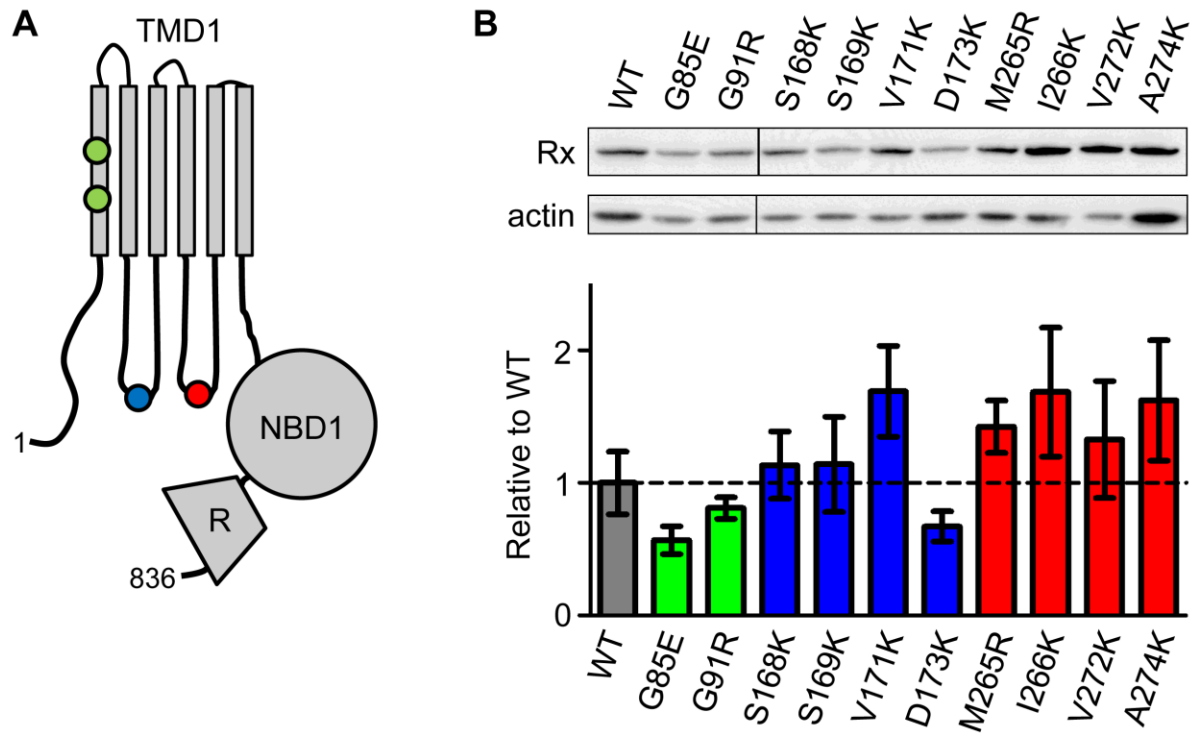

Figure 3.6. TMD1 mutant analysis in the Rx biogenic intermediate. **A.** A schematic of the residues in the Rx construct (1-836) depicts TMD1, NBD1, and R. The approximate locations of mutants in TM1 (green circles), ICL1 (blue circles), and ICL2 (red circles) are marked. **B.** Rx constructs were transiently transfected into HEK293 cells and monitored by Western blot analysis with the antibody MM13-4. CFTR steady-state levels were quantified and normalized to wild type with the average and the standard error of the mean plotted (N=4). TM1 mutants are green, ICL1 mutants are blue, and ICL2 mutants are red. Actin was monitored as a loading control.

close to or the same as wild type, suggesting NBD1 is not altering the ability of TMD1 to be distinguished by cellular quality control.

The R domain of CFTR provides additional potential interaction surfaces for a biogenic intermediate. In other studies, biogenic intermediates truncated after the R domain had a longer half-life than shorter constructs both in cell culture and *in vitro*, suggesting increased stability of this construct (Xiong et al. 1997; Meacham et al. 1999). The CF-causing and ICL mutants were examined in the Rx construct containing residues 1-836 of CFTR (N=4, SEM) (Figure 3.6A). The effects of each different mutant are consistent with the impact of the TMD1x and NBD1x constructs (Figure 3.6B). Therefore, the R domain does not alter the stability of the mutants as compared to wild type.

Effects of mutants at interdomain interfaces are elaborated upon production of TMD2

A CFTR biogenic intermediate containing the first four domains, TMD1-NBD1-R-TMD2, forms a trafficking competent structure as monitored by glycosylation of sites in TMD2 (Cui et al. 2007; Du and Lukacs 2009). The TM1, ICL1, and ICL2 mutations were examined in a TMD2x construct containing residues 1 to 1174 of CFTR (Figure 3.7A). The CF-causing mutants G85E and G91R accumulate in the ER in the TMD2x construct (Figure 3.7B). Misfolding of most ICL mutants is now evident as accumulation in the ER (Figure 3.7B). This is a striking difference from the effect of these mutants on steady-state levels of the TMD1x, NBD1x, and Rx constructs, suggesting that lack of stable interdomain interactions only becomes apparent in the presence of TMD2. The D173K, V272K, and A274K mutants traffic like wild type in TMD2x (Figure 3.7B). Interestingly, the effect of D173K on steady-state levels was

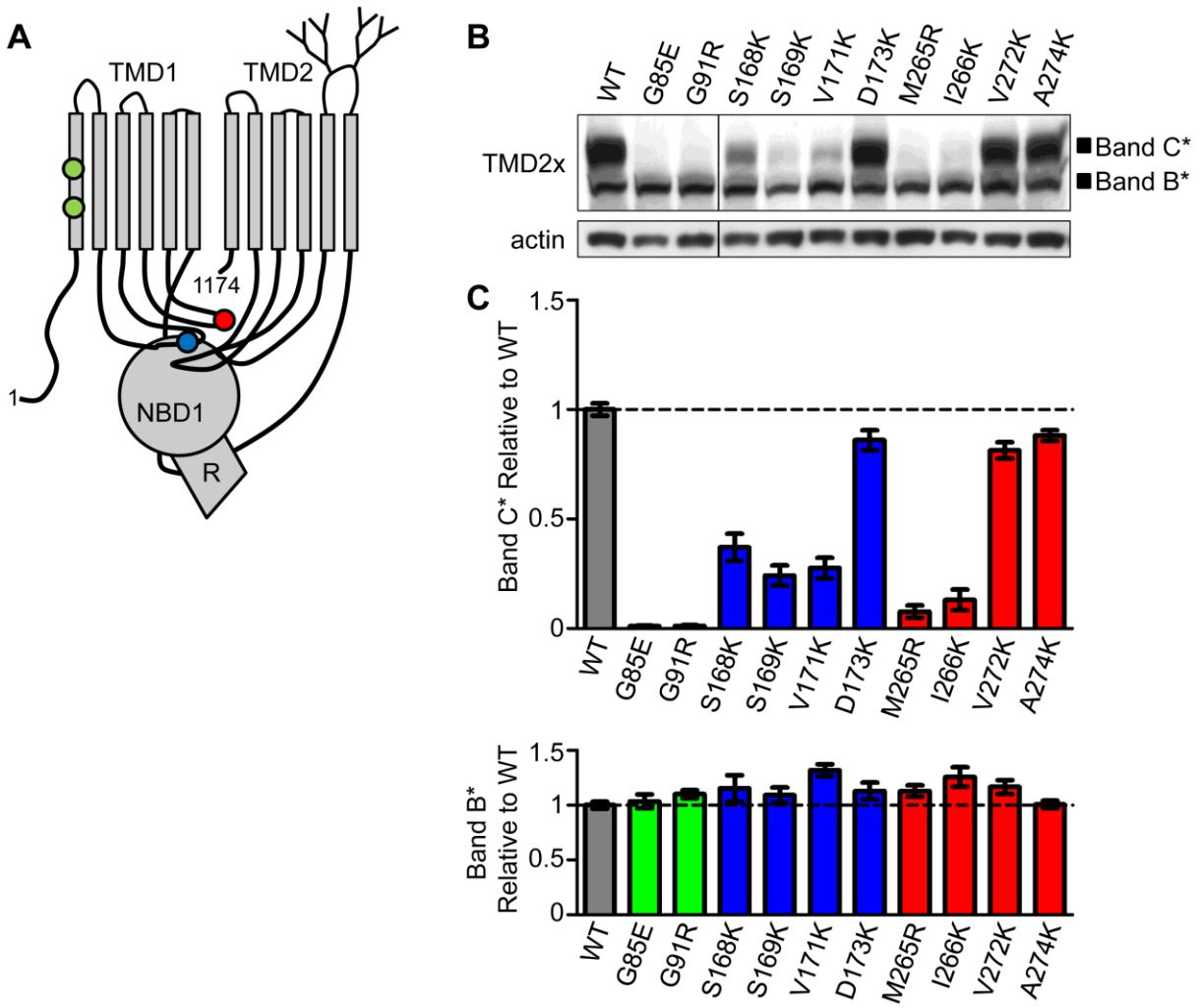

Figure 3.7. TMD1 mutant analysis in the TMD2x biogenic intermediate. **A.** A schematic of the residues in the TMD2x construct (1-1174x) depicts TMD1, NBD1, R, and TMD2. The approximate locations of mutants in TM1 (green circles), ICL1 (blue circles), and ICL2 (red circles) are marked. **B.** TMD2x constructs were transiently transfected into HEK293 cells and monitored by Western blot analysis with the antibody 570. CFTR steady-state levels of Band B* and Band C* were quantified and normalized to wild type. The average is plotted with the standard error of the mean (N=4). TM1 mutants are green, ICL1 mutants are blue, and ICL2 mutants are red. Actin was monitored as a loading control.

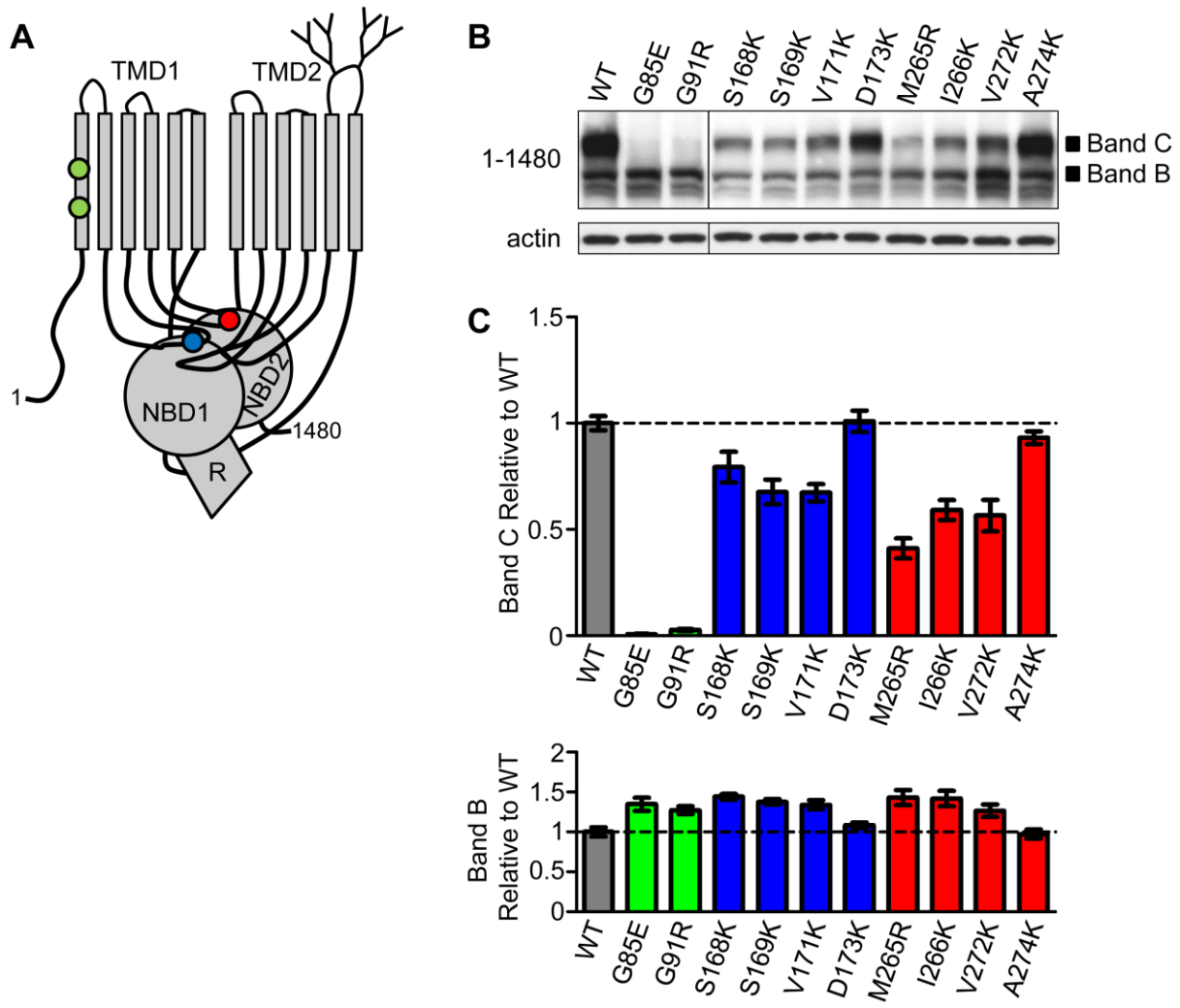

Figure 3.8. TMD1 mutant analysis in full length CFTR. **A.** A schematic of full length CFTR (1-1480) depicts TMD1, NBD1, R, TMD2, and NBD2. The approximate locations of mutants in TM1 (green circles), ICL1 (blue circles), and ICL2 (red circles) are marked. **B.** Full length constructs were transiently transfected into HEK293 cells and monitored by Western blot analysis with the antibody 596. CFTR steady-state levels of Band B and Band C were quantified and normalized to wild type levels. The average is plotted with the standard error of the mean (N=4). TM1 mutants are green, ICL1 mutants are blue, and ICL2 mutants are red. Actin was monitored as a loading control.

more dramatic in TMD1x, NBD1x, and Rx than in TMD2x, consistent with increased stability of this intermediate due to domain association.

NBD2 contributes to stabilization of CFTR

Full length, functional CFTR contains all possible interdomain interactions. The selected mutants were quantified in the full length construct containing residues 1-1480 of CFTR (Figure 3.8A). The CF-causing mutants, G85E and G91R, accumulate in the ER, and have very low levels of Band C as compared to wild type (Figure 3.8B). The D173K and A274K mutants have similar levels of Band C as compared to wild type. In full length, most other mutants had an improved efficiency of trafficking as compared to wild type, consistent with NBD2 conferring stabilization and improved trafficking of CFTR in the cell. The V272K mutant has a measurable effect on the trafficking of the full length protein not observed with the TMD2x construct The V272 position is centrally located within the coupling helix of ICL2. As ICL2 forms major interactions with NBD2, this mutant likely disrupts ICL2 structure required for this interaction and, thus, the effect of V272K only becomes apparent in the presence of NBD2.

Lower temperature confers no benefit to the TMD1 mutants

The ΔF508 full length protein misfolding is temperature sensitive. Incubation at reduced temperatures partially rescues ΔF508, allowing some to traffic from the ER. To test whether reduced temperature can improve maturation of the ICL mutant proteins, the TMD2x and full length constructs were transiently transfected in HEK293 cells, expressed for 24 hours at 37°C, and transferred to 30°C for 24 hours prior to analysis. Lower temperature increased the ΔF508

full length, but conferred no benefit to trafficking of any mutant in TMD2x nor other mutants in full length.

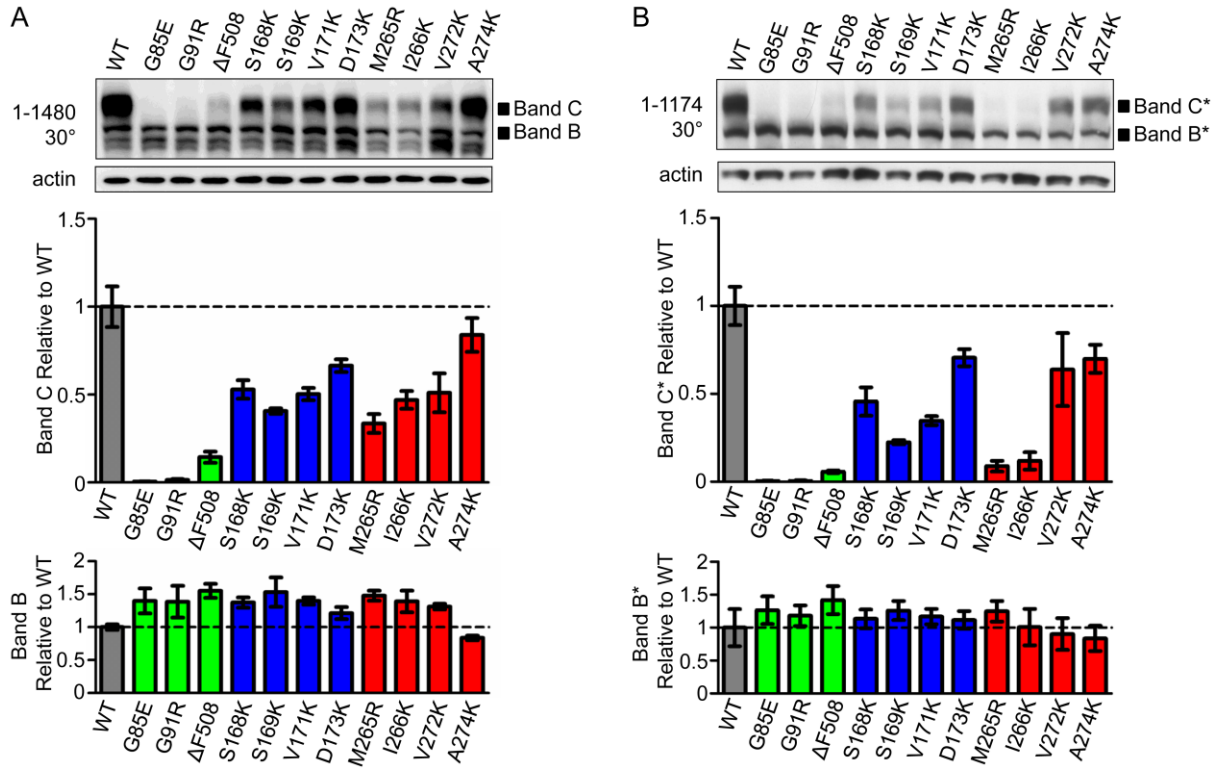

Figure 3.9. Low temperature trafficking of TMD1 mutants in full length or TMD2x. Constructs were transiently transfected into HEK293 cells, expressed at 37°C for 24 hours and moved to 30°C for 24 hours. **A.** Full length construct cellular trafficking was monitored by Western blot analysis with the antibody 596. Steady-state levels of Band B and Band C were quantified and normalized to wild type. The average is plotted with the standard error of the mean (N=3). **B.** TMD2x construct cellular trafficking was monitored by Western blot analysis with the antibody 570. Steady-state levels of Band B* and Band C* were quantified and normalized to wild type. The average is plotted with the standard error of the mean (N=3). TM1 mutants and ΔF508 are green, ICL1 mutants are blue, and ICL2 mutants are red. Actin was monitored as a loading control.

DISCUSSION

These studies provide insight into the molecular pathology of CF-causing mutants within TMD1 and into the role of the ICLs, particularly the coupling helices, in formation of CFTR structure. A rich database of mutations, both CF-associated and polymorphisms, has been generated by sequencing (www.genet.sickkids.on.ca). Mutants have been found throughout TMD1, with many associated with disease introducing charge into the TM spans (Cheung and Deber 2008) or the ICLs (Seibert et al. 1997). More CF-causing mutants have been identified in ICL1 than in ICL2. Of these, very few are near the coupling helices, suggesting that either mutations in these regions do not result in CF or are simply not represented in the database. Consistent with the first interpretation, the experimental introduction of basic residues in these helices did not have profound impacts on folding.

The ICL coupling helices play key roles in CFTR function (He et al. 2008) and folding. The interaction of ICL4 with ΔF508-NBD1 has been shown to directly affect ΔF508-CFTR maturation (Thibodeau et al. 2010). Additionally, in the yeast Yor1p ABC transporter, a deletion mutation mimicking ΔF508 is partially corrected by a combination of two suppressor mutations located at TM-ICL junctions (Pagant et al. 2010). Therefore, a better understanding of how TMD1 is formed and how it interacts with other domains is likely to be important for identifying and characterizing novel mechanisms to correct misfolded CFTR, including ΔF508.

CFTR is monitored by protein folding and quality control proteins during translation (Younger et al. 2006). Quality control involves a protein complex containing the E3 RMA1, E2 Ubc6e, and Derlin-1 that cooperates with the Hcs70/CHIP E3 complex to monitor CFTR structure (Meacham et al. 1999; Meacham et al. 2001; Younger et al. 2004; Younger et al. 2006).

Specifically, the RMA1 complex interactions involve more N-terminal regions and CHIP interactions occur as and after C-terminal regions are produced (Younger et al. 2006). In a hierarchical folding process, the TMD1 mutants in both TM spans and cytosolic ICLs studied here are likely to perturb CFTR structure and be recognized by quality control at different times.

The G85E and G91R mutations in TM1 are mistrafficked and degraded, and *in vitro* work suggests the recognition occurs in multidomain constructs (Xiong et al. 1997). This study shows that the effects of both mutants become apparent in mammalian cells within TMD1, prior to the production of any other domains (Figure 3.10). The G85E mutant CFTR has been shown to be degraded after recognition by the Derlin-1 associated cellular quality control machinery, early during biogenesis (Sun et al. 2006; Younger et al. 2006; Wang et al. 2008a). Derlin-1 mediates the retro translocation and ER-associated degradation of misfolded proteins (Lilley and Ploegh 2004; Ye et al. 2004). Thereby, TMD1 alone likely contains structural signals for the recognition and degradation of the G85E mutant by this machinery, possibly related to the destabilization of TM1 by the mutant (Chapter 2). The G91R mutant CFTR alters cellular trafficking by introduction of arginine at position 91 (Chapter 2)(Xiong et al. 1997), and responds to decreased levels of the RMA1 E3 ubiquitin ligase, which is associated in a complex with Derlin-1 (Younger et al. 2006). This mutation also effects TMD1 stability, suggesting that it, like G85E, produces changes within TMD1 that are recognized by the quality control complex. Of course, loss of appropriate TMD1 structure caused by the G85E and G91R mutants would be expected to propagate to other domains and thus be evident in full length CFTR and the stability of its component domains. Consistent with this, the G91R mutant destabilizes all domains in the full length CFTR (Du and Lukacs 2009).

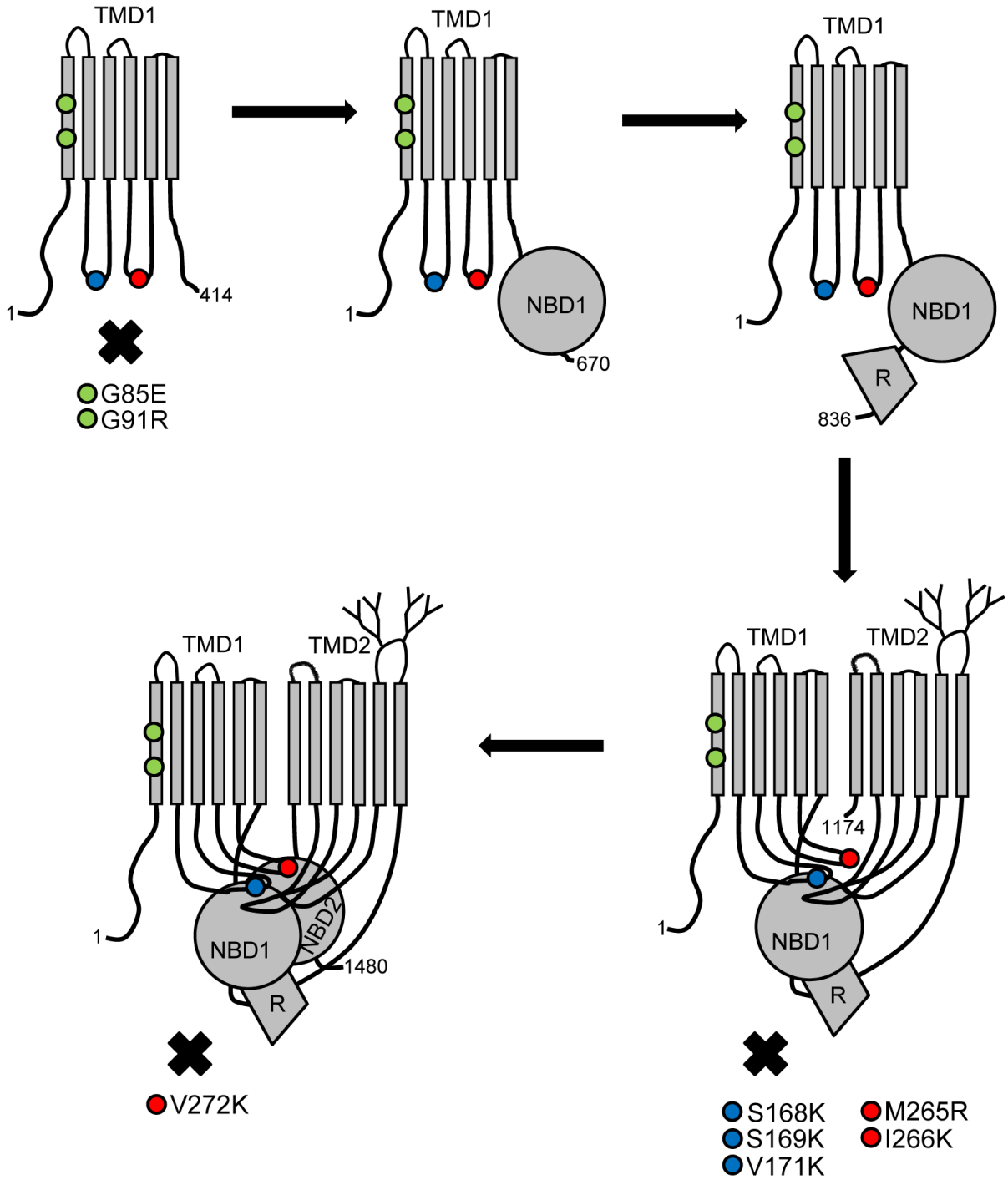

Figure 3.10. A schematic depicting the CFTR biogenic intermediates as they would occur during translation. Below each biogenic intermediate, an X denotes the initial intermediate in which that mutant reduces the steady-state level as compared to wild type.

A proteolytically protected TMD1 structure is formed during translation (Kleizen et al. 2005). In this study, G85E mediated TMD1 perturbations were observed in the 414x and 388x constructs, but not in the 354x construct truncated near the predicted C-terminal end of TM6. Earlier *in vitro* studies demonstrated that if TMD1 is truncated at position 364, TM6 is improperly integrated and translocated into the ER lumen (Tector and Hartl 1999). TM6 contains several basic residues related to formation of the CFTR pore (Cheung and Akabas 1996), making its *in vitro* integration inefficient (Tector and Hartl 1999). Marginally hydrophobic TM spans were found to integrate much more efficiently in the presence of flanking regions and other TM spans (Hedin et al. 2010). This suggests that the presence of residues in the linker region after TM6 may be required for its appropriate insertion in the membrane, and therefore formation of TMD1 structure. The reduced level of 354x TMD1 and the loss of the G85E effect suggests that this construct is unstable and is recognized and degraded in the cell, possibly by a similar mechanism to the CF-causing mutations in TM1.

The roles of ICL1 and ICL2 in CFTR folding are poorly understood. In this study, we focused on the ICL coupling helices. The coupling helices of ABC transporters are architecturally conserved without having a highly conserved sequence (Locher 2009), making prediction of essential positions and residues difficult since there is no high-resolution CFTR structure. In CFTR, the predicted interface between the coupling helices and NBDs is both hydrophilic and hydrophobic for ICL1, and largely hydrophobic for ICL2 (Mendoza and Thomas 2007). Surprisingly, in TMD1x, NBD1x, and Rx constructs, a trend for one mutant in ICL1 and three mutants in ICL2 emerged whereby replacement of a hydrophobic residue with a basic residue increased steady-state construct levels. Thereby, the wild type regions decrease the steady-state levels of these biogenic intermediates. The coupling helices are cytosolic and

located approximately 25Å away from the membrane in homologous structures (Dawson and Locher 2006). The aforementioned Hsc70/CHIP machinery is found in association with TMD1 (Meacham et al. 1999), and cooperates to target immature CFTR for degradation (Meacham et al. 1999; Meacham et al. 2001; Younger et al. 2004). As Hsc70 recognizes short hydrophobic sequences (Rudiger et al. 1997), this is a good candidate to test for direct interactions with the coupling helices. We propose that the coupling helices can be used by the cell to monitor CFTR folding, whereby if the hydrophobic residues remain exposed, the protein is eventually targeted for degradation.

The major impact of most of the positively charged ICL mutants only becomes apparent in the TMD2x construct (Figure 3.10), which is the minimal CFTR construct that can traffic from the ER (Pollet et al. 2000; Cui et al. 2007; Du and Lukacs 2009). In this construct, both TMDs are present, such that TMD rearrangements, ICL helical bundle structure, and interactions with NBD1 have likely formed. The basic residue mutants accumulate in the ER, suggesting inefficient folding related to interactions disrupted and recognized in the presence of TMD2. Interestingly, a di-acidic motif within NBD1 is important for COPII-dependent trafficking of CFTR from the ER (Wang et al. 2004). The exposure of this motif could depend on a structural rearrangement that occurs after TMD2 is produced. The results herein support a cellular mechanism for monitoring the TMD2x construct that is important for trafficking from the ER.

Based on homology models, the S168 and S169 positions are at outer edge of the coupling helix with S169 pointing into the interface. The V171 side chain is predicted to point into the helical bundle, and D173 into the interface towards the nucleotide (Figure 3.1A). Interestingly, the D173K mutation reduces levels of constructs without TMD2 and behaves more like wild type in the presence of TMD2. One possible explanation is that this position is

involved in formation of a nonnative contact that is lost in the constructs containing TMD2. In the full length CFTR basic residue screen, other positions in ICL1 also reduced CFTR levels, suggesting that perturbations in this coupling helix may be more disruptive than those in ICL2. In ICL2, very few mutants tested affected full length trafficking. Of those that do, the M265R and I266K mutants are located proximate to the coupling helix in the inner helical bundle, the V272K mutant is in the helical bundle, and the A274K mutant is in the ICL-NBD interface (Figure 3.1A). In general, alteration of side-chains predicted to point into the ICL structure rather than directly into the ICL-NBD interface was more perturbing. Thus, few individual residues in ICL1 and ICL2 have a major impact on the formation of the ICL-NBD interface, perhaps as required by its critical position for conformational changes associated with channel gating. A similar finding occurs for binding of the human growth hormone receptor to growth hormone, whereby few residue mutations in the protein interface alter binding affinity (Clackson and Wells 1995). This results from the interface ability to alter binding energetics (Pearce et al. 1996) and remodel (Atwell et al. 1997) to maintain similar binding, which could relate to the described observations for CFTR ICL-NBD interactions.

All lysine mutants, with the exception of D173K, A274K, and V272K, trafficked more efficiently in full length as compared to wild type than in the TMD2x construct. The addition of NBD2 confers a greater folding efficiency and trafficking from the ER for the mutants. Thus, although NBD2 is not strictly required for CFTR trafficking (Pollet et al. 2000; Cui et al. 2007; Du and Lukacs 2009; Thibodeau et al. 2010), its posttranslational association into the CFTR structure (Du et al. 2005) imparts stability to the other domains.

Consistent with the prediction that ICL2 interacts mainly with NBD2, the V272K mutant lowered the efficiency of trafficking as compared to wild type in the full length construct (Figure

3.10), more dramatically than in constructs lacking NBD2. This suggests that V272 stabilizes the ICL2-NBD2 interface, as predicted by its conservation in the ABC exporter sequence alignment. In CFTR homology models, V272 points up between the two helical stems, directly supporting ICL structure rather than the ICL2-NBD2 interface itself. The equivalent position in ICL4, L1065, is associated with CF when mutated to proline. L1065P accumulates in the ER and reduces iodide efflux (Cotten et al. 1996; Seibert et al. 1996a). The behavior of CFTR containing mutants in ICL1 and ICL2 provides insight into general properties of the ICLs that may be perturbed by CF-causing mutations. Stabilization of the ICL and coupling helix structures rather than direct stabilization of the NBD/ICL interfaces should be viewed as a potential target for correction of CF-mutant CFTR owing to destabilizing mutations in multiple domains.

MATERIALS AND METHODS

Plasmids, DNA techniques

An expression plasmid of full length, wild type CFTR (pCMV-CFTR- pBQ4.7) was a gift from J. Rommens (The Hospital for Sick Children, Toronto) and was mutagenized using standard protocols for site-directed mutagenesis (Sambrook 1989). Site-directed mutagenesis was performed by PCR techniques using PfuUltra high-fidelity DNA Polymerase (Stratagene). All mutations were confirmed by DNA sequencing. In these constructs, two stop codons were introduced after amino acid residues 414, 670, or 1174. For TMD1 C-terminal truncations, stop codons were introduced after positions 414, 388, and 354 in wild type or G85E mutant CFTR generated from the pBQ4.7 CFTR cloned into a pBI bidirectional vector. For studies including the ECL1 glycosylation site, the stop codons were introduced into the designed CFTR sequence as described above.

Multiple sequence alignment

ABC transporters of the exporter type with solved structures are, *Staphylococcus aureus* Sav1866 (pdb 2ONJ and 2HYD), *Escherichia coli* MsbA (pdb 3B5W), *Vibrio cholerae* MsbA (3B5X), *Salmonella typhimurium* MsbA (3B60), and *Mus musculus* P-glycoprotein (pdb 3G5U, 3G60, 3G61). A multisequence alignment was by entering the UniProt accession numbers for these proteins into ClustalW and selected regions examined. UniProt accession numbers are *Homo sapiens* CFTR (P13569), *Staphylococcus aureus* Sav1866 (Q99T13), *Escherichia coli* MsbA (P60752), *Vibrio cholerae* MsbA (Q9KQW9), and *Salmonella typhimurium* MsbA (P63359), and *Mus musculus* P-glycoprotein (P21447). The coupling helices for CFTR were

selected based on the identified helices in the highest resolution structure, Sav1866 (Dawson and Locher 2006).

Mammalian cell protein expression

HEK293 cells (American Type Culture Collection, ATCC) were maintained in Dulbecco's Modified Eagle Medium (DMEM, Invitrogen) supplemented with 10% Fetal Calf Serum (Gemini Bio-Products), 50 μg mL^{-1} penicillin, and 50 units mL^{-1} streptomycin using standard culture techniques. CFTR constructs were transfected at 20,000 cells per mL in suspension using PEI (polyetheylenimine, Polysciences Inc.) transfection reagent, plated in 24 well plates, and expressed for 48 hours. Cell lysis was performed in RIPA buffer (20mM tris pH7.6, 150mM NaCl, 0.1% SDS, 1% IGEPAL, 0.5% deoxycholic acid, 1mg EDTA-free protease inhibitor tablet (Roche)) at 4°C, and centrifuged at 13000g's to generate cleared lysate. Sample buffer (60mM tris pH6.8, 5% glycerol, 2% SDS, bromophenol blue, 280mM β-mercaptoethanol) was added to cleared lysate and incubated at 37°C for 20 minutes.

For temperature sensitive trafficking of CFTR mutants, HEK293 cells were transfected in suspension as described and expressed for 24 hours at 37°C. The cells were then moved to 30°C for 24 hours. Lysis and protein analysis was performed as described.

Western blot analysis

SDS-PAGE analysis of full length CFTR was performed on equal volumes of lysate. Samples were transferred to PVDF Immobilon membranes (Millipore) and Western blotting performed using antibodies CFTR antibodies as described or actin antibody (Millipore). The CFTR antibody utilized for full length protein was 596 (UNC School of Medicine), for TMD2x

was 570 (UNC School of Medicine), and for TMD1x, NBD1x, and Rx was MM13-4 (AbCAM). The secondary antibody for all primary antibodies was peroxidase-AffiniPure goat anti-mouse IgG (Jackson ImmunoResearch Laboratories, Inc.). All Western blots were developed using Amersham ELCPlus Western blotting detection reagent (GE Healthcare).

Quantitation

Signal from all membranes was collected by film and using a Typhoon 9410 Variable Mode Imager (GE Healthsciences). The TMD1x, NBD1x, and Rx samples were quantified from film and the TMD2x and full length samples were quantified from Typhoon due to signal intensity. Quantification was performed using the Image J Software.

Glycosylation analysis

Glycosylation analysis of the ECL1 site was performed on HEK293 cells transiently transfected with the ECL1 site constructs, expressed for 48 hours, and lysed in RIPA buffer as described. 500U of PNGaseF (New England Biolabs) or Endoglycosidase H (New England Biolabs) was added to 40μL of cleared lysate and incubated at 37° for 2 hours. Sample buffer was added to the reaction and incubated at 37° for 20 minutes before SDS-PAGE and Western blot analysis using antibody MM13-4 (AbCAM). For each transfected construct, mock treated lysate was loaded immediately next to EndoH and PNGaseF treated lysate to detect gel shifts upon removal of glycosylation.

Chapter IV

Perspectives for the Future

Transmembrane span biogenesis and protein misfolding

TM spans are hydrophobic regions that reside within the membrane bilayer with different lengths, tilts, secondary structure, and interactions with molecules. While the hydrophobic region generally determines the membrane integrated residues, proximal residues to this region play a role in its positioning. These residues may be ionizable (von Heijne 1989; Monne et al. 1998; Hessa et al. 2005), aromatic (Braun and von Heijne 1999), and structurally perturbing residues like proline (Nilsson et al. 1998; Nilsson and von Heijne 1998). Furthermore, many TMs incorporate charge and non-membrane compatible regions into the membrane as needed for protein function. In mammals, most membrane spans of multispanning proteins are cotranslationally integrated in a dynamic process involving multiple cellular molecules (Skach 2009).

During translation, membrane spans and signal sequences undergo hydrophobic-mediated interactions with the signal recognition particle (SRP) (Keenan et al. 1998). This ribosome-nascent-chain-SRP complex interacts with the translocon in the ER membrane, which integrates or translocates the TM span or protein (McCormick et al. 2003). In the translocon, TM spans are likely selected and integrated based on hydrophobic partitioning (Mothes et al. 1997), but specific protein interactions (McCormick et al. 2003) and the requirement of ATP for the release of some TM spans (Pitonzo et al. 2009) suggests other factors also play a role.

Each membrane span undergoes this process prior to complete translation of the full length protein, and the TM span(s) behave differently to form each protein. Many pathways exist for a TM span to achieve its final structural location, including rearranging topology (Lu et al. 2000), integrating at one position and shifting (Kauko et al. 2010), and integrating and

remaining at a similar position during later stages of folding. Importantly, the function of many membrane proteins requires TM span movement within the membrane. This is true for the opening and closing of ABC exporters (Ward et al. 2007).

The CFTR TM1 has been the focus of a series of studies relating to biogenesis and span integration. Many protein interactions with TM1 during its biogenesis were observed by cotranslational crosslinking studies, which highlight its interactions with both known and unidentified proteins (A. Karamyshev, manuscript in preparation). The balances of interactions has been observed between a TM span or signal sequence and SRP or other cellular proteins (A. Karamyshev, manuscript in preparation). The role of these interactions for cellular targeting of nascent chains to different regions in the cell, such as the ER, is an ongoing and fundamental biological question. Importantly, mutations in either the TM span or signal sequence altered the balance of the interactions, suggesting a mechanism for cellular recognition of mutant nascent chains (A. Karamyshev, manuscripts in preparation). Moreover, the TM1 span of CFTR interacts inversely with SRP and a component of the N-terminal acetylation machinery (A. Karamyshev, manuscript in preparation). Studies designed to characterize the resulting influence on CFTR are ongoing. However, it is clear that a multitude of known and unknown proteins are involved in TM span biogenesis. The characterization of these components and their role in CFTR biogenesis is a focus for future studies.

These interactions play an essential role in TM1 span membrane integration for both wild type and CF mutants. As described in Chapter 2, core glycosylation analysis was utilized to identify the TM1 ER luminal boundary. Surprisingly, this boundary was determined to reside at a position significantly N-terminal to the previously predicted TM1 span. Consistent with this, the aforementioned crosslinking studies established that the C-terminal residues of the original

predicted TM1 are unnecessary for SRP-TM1 interactions (A. Karamyshev, manuscript in preparation). Taken together, these studies suggest that the biological signals for the steps leading to TM span integration, such as SRP and translocon interactions, may lie within TM1 N-terminal residues (Figure 4.1).

The CF-causing TM1 mutations, G85E and G91R, have normal topology (Xiong et al. 1997). However, both mutants have decreased TM1 crosslinking to SRP (A. Karamyshev, manuscript in preparation), suggesting that the interaction either occurs at a different position or that it does not occur. As described in Chapter 2, the G85E mutant dramatically alters TM1 within the membrane, forcing multiple ER luminal boundaries. This mutation may move the photoprobe position away from SRP or disrupt the interaction. Moreover, the studies described in Chapter 3 reveal that G85E-TMD1 and other G85E multidomain constructs are recognized and removed by the cell. It is clear from these studies that a cascade of events occurs in the presence of CF-causing mutations within TM1.

This series of data highlights the importance of biologic selection and management of the TM1 span and its relevance for CF. It may be inferred that, for example, upon translation of the G85E TM1, SRP binds improperly (A. Karamyshev, manuscript in preparation) which leads to poor translocon integration (Xiong et al. 1997). Thus, resulting in an unstable TM1 (Chapter 2) and a misfolded TMD1 (Chapter 3), which result in CFTR accumulation in the ER and its eventual degradation (Figure 4.1). This process is likely similar for G91R, however the TM1 boundary shift is small. In this case, the arginine may reside close to the membrane surface, and could anchor this TM span such that it cannot shift in the membrane. Taken together, these data highlight the multiple steps involved in CFTR biogenesis that are implicated in the molecular pathology of CF.

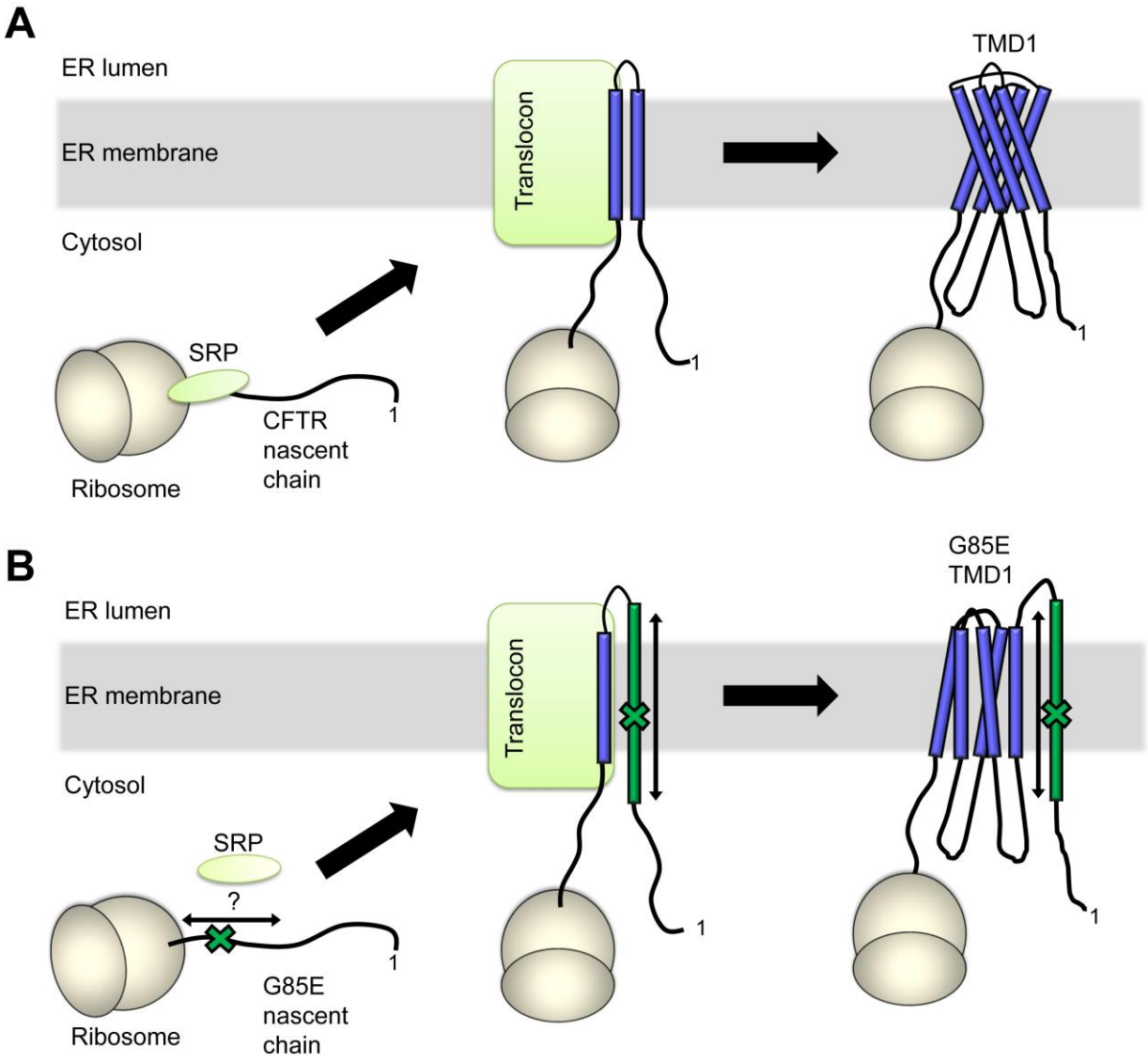

Figure 4.1 A CF-causing mutant alters TM1 span biogenesis. **A.** During translation, TM1 interacts with SRP, resulting in it being brought to the ER membrane and integrated by the translocon. As translation and integration continue, TMD1 obtains cotranslational structure. **B.** The G85E mutation is within TM1 and alters all of these processes, including interactions with SRP, TM1 placement in the ER membrane, and TMD1 structure formation. SRP interactions could be disrupted or shifted along the nascent chain. The G85E TM1 is represented with an elongated green bar with an X indicating G85E.

These data are relevant to both CF-causing mutations in CFTR and other TM spans that naturally contain 'membrane unfriendly' residues. A native TM span can sample multiple positions along a folding path as long as it forms a functional protein. Therefore, TM spans are designed for both initial cellular recognition and integration and final structural placement. The cell must avoid destroying native spans while recognizing mutant TM spans. Moreover, the cellular mechanism for recognizing and removing these misfolding events involves the Derlin-1 associated protein quality control machinery (Lilley and Ploegh 2004; Ye et al. 2004), which associates with the TM1 mutant CFTRs (Sun et al. 2006; Younger et al. 2006; Wang et al. 2008a). Further characterization of the other proteins involved in TM recognition and of the mechanisms for deciphering the cellular management of TM spans is required. Specifically, it is important to determine the cellular criteria that distinguish misfolded from native spans and spans that are merely at a transient step along a normal folding path.

TM spans are dynamically selected, integrated, shifted, and rearranged during folding, but not necessarily so in the final structure. The translational dynamic behavior produces many points where misfolding can occur, precluding formation of a functional membrane protein. Much of membrane protein based human diseases may be associated with these processes. Therefore, generating a better understanding of these basic processes can identify novel targets for therapeutic manipulation of these diseases. Due to the diversity of disease-causing mutations throughout the twelve TM spans of CFTR (Cheung and Deber 2008), it is an excellent model protein for studying these processes.

CFTR and multidomain folding

CFTR is a complex multidomain protein for which each domain obtains structure during translation, as reviewed in Chapter 3. The extensive interdomain interactions in the CFTR homology models resulted in hierarchical folding models (Kleizen et al. 2005; Thibodeau et al. 2005; Cui et al. 2007) that include domains interactions forming after each domain obtains structure (Figure 4.2). If these interdomain interactions form, they could stabilize the intermediate structure, protect exposed surfaces recognizable by the cell protein quality control machinery, or provide a scaffold for domain structure. Experimental evidence supports that the first four domains of CFTR undergo a multidomain rearrangement, since a regulated chloride channel that can traffic to the plasma membrane is formed (Cui et al. 2007). However, models predict that two and three domain hierarchical interactions also form. Though this model is appealing, little evidence exists to support domain associations prior to the translation of TMD2. This disparity may be explained by the dependence of modeling on CF-causing mutants that perturb multidomain structural units. It is clear, however, that the most highly studied mutants, specifically ΔF508, alter domain structure in a manner recognizable by the cell (Du and Lukacs 2009), convoluting the interpretation of multidomain complexes with domain effects. Future analyses of predicted models should address these specific issues.

First, it is important to consider that CFTR cotranslational interactions may be directly related to the order of domain translation. If these interactions are required sequentially for structure formation, then a linear peptide should be essential to produce folded CFTR. This can be tested by expressing CFTR as two pieces and monitoring either functional CFTR or the cellular trafficking of TMD2 by glycosylation. These experiments have been performed with the

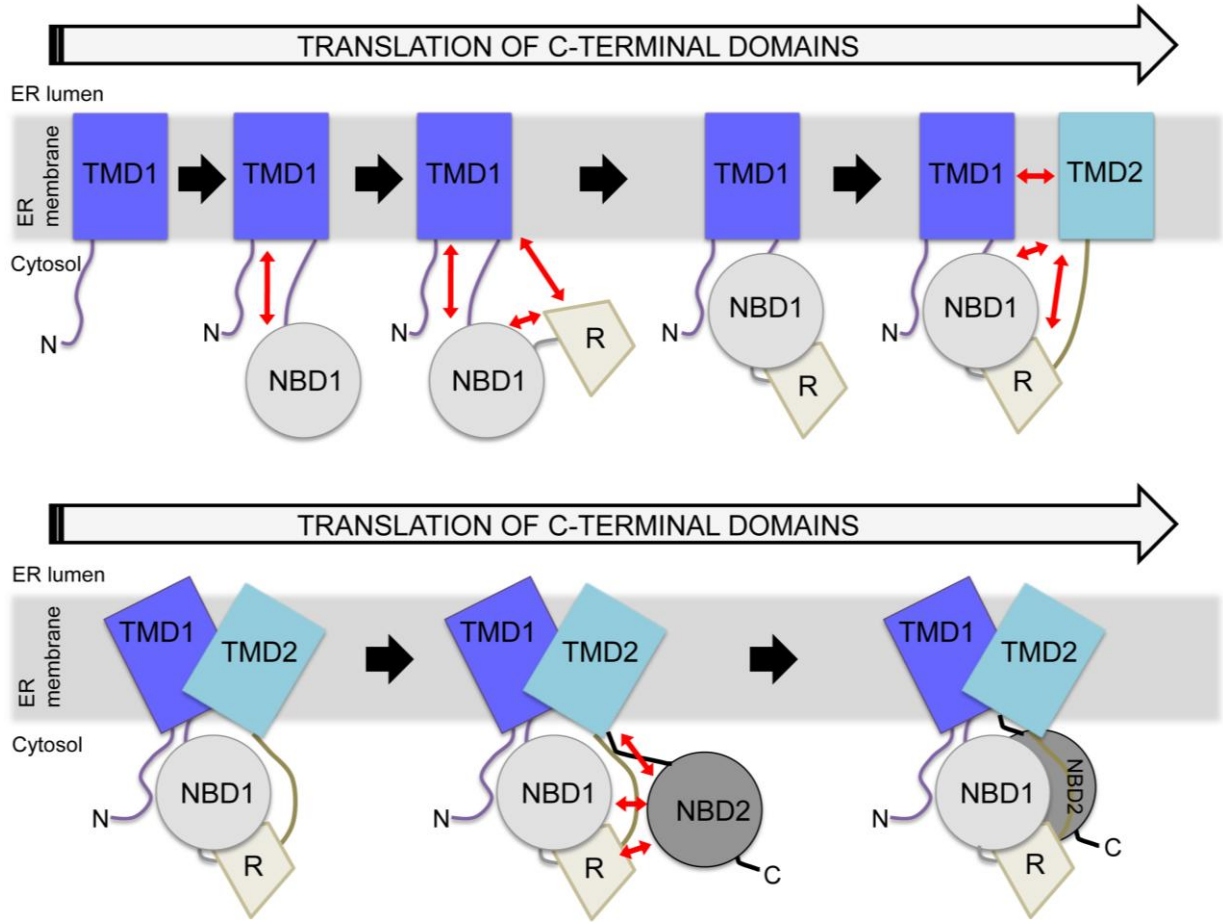

Figure 4.2. Hierarchical folding model of CFTR. Potential interdomain interactions are indicated by red arrows, with several possible structural units included during the translation process. In the cell, constructs lacking TMD2 do not traffic from the ER, whereas constructs containing TMD2 can traffic from the ER. Reflecting this, a major structural rearrangement is depicted in the presence of TMD2, as shown in the bottom panel. Eventually, NBD2 is incorporated as the final step. There are many points during this process at which the cell may monitor perturbations.

split placed at several positions, including within the NBD1 RI, after NBD1, after R, and after TMD2 (Ostedgaard et al. 1997; Chan et al. 2000; Csanady et al. 2000; Du and Lukacs 2009). As described in Chapter 3, most of these components associate and traffic from the ER. Taken together, these data suggest that a linear peptide is clearly not required for formation of functional CFTR that can traffic from the ER, however folding may be much less efficient.

The ability to split CFTR and still obtain function is consistent with other ABC transporters within which the modular formation of domain structure indicates that one domain is not required for the formation of other domains (Locher 2009). Yet, during *in vitro* refolding of the modular ABC transporter, BtuCD, refolding from partially unfolded units resulted in the highest functional measures (Di Bartolo et al. 2011). This suggests that domain interactions during folding may play a role in increasing the production of functional protein. For CFTR, these interactions could be important for generating enough functional protein to maintain normal physiology. Further analyses should examine this process and its relationship to CF.

TMD1 is the first translated domain of CFTR, and it interacts with both NBDs in the final CFTR structure (Mendoza and Thomas 2007). If interactions between TMD1 and NBD1 form and are important during translation, then translation reactions of each construct individually or in combination could reveal differences in construct expression. This was investigated by *in vitro* translation of these domains (Appendix I), but no effects were observed by the techniques performed (data shown and not shown). Notably, for CFTR, the potential interaction complexity is increased by the presence of the R domain, which forms multiple intraprotein interactions (Naren et al. 1999; Baker et al. 2007; Kanelis et al. 2010) but has no homologous structure. The most suggestive evidence of interdomain interactions in two and three domain CFTR constructs is the reported formation of a more stable three domain structure (Meacham et al. 1999; Rosser

et al. 2008; Grove et al. 2009). This structure may include the described interactions between the R region and the N-terminal region of TMD1 as identified in full length CFTR. Yet, within this work there are internal inconsistencies involving the ΔF508 mutation as described later within this chapter. Additionally, the interdomain interactions are implied rather than directly tested.

Specific cotranslational interactions currently cannot be addressed without technique development and application thereof. Further development of the cotranslational *in vitro* photocrosslinking technique (Do et al. 1996; Liao et al. 1997; McCormick et al. 2003) may allow for the interrogation of these interactions. At present, another limitation includes the difficulty of appropriate probe placement, since the crosslinker must be incorporated at a cotranslational interdomain interaction surface. Currently, prediction models are insufficient to accurately predict these surfaces. Therefore, studies of missense mutations in mammalian cell culture must be performed to obtain this information.

If CFTR interdomain interactions form in intermediate structures and are important in the cell, then it must be possible to experimentally monitor their disruption. This approach assumes that interdomain interactions occur based on the hierarchical folding model (Figure 4.2), and that disrupting them with point mutations will alter the cellular stability of multidomain constructs. This is the approach taken in Chapter 3, wherein introduction of lysine or arginine residues in TMD1 ICLs did not disrupt TMD1, but altered CFTR biogenic intermediates containing TMD2. The observed effects do not support a role for interdomain interactions before TMD2 is translated. However, interactions between the R domain and the N-terminus of TMD1 or NBD1 were not examined. Future studies should interrogate these interactions.

CF-causing mutants and CFTR cotranslational folding

Protein folding has been a primary focus in the study of CFTR since ΔF508 was characterized as a misfolding mutation that accumulates in the ER (Cheng et al. 1990). Interestingly, it has been shown that ΔF508 and other CF-causing mutants have effects on the individual domain or subdomain within which they reside (Chapter 3)(Thomas et al. 1992; Qu and Thomas 1996; Kleizen et al. 2005; Thibodeau et al. 2005). Examination of CF-mutant full length CFTR by crosslinking and proteolysis techniques revealed that in many cases, all final contacts are disrupted (Zhang et al. 1998; Du et al. 2005; Cui et al. 2007; Du and Lukacs 2009). Therefore, it is likely that a mutation can propagate to cause both domain and multidomain misfolding. However, it is difficult to determine if the initial or propagated perturbation is responsible for mutant protein cellular recognition. It is important to determine the nature of these mutant effects in order to therapeutically target the most relevant perturbation. It may be that a combination of defects results in misfolding, including inappropriate interactions with cellular machinery. A mutation could propagate to each domain during translation or only during later steps, such as the proposed multidomain rearrangement step. These questions may be addressed by further characterization of the TMD1 mutants studied in Chapters 2 and 3 to yield further insights into CFTR domain structure and interdomain interactions.

It is clear that the G85E and G91R mutations in TM1 disrupt TMD1 and preclude formation of CFTR. However, the effects of these mutations on NBD1 have not been analyzed in detail. As described above, split CFTR is capable of appropriately folding. These data suggest that perhaps NBD1 structure can form in the absence of TMD1. Yet, it is possible that NBD1 folding may be different in the presence of stable versus misfolded TMD1, which can be

addressed experimentally by proteolytic analysis of domains. Future studies should aim to analyze the effects of these mutations on the cotranslational folding of other CFTR domains.

The ICL1 and ICL2 studies presented in Chapter 3 bring about important questions regarding the normal cellular monitoring of CFTR. Hydrophobic residues in the ICL coupling helices negatively impact biogenic intermediate stability in the cell, suggesting a tradeoff between stability of these residues and later interactions in the CFTR structure. Mutation of the hydrophobic residues have no negative effect until TMD2 is present, therefore the later interactions most likely occur in the presence of TMD2. Based on homologous positions, these mutants likely affect structure at the helical ICL bundle or in the coupling helix interface, which both could alter ICL interactions with NBDs. While the ICL helical bundle likely forms when TMD1 and TMD2 are present, this has not been tested experimentally. Similarly, a requirement of this structure for NBD docking onto the ICLs has not been examined. The timing of this structure formation and its role in TMD-NBD interactions should be addressed in future experiments.

The cell is able to monitor and determine whether the TMD2 containing construct should traffic from the ER (Chapter 3)(Cui et al. 2007; Du and Lukacs 2009). This suggests that, upon the translation of TMD2, the protein quality control machinery makes a distinction between folded and unfolded CFTR (Figure 4.2). In the cell, the COPII machinery is implicated in CFTR export from (Yoo et al. 2002; Wang et al. 2004) or sorting for degradation within the ER (Fu and Sztul 2003), with a diacidic motif located within NBD1 potentially being important for the export function (Wang et al. 2004). However, a direct interaction has not been shown, and further characterization of these interactions as they relate to TMD2 should be performed. The studies in Chapter 3 suggest that the coupling helices may also be monitored by the cell, which

could play a role in distinguishing structures formed in the presence of TMD2. This monitoring of ICL interfaces may represent a mechanism by which the cell could facilitate removal of both misfolded wild type and CF-mutant CFTR. The different interactions responsible for deciding whether CFTR should traffic or be degraded are therapeutically relevant since modification thereof could increase production of cellular CFTR.

How does this relate to ΔF508 and how do we cure CF?

CF is a loss-of-function disease effecting more than 70,000 people worldwide (www.cff.org), with greater than 90% of these patients having at least one ΔF508 mutation (Kerem et al. 1989). The clinical ramifications affect multiple organ systems, such that treatment of the basic defect in CFTR is the best way to address the widespread morbidities. As discussed in Chapter 1, novel therapeutics show tremendous promise for altering the molecular pathologies of CF, however, implementation of therapeutics designed to correct ΔF508 is difficult. The ΔF508 molecular pathology is complex and involves multiple levels of misfolding and recognition thereof in the cell. Indeed, ΔF508-CFTR misfolds and is accumulated in the ER (Cheng et al. 1990). Moreover, if the trafficking defect is overcome, cell surface ΔF508-CFTR displays reduced chloride transport (Dalemans et al. 1991) and an accelerated turnover rate (Lukacs et al. 1993). Addressing each effect individually is inadequate, and a successful combination of therapeutics has not yet been identified to effectively rescue the ΔF508 mutation. Correction of the basic folding defect of ΔF508 CFTR is one therapeutic option, however, the most relevant basic defect remains unclear. Suppressor mutations of ΔF508 have been identified within NBD1 (Teem et al. 1993) and within ICL4 (Thibodeau et al. 2010), which correct NBD1

folding and/or multidomain folding. But, individually, these suppressors have limited efficacy. Taken together, these studies suggest that a diverse number of steps in CFTR misfolding may be therapeutically targeted.

The major recognition of many CFTR mutants within the cell requires the presence and thus translation of TMD2. In contrast, other reports indicate that ΔF508 minimally reduces stability of TMD1-NBD1 constructs but significantly reduces stability of constructs containing the R domain (Rosser et al. 2008; Grove et al. 2009). However, there are internal inconsistencies in the published data (Rosser et al. 2008; Grove et al. 2009). In this work, the rate of degradation of ΔF508 CFTR containing residues 1-653, 1-673, or 1-837 was lower than WT (Rosser et al. 2008; Grove et al. 2009). However, the difference in the rates for WT as compared to ΔF508 was modest (13 to 18% reductions) as compared to the dramatic (approximately 80%) decrease in starting levels (Rosser et al. 2008). Therefore the differences in degradation cannot explain the observed levels of construct expression.

To address this discrepancy, multiple ΔF508 biogenic intermediates, truncated after NBD1 or R, were generated and transiently expressed in HEK293 cell culture (Figure 4.3A). The steady-state levels of NBD1x ΔF508 are reduced from wild type, yet the Rx ΔF508 constructs are not altered from wild type (Figure 4.3A). These data are inconsistent with previous reports, but could easily be explained by the observed differences in the range of expressed individual constructs.

While earlier recognition of ΔF508 may occur, the cell does not mark it for disposal until TMD2 is present (Figure 4.3). This suggests that stabilization of the structure formed after TMD2 production is perhaps the most relevant mechanism for ΔF508 correction in the cell. This stabilization could maximally occur by correcting unstable ΔF508-NBD1 or the multidomain

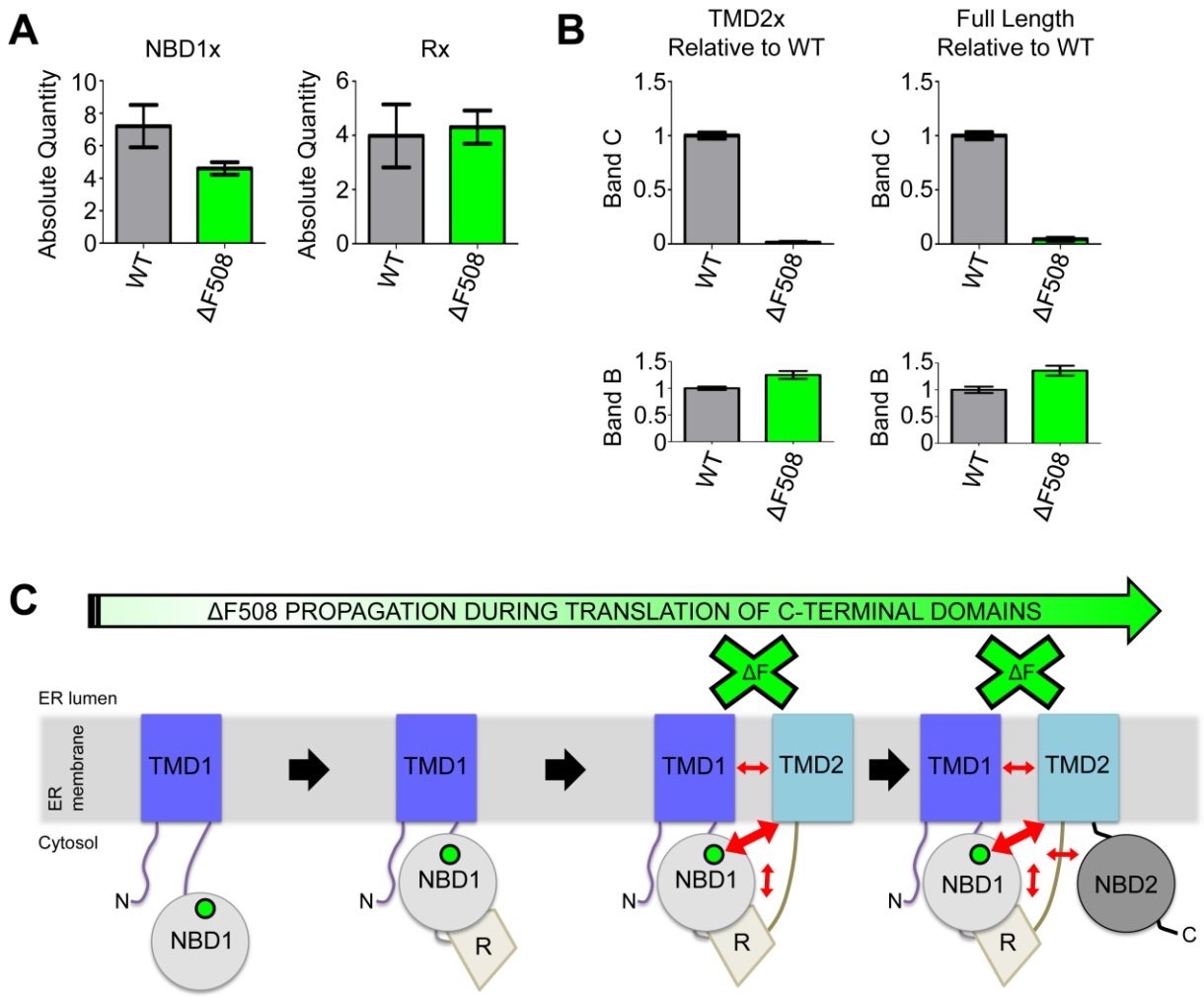

Figure 4.3 ΔF508 dramatically alters CFTR in the presence of TMD2. **A.** Wild type (WT) and ΔF508 NBD1x and Rx constructs are as described in Chapter3. NBD1x and Rx constructs were transiently transfected into HEK293 cells and monitored by Western blot analysis. The average and standard error of the mean for NBD1x, WT(N=2) and ΔF508(N=9), and Rx, WT(N=2) and ΔF508 (N=7), are from a single transfection. **B.** TMD2x and full length constructs were transiently transfected into HEK293 cells and monitored by Western blot analysis. CFTR steady-state levels of Band B and Band C were quantified and normalized to WT levels. The average is plotted with the standard error of the mean (N=4). **C.** A schematic from the hierarchical folding model depicting ΔF508 in the presence of different multidomain intermediates and potential interactions within those intermediates. The major cellular effect observed in the TMD2x and full length constructs containing ΔF508 are marked by a large X.

construct. Notably, many individual domains, such as NBD1, are commonly present in the cell with different stabilities suggesting that distinguishing amongst these domains for degradation could be biologically inefficient. However, failing to achieve a complex fold (Figure 4.2, Figure 4.3) could be an efficient way for the cell to distinguish misfolded from appropriately folded protein. These situations may be the case for ΔF508-CFTR, wherein the reduction in the ΔF508-NBD1 domain is not dramatic until the presence of TMD2 (Figure 4.3).

The effects of suppressor mutations for ΔF508, either within NBD1 or distant in the CFTR protein, and compounds that rescue ΔF508 could be mimicked by therapeutics. Reports of compounds and suppressor mutations that work within NBD1 exist (Teem et al. 1993; Qu et al. 1997; Sampson et al. 2011). Additionally, other compounds rescue the ΔF508 mutation by interactions with the TMDs (Loo et al. 2011). ΔF508 or other mutant CFTRs were also partially rescued by transcomplementation, in which coexpression of parts of CFTR were able to cause trafficking of CF-mutant CFTR from the ER (Cormet-Boyaka et al. 2004; Cebotaru et al. 2008).

Other methods to rescue the ΔF508 mutation have been explored using the yeast homologous ABC exporter, Yor1p (Pagant et al. 2007; Pagant et al. 2008). When a ΔF508 mimic is introduced into Yor1p, consequent mistrafficking and degradation occurs (Pagant et al. 2007). Interestingly, a Yor1p suppressor mutation combination in the TM-ICL junctions partially corrected this ΔF508 mimic (Pagant et al. 2010). Also, a co-expressed Yor1p NBD1 was able to swap into the ΔF508 mimic-Yor1p to replace the defective domain (Louie et al. 2010). Notable differences exist between the Yor1p protein and CFTR, however these findings provide novel insight into potential mechanisms for ΔF508-CFTR correction that should be investigated in mammalian cell culture with CFTR.

It is clear from these studies that the identification of disease mechanisms that may be targeted therapeutically requires a global understanding of CFTR structure. High throughput screens are an excellent method to find relevant compounds, however better identification of the most relevant biological defect will help us design better, more biologically productive screens. The recent discovery of Vx770, a compound that targets the G551D mutation, has generated a spark of hope for CF therapeutics (Accurso et al. 2010). Using these methods, similar compounds that target the ΔF508 mutation may be identified. This is a very exciting time to be involved in CF research as collaborations between basic and clinical science are changing CF therapeutics.

MATERIALS AND METHODS

Expression and quantitation for ΔF508 constructs

Protocols described in Chapter 3 were utilized for plasmids and DNA techniques. Stop codons were introduced into full length CFTR containing ΔF508. The nine NBD1x and seven Rx constructs were generated from two separate mutagenesis reactions with constructs validated by DNA sequence analysis. Constructs were expressed in HEK293 cell culture and analyzed as described. NBD1x and Rx constructs were analyzed from a single experiment to eliminate variation due to single construct expression. Results presented are representative of multiple experiments. TMD2x and full length constructs were analyzed as described in Chapter 3.

Appendix I

Development of *In Vitro* Translation Protocols for CFTR

Introduction to *in vitro* translation of CFTR

The cotranslational formation of CFTR structure can be studied using i*n vitro* translation. In i*n vitro* translation systems, a defined mRNA is translated in the presence of radiolabeled methionine that gets incorporated into the protein nascent chain. By synchronization of the ribosomes, a selected pool of nascent chains can be followed as structure is obtained, either cotranslationally or posttranslationally. CFTR has been studied using this technique, revealing through limited proteolysis that each domain obtains structure cotranslationally (Kleizen et al. 2005), and NBD2 is posttranslationally incorporated into the CFTR structure (Du et al. 2005). In NBD1, cotranslational structure formation includes collapse of a ligand dependent N-terminal subdomain and further collapse upon completion of NBD1 translation (Khushoo et al. 2011). Other studies have also identified details of CFTR TM span topology and integration (Xiong et al. 1997; Lu et al. 1998; Tector and Hartl 1999). Most importantly, these systems determined that ΔF508 mediated effects are apparent during both NBD1 and full length CFTR translation (Zhang et al. 1998; Du et al. 2005; Hoelen et al. 2010).

The *in vitro* translation systems are also used to site-specifically incorporate a photocrosslinkable amino acid into the protein nascent chain (Do et al. 1996; Liao et al. 1997; McCormick et al. 2003). In order to extend this system to study CFTR, different system components were generated and optimized.

CFTR is a complex membrane spanning protein. *In vitro* translation systems for CFTR require many components, including translationally active ribosomes and translocation competent ER membranes. All of the molecules required for active ribosomes and translocons are not known, so both materials are collected from primary sources. The ribosomes can be

generated from wheat germ (WG) and rabbit reticulocyte (RRL) cell lysates, both of which are immature cell types containing high levels of ribosomes. The translocons can be collected as canine pancreatic microsomes. The canine pancreas contains high levels of professional secretory cells with extensive ER membranes and translocons and relatively low levels of RNases.

In vitro translation protocols are complex, and the WG and RRL systems require different reagents for translation of cytosolic, secreted, or membrane proteins. During all *in vitro* translation reactions, protein nascent chains were generated by addition of mRNA prepared by *in vitro* transcription using SP6 RNA polymerase (Woolhead et al. 2004). Translation was performed in the presence of ^{35}S-methionine, and the nascent chains detected by SDS-PAGE and phosphorimage analysis. The previously described protocols for *in vitro* translation in WG and RRL systems were followed (Do et al. 1996; Liao et al. 1997; Etchells et al. 2005).

Preparation and characterization of wheat germ lysate

WG lysate is a processed *in vitro* translation system, which results in removal of SRP. To translate secreted and membrane proteins in the WG system, both SRP and column washed canine pancreatic microsomes (CRMs) must be added, both of which are difficult to prepare. The translation efficiency of larger constructs is low, making this system less optimal for CFTR multidomain constructs.

Protocols for the preparation of WG lysate were followed as described (Erickson and Blobel 1983). In brief, WG was mixed in 87% carbon tetrachloride/ 13% cyclohexane and floating wheat germ collected and dried. This WG was added to homogenization buffer (40mM

HEPEs, 100mM KOAc, 1mM $Mg(OAc)_2$, 2mM $CaCl_2$, 4mM DTT, pH 7.5) and ground into a paste in a liquid nitrogen cooled mortar and pestle to disrupt the cell walls. The resulting mixture was separated by centrifugation at 20,000g's, and column chromatography performed on the supernatant using Sephadex G-25 resin with buffer (40mM HEPEs, 100mM KOAc, 5mM $Mg(OAc)_2$, 2mM glutathione, pH 7.5). The most turbid fractions were collected and nuclease treated with *Staphylococcus aureus* Nuclease S7 to remove endogenous mRNAs. The resulting mix was separated by centrifugation at 20,000g's, the supernatant collected, and then centrifuged at 200,000g's to collect the ribosomes.

Preparation and characterization of rabbit reticulocyte lysate

RRL is a less processed lysate than WG, which is more efficient for translation of larger protein constructs. SRP is present in RRL, and either CRMs or rough microsomes (RMs) can be added for translocation activity. Rabbit reticulocytes contain high levels of active proteasome, which is inhibited in the utilized translation reactions. The optimized *in vitro* translation protocol for CFTR translation includes a 10 minute 30°C incubation prior to addition of ^{35}S-methionine and mRNA, and addition of a translation initiation inhibitor, aurin tricarboxylic acid (ATA), 15 minutes after start of the reaction to synchronize the nascent chains (Oberdorf and Skach 2002).

RRL from Green Hectares (Oregon, WI) was purchased that had been washed, lysed in pure water, membranes and nuclei removed, and frozen. Before use, endogenous mRNAs were removed by treatment with *Staphylococcus aureus* Nuclease S7, and proteasome was inhibited by inclusion of hemin in storage buffer (40μM hemin/1mN KOH/0.4mM HEPEs/3.5%ethylene

glycol/0.7mM HCl). Translation activity was tested for RRL without nuclease treatment to monitor background translation from endogenous mRNAs, with nuclease treatment to monitor removal of endogenous mRNAs, and with addition of external mRNA encoding the model protein preprolactin (pPL) to nuclease treated RRL (Figure 5.1A,B).

Preparation and characterization of rough canine pancreatic microsomes

ER membranes contain the translocation machinery for moving secreted proteins into the ER lumen and integrating transmembrane spans. ER membranes in the form of microsomes were collected from seven individual canine pancreases on separate days. Classic protocols were followed for collection of rough microsomes (Walter and Blobel 1983a; Walter and Blobel 1983b). During this process, all steps are performed at 4°C, on ice, and as quickly as possible to generate high quality microsomes. In brief, pancreas was collected immediately postmortem, undesired tissues removed, weighed, and chopped into small pieces. Buffer (250mM sucrose, 50mM TEA, 50mM KOAc, 6mM $Mg(OAc)_2$, 1mM EDTA, 1mM DTT, and 0.5mM PMSF) was added and the mixture, which was then ground gently and homogenized by drill press. A 1,000g centrifugation was performed and pelleted debris and floating fat separated from supernatant. This supernatant was then loaded into tubes, under layered with high sucrose buffer (1300mM sucrose, 50mM TEA, 50mM KOAc, 6mM $Mg(OAc)_2$, 1mM EDTA, 1mM DTT, and 0.5mM PMSF), and centrifuged at 145,000g's for 150 minutes to pellet microsomes. The pellet was gently resuspended (250mM sucrose, 50mM TEA, 1mM DTT) and dounce homogenized 3 times. Each rough microsome preparation was separately stored, #1-7, and quantified as A_{280} units, which determines the quantity added per *in vitro* translation reaction. In summation,

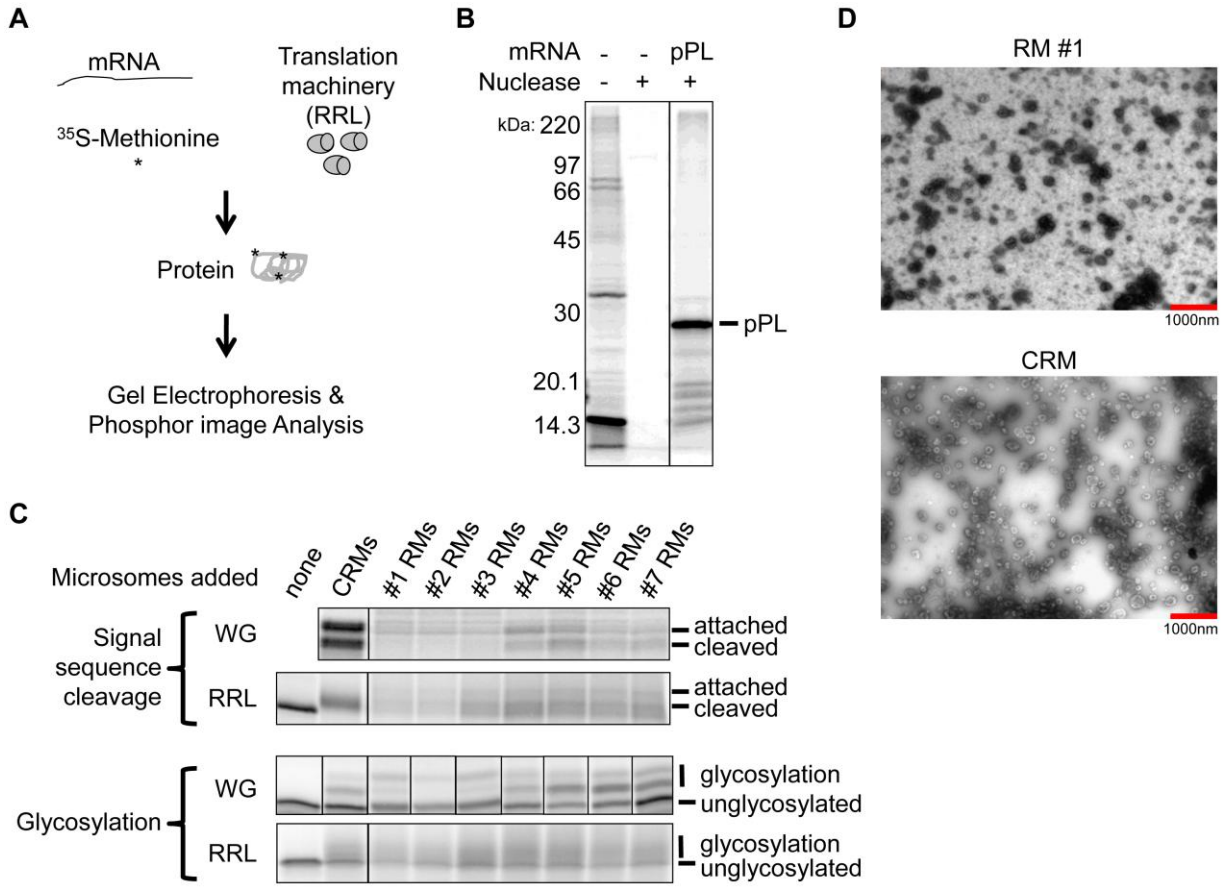

Figure 5.1 RRL and RM *in vitro* translation materials. **A.** Schematic depicting materials added into a standard RRL translation reaction, formation of radiolabeled protein, and analysis of this protein. **B.** RRL control reactions monitoring translation in non-nuclease treated RRL containing endogenous mRNAs, nuclease-treated RRL without endogenous mRNAs, and translation of an added mRNA encoding preprolactin (pPL) in nuclease-treated RRL. Positions of molecular weight markers in kDa are shown. **C.** Collected RMs were compared in WG and RRL translation reactions with no addition and CRMs controls. mRNAs that undergo signal sequence cleavage or core glycosylation were examined, with signal sequence cleavage and core glycosylation resulting in respective decreased and increased electrophoretic mobility. **D.** RM#1 was examined by negative stain electron microscopy in the Electron Microscopy Core Facility at UT Southwestern and compared to CRMs as control.

approximately 250mL of rough canine pancreatic microsomes (RMs) totaling 22,000 A_{280} units were collected from 295g of pancreas.

The RM preparations, #1-7, were characterized in both RRL and WG *in vitro* translation systems. The translocation machinery is associated with oligosaccharyl transferase (OST), which core glycosylates sequences in the ER lumen, and signal peptidase, which removes the signal sequences from secreted proteins (Johnson and van Waes 1999). The glycosylation and signal sequence cleavage activities of the collected RMs were monitored by adding mRNA encoding the following: 1) a three TM span CFTR construct containing a glycosylation site and 2) a preprolactin construct containing a cleavable signal sequence (Figure 5.1C). RM preparations were compared to high quality CRMs, which have undergone a column washing step, from the A.E. Johnson laboratory. RMs were examined without nuclease treatment, resulting in high background and lower signal of translated products as compared to no microsome and CRM samples (Figure 5.1C). The use of CRMs versus RMs in the WG system can be compared, highlighting the requirement of CRMs for this system. Additionally, the later microsome preparations (#4-7) have higher activity, suggesting that microsome quality is directly related to the experience of the collectors. Microsomes from RM#1 were examined in the Electron Microscopy Core Facility at UT Southwestern by negative stain electron microscopy, and found to be ultrastructurally comparable to the CRM control (Figure 5.1D).

In vitro translation of TMD1 and NBD1

CFTR heiarchical folding models show TMD1 and NBD1 interacting during translation, however this has not been experimentally tested. The prepared materials were utilized to

examine TMD1 and NBD1 translation. mRNAs encoding TMD1, residues 1 to 383, or NBD1, residues 389 to 710, were prepared with no stop codon at the 3' end, such that the ribosomes remain bound to mRNA and the protein nascent chain (Figure 5.2A). NBD1 is a cytosolic domain and should not require ER membranes for translation. TMD1 and NBD1 were translated in the WG system (Figure 5.2B) or in the RRL system (Figure 5.2C). In the WG system, NBD1 is formed in the presence or absence of TMD1 and CRMs (Figure 5.2B). In contrast, NBD1 formed a low molecular weight (LMW) translation product in RRL alone, and an expected molecular weight product in the presence of TMD1 and RMs (Figure 5.2C). Since the RRL system is optimal for producing CFTR constructs, the LMW product of NBD1 presents a challenge for future studies.

In order to separate the effects of TMD1 and RMs on NBD1 translation, NBD1 was translated in the presence of RRL supplemented with buffer, CRMs, or RMs and collected over a time course (Figure 5.3A). During NBD1 translation, in buffer the LMW product is produced, in CRMs the LWM product is produced with a partial transition to full length product with time, and in RMs full length product is formed (Figure 5.3A). With time, the quantity of the LMW product decreases as the quantity of full length NBD1 increases, suggesting the bands are directly related. The effect of ΔF508 on formation of the LWM product was examined in RRL with RMs over a short time course, with the resulting NBD1 and ΔF508-NBD1 having indistinguishable translation products (Figure 5.3B). In order to test if NBD1 translation is effected by the presence of TMD1, TMD1 and NBD1 or ΔF508-NBD1 were translated in RRL with RMs separately, then mixed and followed over time (Figure 5.3C). This translation experiment was compared to an experiment wherein TMD1 and NBD1 or ΔF508-NBD1 were translated in RRL with RMs *in trans* and followed over time (Figure 5.3D). In both sets of

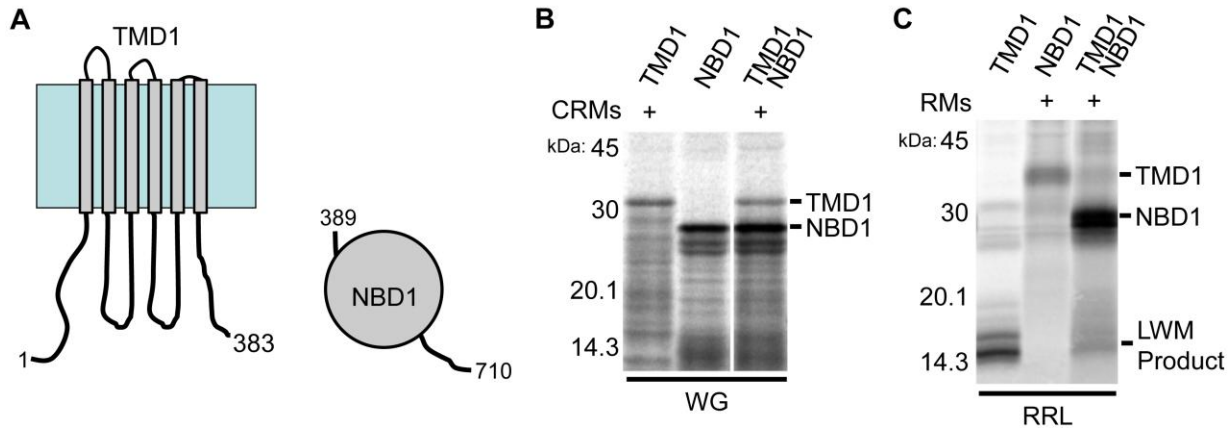

Figure 5.2 TMD1 and NBD1 translation in WG and RRL *in vitro* translation systems. **A.** Schematic showing the TMD1 and NBD1 constructs containing residues 1 to 383 and 389 to 710 respectively. TMD1 and NBD1 were translated separately or *in trans* in WG (**B**) and RRL (**C**) *in vitro* translation systems supplemented by CRMs or RMs respectively. Positions of molecular weight markers in kDa are shown.

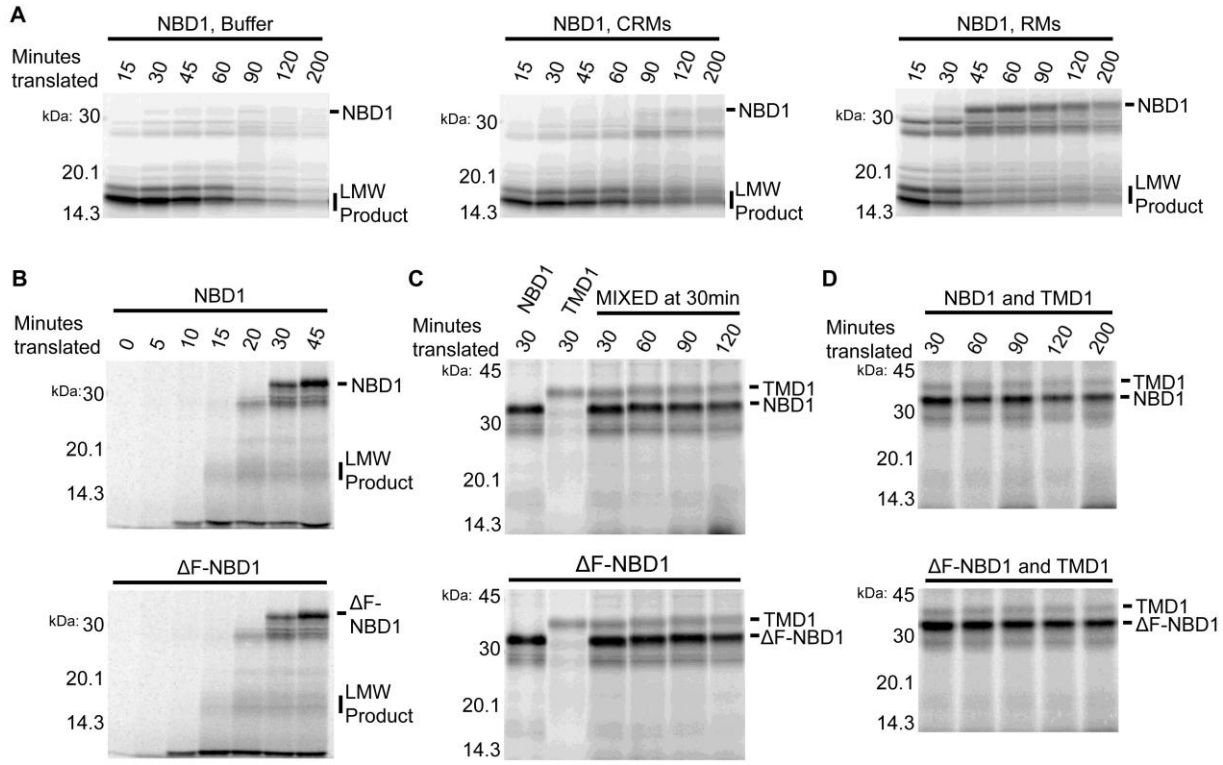

Figure 5.3 NBD1 and ΔF508-NBD1 translations behave similarly. **A.** NBD1 was translated in an RRL *in vitro* translation system supplemented with buffer (left), CRMs (middle), or RMs (right). Translation products were monitored over time. **B.** NBD1 (top) and ΔF508-NBD1 (bottom) were translated in RRL supplemented with RMs. **C.** NBD1 (top) or ΔF508-NBD1 (bottom) and TMD1 were translated in separate RRL translation reactions supplemented with RMs for 30 minutes, mixed, and followed over time. **D.** NBD1 (top) or ΔF508-NBD1 (bottom) and TMD1 were translated *in trans* in the same RRL translation reactions supplemented with RMs and followed over time. Positions of molecular weight markers in kDa are shown.

carefully controlled reactions, no effect was observed, suggesting NBD1 and TMD1 do not strongly affect each other during this process. Notably, mixing of NBD1 and TMD1 mRNAs resulted in low production of TMD1, making *in trans* experiments inefficient.

NBD1 forms a translationally paused product in RRL

The formation of a NBD1 LMW product in RRL and its rescue by RMs was unexpected. To determine the reproducibility and specificity of this observation, the *in vitro* translation protein products were identified by immunoprecipitation (IP) and multiple RRL and RM preparations tested. IPs were performed with multiple antibodies having epitopes in NBD1 (Figure 5.4A). NBD1 translation reactions were performed in RRL with or without RMs and immunoprecipitated with these antibodies (Figure 5.4B). A table listing the results of tested antibodies is shown (Figure 5.4C). The full length and LMW products were both verified as NBD1, and the C-terminal boundary of the LMW product was grossly mapped between residues 540 to 589 (Figure 5.4C). Multiple translation materials were able to reproduce the observed NBD1 behavior, including three independent RRLs and multiple pancreas preparations (data not shown). Notably, commercially available RRL did not form the LMW band (data not shown).

The LMW band specificity for NBD1 was tested by translating other mRNA constructs in RRL with or without RMs. These tested mRNAs encode NBD2 of CFTR, luciferase, β-lactamase that undergoes signal sequence cleavage, and α-factor that undergoes signal sequence cleavage and multiple core glycosylations (Figure 5.4D). Core glycosylation and signal sequence cleavage only occur in the presence of microsomes, with the noted modifications observed (Figure 5.4D). The LMW band was only present for NBD1 (Figure 5.4D).

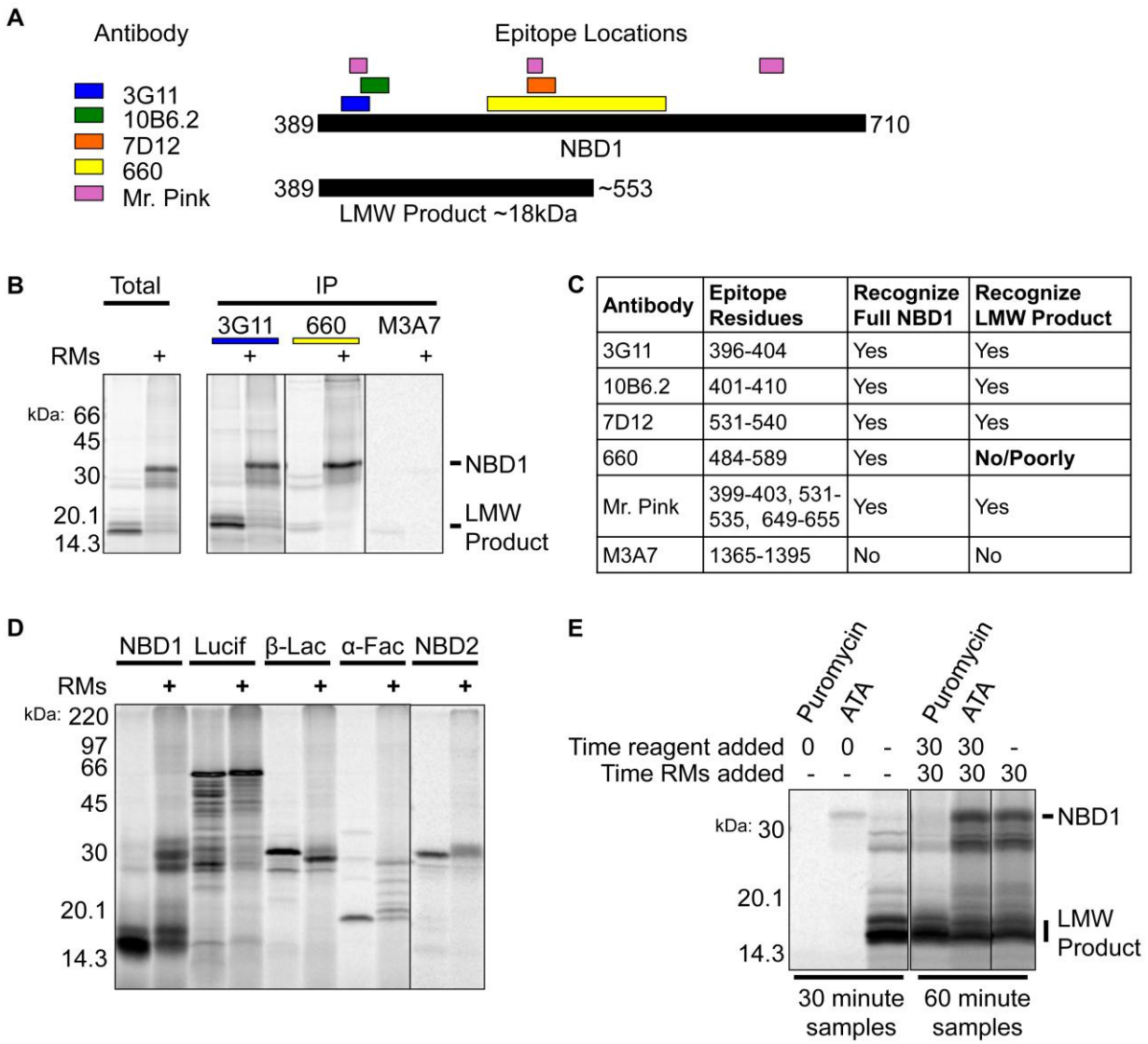

Figure 5.4 The LWM product is translationally paused NBD1. **A.** A schematic showing antibodies to NBD1 and the epitope positions with respect to NBD1 and the LMW product. **B.** A translation reaction was performed in RRL with or without RMs, with the total translation product shown (left). The total translation was split and immunoprecipitated (IP) by the antibodies in panel A. The M3A7 is a control that does not recognize NBD1. **C.** A table listing the results of the IPs. **D.** Other mRNAs encoding luciferase, β-lactamase, α-factor, and NBD2 of CFTR were translated in the RRL with or without RMs. In the presence of RMs, β-lactamase and α-factor undergo signal sequence cleavage (increased electrophoretic mobility band) and α-factor is core glycosylated (multiple decreased electrophoretic mobility bands). **E.** NBD1 was translated in RRL reactions immediately treated translation elongation and initiation inhibitors, respectively puromycin and ATA, or without inhibitors for 30 minutes. Translation reactions represented by lane 3 were then continued with inhibitors or no inhibitor and RMs added. Positions of molecular weight markers in kDa are shown.

The LMW product appears to have an inverse relationship with full length NBD1. To test if the LMW product is translationally paused, a combination of translation inhibitors and RM additions was performed. The inhibitor puromycin inhibits translation elongation, and ATA inhibits translation initiation. The LMW product was produced by translation of NBD1 in RRL, then inhibitors and RMs were added and translation continued (Figure 5.4E). The addition of puromycin blocked all translation, whereas addition of ATA only blocked initiation of translation. In the presence of ATA, the LMW band was able to transition to the full length product in the presence of RMs, supporting a direct relationship between the bands.

While the LMW band appears specific to NBD1, its relevance during full length CFTR translation is unclear. In order for TMD1 structure to form, it must be translated in the presence of CRMs or RMs. The LMW product formation in NBD1 displayed differences in CRMs and RMs (Figure 5.3A). An mRNA encoding CFTR residues 1 to 710 was translated in RRL in the presence of CRMs or RMs (Figure 5.5). Immunoprecipitation to validate the translated product revealed no detectable low molecular weight product. Future directions should require the identification of this product as relevant to multiple NBD1 constructs and to the full length translation of CFTR.

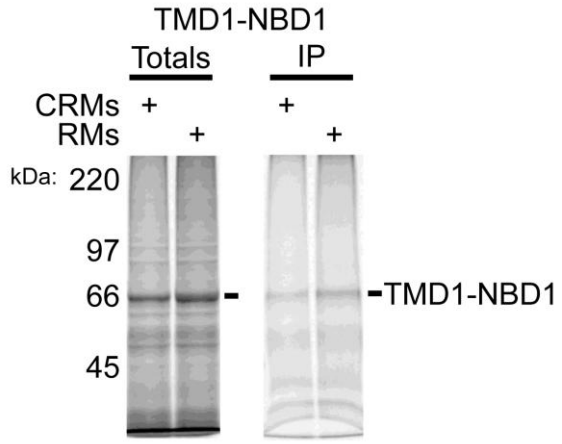

Figure 5.5. LMW product is not present in all CFTR constructs. An mRNA encoding residues 1 to 710 of CFTR was translated in an RRL *in vitro* translation system supplemented with CRMs or RMs. Total translation products (left) were immunoprecipitated by antibody 10B6.2 (Figure 5.4)(right) and examined for lower truncation product formation. No significant lower molecular weight products are detected. Positions of molecular weight markers in kDa are shown.

BIBLIOGRAPHY

Accurso FJ, Rowe SM, Clancy JP, Boyle MP, Dunitz JM, Durie PR, Sagel SD, Hornick DB, Konstan MW, Donaldson SH et al. 2010. Effect of VX-770 in persons with cystic fibrosis and the G551D-CFTR mutation. *N Engl J Med* **363**: 1991-2003.

Aigner B, Renner S, Kessler B, Klymiuk N, Kurome M, Wunsch A, Wolf E. 2010. Transgenic pigs as models for translational biomedical research. *Journal of molecular medicine* **88**: 653-664.

Aleksandrov AA, Aleksandrov LA, Riordan JR. 2007. CFTR (ABCC7) is a hydrolyzable-ligand-gated channel. *Pflugers Arch* **453**: 693-702.

Aleksandrov AA, Kota P, Aleksandrov LA, He L, Jensen T, Cui L, Gentzsch M, Dokholyan NV, Riordan JR. 2010. Regulatory insertion removal restores maturation, stability and function of DeltaF508 CFTR. *Journal of molecular biology* **401**: 194-210.

Aleksandrov L, Aleksandrov AA, Chang XB, Riordan JR. 2002. The First Nucleotide Binding Domain of Cystic Fibrosis Transmembrane Conductance Regulator Is a Site of Stable Nucleotide Interaction, whereas the Second Is a Site of Rapid Turnover. *The Journal of biological chemistry* **277**: 15419-15425.

Aller SG, Yu J, Ward A, Weng Y, Chittaboina S, Zhuo R, Harrell PM, Trinh YT, Zhang Q, Urbatsch IL et al. 2009. Structure of P-glycoprotein reveals a molecular basis for poly-specific drug binding. *Science* **323**: 1718-1722.

Anderson MP, Gregory RJ, Thompson S, Souza DW, Paul S, Mulligan RC, Smith AE, Welsh MJ. 1991. Demonstration that CFTR is a chloride channel by alteration of its anion selectivity. *Science* **253**: 202-205.

Atwell S, Ultsch M, De Vos AM, Wells JA. 1997. Structural plasticity in a remodeled protein-protein interface. *Science* **278**: 1125-1128.

Baker JM, Hudson RP, Kanelis V, Choy WY, Thibodeau PH, Thomas PJ, Forman-Kay JD. 2007. CFTR regulatory region interacts with NBD1 predominantly via multiple transient helices. *Nat Struct Mol Biol* **14**: 738-745.

Basso C, Vergani P, Nairn AC, Gadsby DC. 2003. Prolonged nonhydrolytic interaction of nucleotide with CFTR's NH2-terminal nucleotide binding domain and its role in channel gating. *J Gen Physiol* **122**: 333-348.

Bear CE, Li CH, Kartner N, Bridges RJ, Jensen TJ, Ramjeesingh M, Riordan JR. 1992. Purification and functional reconstitution of the cystic fibrosis transmembrane conductance regulator (CFTR). *Cell* **68**: 809-818.

Biemans-Oldehinkel E, Doeven MK, Poolman B. 2006. ABC transporter architecture and regulatory roles of accessory domains. *FEBS Lett* **580**: 1023-1035.

Borowitz D, Baker RD, Stallings V. 2002. Consensus report on nutrition for pediatric patients with cystic fibrosis. *J Pediatr Gastroenterol Nutr* **35**: 246-259.

Borst P, Elferink RO. 2002. Mammalian ABC transporters in health and disease. *Annu Rev Biochem* **71**: 537-592.

Braun P, von Heijne G. 1999. The aromatic residues Trp and Phe have different effects on the positioning of a transmembrane helix in the microsomal membrane. *Biochemistry* **38**: 9778-9782.

Brown CR, Hong-Brown LQ, Biwersi J, Verkman AS, Welch WJ. 1996. Chemical chaperones correct the mutant phenotype of the delta F508 cystic fibrosis transmembrane conductance regulator protein. *Cell stress & chaperones* **1**: 117-125.

Campodonico VL, Gadjeva M, Paradis-Bleau C, Uluer A, Pier GB. 2008. Airway epithelial control of Pseudomonas aeruginosa infection in cystic fibrosis. *Trends Mol Med* **14**: 120-133.

Cebotaru L, Vij N, Ciobanu I, Wright J, Flotte T, Guggino WB. 2008. Cystic fibrosis transmembrane regulator missing the first four transmembrane segments increases wild type and DeltaF508 processing. *J Biol Chem* **283**: 21926-21933.

CFFRegistry. 2011. Cystic Fibrosis Foundation Patient Registry 2009 Annual Data Report. Cystic Fibrosis Foundation, Bethesda, MD.

Chan KW, Csanady L, Seto-Young D, Nairn AC, Gadsby DC. 2000. Severed molecules functionally define the boundaries of the cystic fibrosis transmembrane conductance regulator's NH(2)-terminal nucleotide binding domain. *The Journal of general physiology* **116**: 163-180.

Chang XB, Hou YX, Jensen TJ, Riordan JR. 1994. Mapping of cystic fibrosis transmembrane conductance regulator membrane topology by glycosylation site insertion. *The Journal of biological chemistry* **269**: 18572-18575.

Chang XB, Mengos A, Hou YX, Cui L, Jensen TJ, Aleksandrov A, Riordan JR, Gentzsch M. 2008. Role of N-linked oligosaccharides in the biosynthetic processing of the cystic fibrosis membrane conductance regulator. *J Cell Sci* **121**: 2814-2823.

Chappe V, Irvine T, Liao J, Evagelidis A, Hanrahan JW. 2005. Phosphorylation of CFTR by PKA promotes binding of the regulatory domain. *Embo J* **24**: 2730-2740.

Chavan M, Lennarz W. 2006. The molecular basis of coupling of translocation and N-glycosylation. *Trends Biochem Sci* **31**: 17-20.

Chen EY, Bartlett MC, Loo TW, Clarke DM. 2004. The DeltaF508 mutation disrupts packing of the transmembrane segments of the cystic fibrosis transmembrane conductance regulator. *J Biol Chem* **279**: 39620-39627.

Chen M, Zhang JT. 1999. Topogenesis of cystic fibrosis transmembrane conductance regulator (CFTR): regulation by the amino terminal transmembrane sequences. *Biochemistry* **38**: 5471-5477.

Cheng SH, Gregory RJ, Marshall J, Paul S, Souza DW, White GA, O'Riordan CR, Smith AE. 1990. Defective intracellular transport and processing of CFTR is the molecular basis of most cystic fibrosis. *Cell* **63**: 827-834.

Cheung JC, Deber CM. 2008. Misfolding of the cystic fibrosis transmembrane conductance regulator and disease. *Biochemistry* **47**: 1465-1473.

Cheung JC, Reithmeier RA. 2005. Membrane integration and topology of the first transmembrane segment in normal and Southeast Asian ovalocytosis human erythrocyte anion exchanger 1. *Mol Membr Biol* **22**: 203-214.

-. 2007. Scanning N-glycosylation mutagenesis of membrane proteins. *Methods* **41**: 451-459.

Cheung M, Akabas MH. 1996. Identification of cystic fibrosis transmembrane conductance regulator channel-lining residues in and flanking the M6 membrane-spanning segment. *Biophys J* **70**: 2688-2695.

Choi JY, Muallem D, Kiselyov K, Lee MG, Thomas PJ, Muallem S. 2001. Aberrant CFTR-dependent HCO3- transport in mutations associated with cystic fibrosis. *Nature* **410**: 94-97.

Clackson T, Wells JA. 1995. A hot spot of binding energy in a hormone-receptor interface. *Science* **267**: 383-386.

Claros MG, von Heijne G. 1994. TopPred II: an improved software for membrane protein structure predictions. *Comput Appl Biosci* **10**: 685-686.

Combet C, Blanchet C, Geourjon C, Deleage G. 2000. NPS@: network protein sequence analysis. *Trends Biochem Sci* **25**: 147-150.

Cormet-Boyaka E, Jablonsky M, Naren AP, Jackson PL, Muccio DD, Kirk KL. 2004. Rescuing cystic fibrosis transmembrane conductance regulator (CFTR)-processing mutants by transcomplementation. *Proceedings of the National Academy of Sciences of the United States of America* **101**: 8221-8226.

Cotten JF, Ostedgaard LS, Carson MR, Welsh MJ. 1996. Effect of cystic fibrosis-associated mutations in the fourth intracellular loop of cystic fibrosis transmembrane conductance regulator. *J Biol Chem* **271**: 21279-21284.

Csanady L, Chan KW, Seto-Young D, Kopsco DC, Nairn AC, Gadsby DC. 2000. Severed channels probe regulation of gating of cystic fibrosis transmembrane conductance regulator by its cytoplasmic domains. *J Gen Physiol* **116**: 477-500.

Cui L, Aleksandrov L, Chang XB, Hou YX, He L, Hegedus T, Gentzsch M, Aleksandrov A, Balch WE, Riordan JR. 2007. Domain interdependence in the biosynthetic assembly of CFTR. *J Mol Biol* **365**: 981-994.

Curran AR, Engelman DM. 2003. Sequence motifs, polar interactions and conformational changes in helical membrane proteins. *Curr Opin Struct Biol* **13**: 412-417.

Cutting GR. 2010. Modifier genes in Mendelian disorders: the example of cystic fibrosis. *Ann N Y Acad Sci* **1214**: 57-69.

Dalemans W, Barbry P, Champigny G, Jallat S, Dott K, Dreyer D, Crystal RG, Pavirani A, Lecocq JP, Lazdunski M. 1991. Altered chloride ion channel kinetics associated with the delta F508 cystic fibrosis mutation. *Nature* **354**: 526-528.

Dawson RJ, Hollenstein K, Locher KP. 2007. Uptake or extrusion: crystal structures of full ABC transporters suggest a common mechanism. *Mol Microbiol* **65**: 250-257.

Dawson RJ, Locher KP. 2006. Structure of a bacterial multidrug ABC transporter. *Nature* **443**: 180-185.

-. 2007. Structure of the multidrug ABC transporter Sav1866 from Staphylococcus aureus in complex with AMP-PNP. *FEBS Lett* **581**: 935-938.

Dean M, Rzhetsky A, Allikmets R. 2001. The human ATP-binding cassette (ABC) transporter superfamily. *Genome Res* **11**: 1156-1166.

DeCarvalho AC, Gansheroff LJ, Teem JL. 2002. Mutations in the nucleotide binding domain 1 signature motif region rescue processing and functional defects of cystic fibrosis transmembrane conductance regulator delta f508. *J Biol Chem* **277**: 35896-35905.

Denning GM, Anderson MP, Amara JF, Marshall J, Smith AE, Welsh MJ. 1992. Processing of mutant cystic fibrosis transmembrane conductance regulator is temperature-sensitive. *Nature* **358**: 761-764.

Devidas S, Yue H, Guggino WB. 1998. The second half of the cystic fibrosis transmembrane conductance regulator forms a functional chloride channel. *J Biol Chem* **273**: 29373-29380.

Di Bartolo ND, Hvorup RN, Locher KP, Booth PJ. 2011. In Vitro folding and assembly of the Escherichia coli ATP-binding cassette transporter, BtuCD. *J Biol Chem*.

Do H, Falcone D, Lin J, Andrews DW, Johnson AE. 1996. The cotranslational integration of membrane proteins into the phospholipid bilayer is a multistep process. *Cell* **85**: 369-378.

Donaldson SH, Boucher RC. 2007. Sodium channels and cystic fibrosis. *Chest* **132**: 1631-1636.

Du K, Lukacs GL. 2009. Cooperative assembly and misfolding of CFTR domains in vivo. *Mol Biol Cell* **20**: 1903-1915.

Du K, Sharma M, Lukacs GL. 2005. The DeltaF508 cystic fibrosis mutation impairs domain-domain interactions and arrests post-translational folding of CFTR. *Nat Struct Mol Biol* **12**: 17-25.

Durno C, Corey M, Zielenski J, Tullis E, Tsui LC, Durie P. 2002. Genotype and phenotype correlations in patients with cystic fibrosis and pancreatitis. *Gastroenterology* **123**: 1857-1864.

Ellsworth RE, Jamison DC, Touchman JW, Chissoe SL, Braden Maduro VV, Bouffard GG, Dietrich NL, Beckstrom-Sternberg SM, Iyer LM, Weintraub LA et al. 2000. Comparative genomic sequence analysis of the human and mouse cystic fibrosis transmembrane conductance regulator genes. *Proc Natl Acad Sci U S A* **97**: 1172-1177.

Enquist K, Fransson M, Boekel C, Bengtsson I, Geiger K, Lang L, Pettersson A, Johansson S, von Heijne G, Nilsson I. 2009. Membrane-integration characteristics of two ABC transporters, CFTR and P-glycoprotein. *J Mol Biol* **387**: 1153-1164.

Erickson AH, Blobel G. 1983. Cell-free translation of messenger RNA in a wheat germ system. *Methods Enzymol* **96**: 38-50.

Etchells SA, Meyer AS, Yam AY, Roobol A, Miao Y, Shao Y, Carden MJ, Skach WR, Frydman J, Johnson AE. 2005. The cotranslational contacts between ribosome-bound nascent polypeptides and the subunits of the hetero-oligomeric chaperonin TRiC probed by photocross-linking. *The Journal of biological chemistry* **280**: 28118-28126.

Fahy JV, Dickey BF. Airway mucus function and dysfunction. *N Engl J Med* **363**: 2233-2247.

Farrell PM, Kosorok MR, Laxova A, Shen G, Koscik RE, Bruns WT, Splaingard M, Mischler EH. 1997. Nutritional benefits of neonatal screening for cystic fibrosis. Wisconsin Cystic Fibrosis Neonatal Screening Study Group. *N Engl J Med* **337**: 963-969.

Farrell PM, Kosorok MR, Rock MJ, Laxova A, Zeng L, Lai HC, Hoffman G, Laessig RH, Splaingard ML. 2001. Early diagnosis of cystic fibrosis through neonatal screening prevents severe malnutrition and improves long-term growth. Wisconsin Cystic Fibrosis Neonatal Screening Study Group. *Pediatrics* **107**: 1-13.

Farrell PM, Lai HJ, Li Z, Kosorok MR, Laxova A, Green CG, Collins J, Hoffman G, Laessig R, Rock MJ et al. 2005. Evidence on improved outcomes with early diagnosis of cystic fibrosis through neonatal screening: enough is enough! *J Pediatr* **147**: S30-36.

Farrell PM, Rosenstein BJ, White TB, Accurso FJ, Castellani C, Cutting GR, Durie PR, Legrys VA, Massie J, Parad RB et al. 2008. Guidelines for diagnosis of cystic fibrosis in newborns through older adults: Cystic Fibrosis Foundation consensus report. *J Pediatr* **153**: S4-S14.

Fu L, Sztul E. 2003. Traffic-independent function of the Sar1p/COPII machinery in proteasomal sorting of the cystic fibrosis transmembrane conductance regulator. *J Cell Biol* **160**: 157-163.

Gadsby DC. 2009. Ion channels versus ion pumps: the principal difference, in principle. *Nat Rev Mol Cell Biol* **10**: 344-352.

Gadsby DC, Vergani P, Csanady L. 2006. The ABC protein turned chloride channel whose failure causes cystic fibrosis. *Nature* **440**: 477-483.

Glozman R, Okiyoneda T, Mulvihill CM, Rini JM, Barriere H, Lukacs GL. 2009. N-glycans are direct determinants of CFTR folding and stability in secretory and endocytic membrane traffic. *J Cell Biol* **184**: 847-862.

Gottesman MM, Ambudkar SV. 2001. Overview: ABC transporters and human disease. *Journal of bioenergetics and biomembranes* **33**: 453-458.

Gregory RJ, Rich DP, Cheng SH, Souza DW, Paul S, Manavalan P, Anderson MP, Welsh MJ, Smith AE. 1991. Maturation and function of cystic fibrosis transmembrane conductance regulator variants bearing mutations in putative nucleotide-binding domains 1 and 2. *Mol Cell Biol* **11**: 3886-3893.

Griesenbach U, Alton EW. 2009. Gene transfer to the lung: lessons learned from more than 2 decades of CF gene therapy. *Adv Drug Deliv Rev* **61**: 128-139.

Grosse SD, Boyle CA, Cordero JF. 2005. Newborn screening for cystic fibrosis: recommendations from the Centers for Disease Control and Prevention. *Am Fam Physician* **71**: 1482, 1487.

Grove DE, Fan CY, Ren HY, Cyr DM. 2011. The endoplasmic reticulum-associated Hsp40 DNAJB12 and Hsc70 cooperate to facilitate RMA1 E3-dependent degradation of nascent CFTRDeltaF508. *Mol Biol Cell* **22**: 301-314.

Grove DE, Rosser MF, Ren HY, Naren AP, Cyr DM. 2009. Mechanisms for rescue of correctable folding defects in CFTRDelta F508. *Mol Biol Cell* **20**: 4059-4069.

Guilbault C, Saeed Z, Downey GP, Radzioch D. 2007. Cystic fibrosis mouse models. *American journal of respiratory cell and molecular biology* **36**: 1-7.

Hamosh A, FitzSimmons SC, Macek M, Jr., Knowles MR, Rosenstein BJ, Cutting GR. 1998. Comparison of the clinical manifestations of cystic fibrosis in black and white patients. *J Pediatr* **132**: 255-259.

Hartmann E, Rapoport TA, Lodish HF. 1989. Predicting the orientation of eukaryotic membrane-spanning proteins. *Proc Natl Acad Sci U S A* **86**: 5786-5790.

He L, Aleksandrov AA, Serohijos AW, Hegedus T, Aleksandrov LA, Cui L, Dokholyan NV, Riordan JR. 2008. Multiple membrane-cytoplasmic domain contacts in the cystic fibrosis transmembrane conductance regulator (CFTR) mediate regulation of channel gating. *J Biol Chem* **283**: 26383-26390.

Hedin LE, Ojemalm K, Bernsel A, Hennerdal A, Illergard K, Enquist K, Kauko A, Cristobal S, von Heijne G, Lerch-Bader M et al. 2010. Membrane insertion of marginally hydrophobic transmembrane helices depends on sequence context. *J Mol Biol* **396**: 221-229.

Helenius A, Aebi M. 2001. Intracellular functions of N-linked glycans. *Science* **291**: 2364-2369.

Hermann T. 2007. Aminoglycoside antibiotics: old drugs and new therapeutic approaches. *Cell Mol Life Sci* **64**: 1841-1852.

Hessa T, Kim H, Bihlmaier K, Lundin C, Boekel J, Andersson H, Nilsson I, White SH, von Heijne G. 2005. Recognition of transmembrane helices by the endoplasmic reticulum translocon. *Nature* **433**: 377-381.

Hessa T, Meindl-Beinker NM, Bernsel A, Kim H, Sato Y, Lerch-Bader M, Nilsson I, White SH, von Heijne G. 2007. Molecular code for transmembrane-helix recognition by the Sec61 translocon. *Nature* **450**: 1026-1030.

Hoelen H, Kleizen B, Schmidt A, Richardson J, Charitou P, Thomas PJ, Braakman I. 2010. The primary folding defect and rescue of DeltaF508 CFTR emerge during translation of the mutant domain. *PLoS One* **5**: e15458.

Hofmann KaS, W. 1993. A database of membrane spanning proteins segments. *Biological Chemistry Hoppe-Seyler* **374**: 166.

Holland IB. 2003. *ABC proteins : from bacteria to man*. Academic Press, Amsterdam ; Boston.

Hollenstein K, Frei DC, Locher KP. 2007. Structure of an ABC transporter in complex with its binding protein. *Nature* **446**: 213-216.

Howard M, DuVall MD, Devor DC, Dong JY, Henze K, Frizzell RA. 1995. Epitope tagging permits cell surface detection of functional CFTR. *The American journal of physiology* **269**: C1565-1576.

Howard M, Frizzell RA, Bedwell DM. 1996. Aminoglycoside antibiotics restore CFTR function by overcoming premature stop mutations. *Nat Med* **2**: 467-469.

Jensen TJ, Loo MA, Pind S, Williams DB, Goldberg AL, Riordan JR. 1995. Multiple proteolytic systems, including the proteasome, contribute to CFTR processing. *Cell* **83**: 129-135.

Johnson AE, van Waes MA. 1999. The translocon: a dynamic gateway at the ER membrane. *Annu Rev Cell Dev Biol* **15**: 799-842.

Jordan IK, Kota KC, Cui G, Thompson CH, McCarty NA. 2008. Evolutionary and functional divergence between the cystic fibrosis transmembrane conductance regulator and related ATP-binding cassette transporters. *Proc Natl Acad Sci U S A* **105**: 18865-18870.

Jorde LB, Lathrop GM. 1988. A test of the heterozygote-advantage hypothesis in cystic fibrosis carriers. *Am J Hum Genet* **42**: 808-815.

Kanelis V, Hudson RP, Thibodeau PH, Thomas PJ, Forman-Kay JD. 2010. NMR evidence for differential phosphorylation-dependent interactions in WT and DeltaF508 CFTR. *Embo J* **29**: 263-277.

Kauko A, Hedin LE, Thebaud E, Cristobal S, Elofsson A, von Heijne G. 2010. Repositioning of transmembrane alpha-helices during membrane protein folding. *J Mol Biol* **397**: 190-201.

Keenan RJ, Freymann DM, Walter P, Stroud RM. 1998. Crystal structure of the signal sequence binding subunit of the signal recognition particle. *Cell* **94**: 181-191.

Kerem B, Rommens JM, Buchanan JA, Markiewicz D, Cox TK, Chakravarti A, Buchwald M, Tsui LC. 1989. Identification of the cystic fibrosis gene: genetic analysis. *Science* **245**: 1073-1080.

Kerem E. 2004. Pharmacologic therapy for stop mutations: how much CFTR activity is enough? *Curr Opin Pulm Med* **10**: 547-552.

Kerem E, Hirawat S, Armoni S, Yaakov Y, Shoseyov D, Cohen M, Nissim-Rafinia M, Blau H, Rivlin J, Aviram M et al. 2008. Effectiveness of PTC124 treatment of cystic fibrosis caused by nonsense mutations: a prospective phase II trial. *Lancet* **372**: 719-727.

Kerem E, Kerem B. 1996. Genotype-phenotype correlations in cystic fibrosis. *Pediatr Pulmonol* **22**: 387-395.

Khushoo A, Yang Z, Johnson AE, Skach WR. 2011. Ligand-Driven Vectorial Folding of Ribosome-Bound Human CFTR NBD1. *Mol Cell* **41**: 682-692.

Kleizen B, van Vlijmen T, de Jonge HR, Braakman I. 2005. Folding of CFTR is predominantly cotranslational. *Mol Cell* **20**: 277-287.

Ko SB, Shcheynikov N, Choi JY, Luo X, Ishibashi K, Thomas PJ, Kim JY, Kim KH, Lee MG, Naruse S et al. 2002. A molecular mechanism for aberrant CFTR-dependent HCO(3)(-) transport in cystic fibrosis. *Embo J* **21**: 5662-5672.

Kramer G, Ramachandiran V, Hardesty B. 2001. Cotranslational folding--omnia mea mecum porto? *Int J Biochem Cell Biol* **33**: 541-553.

Lai HJ, Cheng Y, Farrell PM. 2005. The survival advantage of patients with cystic fibrosis diagnosed through neonatal screening: evidence from the United States Cystic Fibrosis Foundation registry data. *J Pediatr* **147**: S57-63.

Lao O, Andres AM, Mateu E, Bertranpetit J, Calafell F. 2003. Spatial patterns of cystic fibrosis mutation spectra in European populations. *Eur J Hum Genet* **11**: 385-394.

Lewis HA, Buchanan SG, Burley SK, Conners K, Dickey M, Dorwart M, Fowler R, Gao X, Guggino WB, Hendrickson WA et al. 2004. Structure of nucleotide-binding domain 1 of the cystic fibrosis transmembrane conductance regulator. *Embo J* **23**: 282-293.

Lewis HA, Zhao X, Wang C, Sauder JM, Rooney I, Noland BW, Lorimer D, Kearins MC, Conners K, Condon B et al. 2005. Impact of the deltaF508 mutation in first nucleotide-binding domain of human cystic fibrosis transmembrane conductance regulator on domain folding and structure. *J Biol Chem* **280**: 1346-1353.

Liao S, Lin J, Do H, Johnson AE. 1997. Both lumenal and cytosolic gating of the aqueous ER translocon pore are regulated from inside the ribosome during membrane protein integration. *Cell* **90**: 31-41.

Lilley BN, Ploegh HL. 2004. A membrane protein required for dislocation of misfolded proteins from the ER. *Nature* **429**: 834-840.

Linsdell P. 2006. Mechanism of chloride permeation in the cystic fibrosis transmembrane conductance regulator chloride channel. *Exp Physiol* **91**: 123-129.

Linton KJ, Higgins CF. 1998. The Escherichia coli ATP-binding cassette (ABC) proteins. *Mol Microbiol* **28**: 5-13.

Locher KP. 2009. Review. Structure and mechanism of ATP-binding cassette transporters. *Philos Trans R Soc Lond B Biol Sci* **364**: 239-245.

Locher KP, Lee AT, Rees DC. 2002. The E. coli BtuCD structure: a framework for ABC transporter architecture and mechanism. *Science* **296**: 1091-1098.

Loo TW, Bartlett MC, Clarke DM. 2011. Benzbromarone Stabilizes DeltaF508 CFTR at the Cell Surface. *Biochemistry*.

Loo TW, Clarke DM. 2008. Mutational analysis of ABC proteins. *Arch Biochem Biophys* **476**: 51-64.

Louie RJ, Pagant S, Youn JY, Halliday JJ, Huyer G, Michaelis S, Miller EA. 2010. Functional rescue of a misfolded eukaryotic ATP-binding cassette transporter by domain replacement. *J Biol Chem* **285**: 36225-36234.

Lu Y, Turnbull IR, Bragin A, Carveth K, Verkman AS, Skach WR. 2000. Reorientation of aquaporin-1 topology during maturation in the endoplasmic reticulum. *Mol Biol Cell* **11**: 2973-2985.

Lu Y, Xiong X, Helm A, Kimani K, Bragin A, Skach WR. 1998. Co- and posttranslational translocation mechanisms direct cystic fibrosis transmembrane conductance regulator N terminus transmembrane assembly. *J Biol Chem* **273**: 568-576.

Lukacs GL, Chang XB, Bear C, Kartner N, Mohamed A, Riordan JR, Grinstein S. 1993. The delta F508 mutation decreases the stability of cystic fibrosis transmembrane conductance regulator in the plasma membrane. Determination of functional half-lives on transfected cells. *J Biol Chem* **268**: 21592-21598.

Lukacs GL, Mohamed A, Kartner N, Chang XB, Riordan JR, Grinstein S. 1994. Conformational maturation of CFTR but not its mutant counterpart (delta F508) occurs in the endoplasmic reticulum and requires ATP. *Embo J* **13**: 6076-6086.

Lundin C, Kim H, Nilsson I, White SH, von Heijne G. 2008. Molecular code for protein insertion in the endoplasmic reticulum membrane is similar for N(in)-C(out) and N(out)-C(in) transmembrane helices. *Proc Natl Acad Sci U S A* **105**: 15702-15707.

Ma T, Vetrivel L, Yang H, Pedemonte N, Zegarra-Moran O, Galietta LJ, Verkman AS. 2002. High-affinity activators of cystic fibrosis transmembrane conductance regulator (CFTR) chloride conductance identified by high-throughput screening. *J Biol Chem* **277**: 37235-37241.

Mall M, Grubb BR, Harkema JR, O'Neal WK, Boucher RC. 2004. Increased airway epithelial Na+ absorption produces cystic fibrosis-like lung disease in mice. *Nat Med* **10**: 487-493.

McCormick PJ, Miao Y, Shao Y, Lin J, Johnson AE. 2003. Cotranslational protein integration into the ER membrane is mediated by the binding of nascent chains to translocon proteins. *Mol Cell* **12**: 329-341.

Meacham GC, Lu Z, King S, Sorscher E, Tousson A, Cyr DM. 1999. The Hdj-2/Hsc70 chaperone pair facilitates early steps in CFTR biogenesis. *Embo J* **18**: 1492-1505.

Meacham GC, Patterson C, Zhang W, Younger JM, Cyr DM. 2001. The Hsc70 co-chaperone CHIP targets immature CFTR for proteasomal degradation. *Nat Cell Biol* **3**: 100-105.

Mendoza JL, Thomas PJ. 2007. Building an understanding of cystic fibrosis on the foundation of ABC transporter structures. *J Bioenerg Biomembr* **39**: 499-505.

Mense M, Vergani P, White DM, Altberg G, Nairn AC, Gadsby DC. 2006. In vivo phosphorylation of CFTR promotes formation of a nucleotide-binding domain heterodimer. *Embo J* **25**: 4728-4739.

Meyerholz DK, Stoltz DA, Pezzulo AA, Welsh MJ. 2010. Pathology of gastrointestinal organs in a porcine model of cystic fibrosis. *The American journal of pathology* **176**: 1377-1389.

Mingarro I, Nilsson I, Whitley P, von Heijne G. 2000. Different conformations of nascent polypeptides during translocation across the ER membrane. *BMC Cell Biol* **1**: 3.

Monne M, Nilsson I, Johansson M, Elmhed N, von Heijne G. 1998. Positively and negatively charged residues have different effects on the position in the membrane of a model transmembrane helix. *J Mol Biol* **284**: 1177-1183.

Moody JE, Millen L, Binns D, Hunt JF, Thomas PJ. 2002. Cooperative, ATP-dependent association of the nucleotide binding cassettes during the catalytic cycle of ATP-binding cassette transporters. *J Biol Chem* **277**: 21111-21114.

Moran A, Brunzell C, Cohen RC, Katz M, Marshall BC, Onady G, Robinson KA, Sabadosa KA, Stecenko A, Slovis B. 2010. Clinical care guidelines for cystic fibrosis-related diabetes: a position statement of the American Diabetes Association and a clinical practice guideline of the Cystic Fibrosis Foundation, endorsed by the Pediatric Endocrine Society. *Diabetes Care* **33**: 2697-2708.

Moran O, Zegarra-Moran O. 2008. On the measurement of the functional properties of the CFTR. *Journal of cystic fibrosis : official journal of the European Cystic Fibrosis Society* **7**: 483-494.

Mornon JP, Lehn P, Callebaut I. 2008. Atomic model of human cystic fibrosis transmembrane conductance regulator: membrane-spanning domains and coupling interfaces. *Cellular and molecular life sciences : CMLS* **65**: 2594-2612.

-. 2009. Molecular models of the open and closed states of the whole human CFTR protein. *Cellular and molecular life sciences : CMLS* **66**: 3469-3486.

Moskowitz SM, Chmiel JF, Sternen DL, Cheng E, Gibson RL, Marshall SG, Cutting GR. 2008. Clinical practice and genetic counseling for cystic fibrosis and CFTR-related disorders. *Genet Med* **10**: 851-868.

Mothes W, Heinrich SU, Graf R, Nilsson I, von Heijne G, Brunner J, Rapoport TA. 1997. Molecular mechanism of membrane protein integration into the endoplasmic reticulum. *Cell* **89**: 523-533.

Muallem D, Vergani P. 2009. Review. ATP hydrolysis-driven gating in cystic fibrosis transmembrane conductance regulator. *Philos Trans R Soc Lond B Biol Sci* **364**: 247-255.

Naren AP, Cormet-Boyaka E, Fu J, Villain M, Blalock JE, Quick MW, Kirk KL. 1999. CFTR chloride channel regulation by an interdomain interaction. *Science* **286**: 544-548.

Nikles D, Tampe R. 2007. Targeted degradation of ABC transporters in health and disease. *Journal of bioenergetics and biomembranes* **39**: 489-497.

Nilsson I, Kelleher DJ, Miao Y, Shao Y, Kreibich G, Gilmore R, von Heijne G, Johnson AE. 2003. Photocross-linking of nascent chains to the STT3 subunit of the oligosaccharyltransferase complex. *J Cell Biol* **161**: 715-725.

Nilsson I, Saaf A, Whitley P, Gafvelin G, Waller C, von Heijne G. 1998. Proline-induced disruption of a transmembrane alpha-helix in its natural environment. *J Mol Biol* **284**: 1165-1175.

Nilsson I, von Heijne G. 1998. Breaking the camel's back: proline-induced turns in a model transmembrane helix. *J Mol Biol* **284**: 1185-1189.

Nilsson IM, von Heijne G. 1993. Determination of the distance between the oligosaccharyltransferase active site and the endoplasmic reticulum membrane. *J Biol Chem* **268**: 5798-5801.

O'Riordan CR, Erickson A, Bear C, Li C, Manavalan P, Wang KX, Marshall J, Scheule RK, McPherson JM, Cheng SH et al. 1995. Purification and characterization of recombinant cystic fibrosis transmembrane conductance regulator from Chinese hamster ovary and insect cells. *J Biol Chem* **270**: 17033-17043.

O'Sullivan BP, Flume P. 2009. The clinical approach to lung disease in patients with cystic fibrosis. *Semin Respir Crit Care Med* **30**: 505-513.

O'Sullivan BP, Freedman SD. 2009. Cystic fibrosis. *Lancet* **373**: 1891-1904.

Oberdorf J, Skach WR. 2002. In vitro reconstitution of CFTR biogenesis and degradation. *Methods Mol Med* **70**: 295-310.

Okiyoneda T, Barriere H, Bagdany M, Rabeh WM, Du K, Hohfeld J, Young JC, Lukacs GL. 2010. Peripheral protein quality control removes unfolded CFTR from the plasma membrane. *Science* **329**: 805-810.

Okiyoneda T, Lukacs GL. 2007. Cell surface dynamics of CFTR: the ins and outs. *Biochim Biophys Acta* **1773**: 476-479.

Ostedgaard LS, Meyerholz DK, Chen JH, Pezzulo AA, Karp PH, Rokhlina T, Ernst SE, Hanfland RA, Reznikov LR, Ludwig PS et al. 2011. The {Delta}F508 Mutation Causes CFTR Misprocessing and Cystic Fibrosis-Like Disease in Pigs. *Sci Transl Med* **3**: 74ra24.

Ostedgaard LS, Rich DP, DeBerg LG, Welsh MJ. 1997. Association of domains within the cystic fibrosis transmembrane conductance regulator. *Biochemistry* **36**: 1287-1294.

Ostedgaard LS, Rogers CS, Dong Q, Randak CO, Vermeer DW, Rokhlina T, Karp PH, Welsh MJ. 2007. Processing and function of CFTR-DeltaF508 are species-dependent. *Proceedings of the National Academy of Sciences of the United States of America* **104**: 15370-15375.

Pagant S, Brovman EY, Halliday JJ, Miller EA. 2008. Mapping of interdomain interfaces required for the functional architecture of Yor1p, a eukaryotic ATP-binding cassette (ABC) transporter. *J Biol Chem* **283**: 26444-26451.

Pagant S, Halliday JJ, Kougentakis C, Miller EA. 2010. Intragenic suppressing mutations correct the folding and intracellular traffic of misfolded mutants of Yor1p, a eukaryotic drug transporter. *J Biol Chem* **285**: 36304-36314.

Pagant S, Kung L, Dorrington M, Lee MC, Miller EA. 2007. Inhibiting endoplasmic reticulum (ER)-associated degradation of misfolded Yor1p does not permit ER export despite the presence of a diacidic sorting signal. *Molecular biology of the cell* **18**: 3398-3413.

Partridge AW, Therien AG, Deber CM. 2002. Polar mutations in membrane proteins as a biophysical basis for disease. *Biopolymers* **66**: 350-358.

Pearce KH, Jr., Ultsch MH, Kelley RF, de Vos AM, Wells JA. 1996. Structural and mutational analysis of affinity-inert contact residues at the growth hormone-receptor interface. *Biochemistry* **35**: 10300-10307.

Pier GB, Grout M, Zaidi TS, Olsen JC, Johnson LG, Yankaskas JR, Goldberg JB. 1996. Role of mutant CFTR in hypersusceptibility of cystic fibrosis patients to lung infections. *Science* **271**: 64-67.

Pind S, Riordan JR, Williams DB. 1994. Participation of the endoplasmic reticulum chaperone calnexin (p88, IP90) in the biogenesis of the cystic fibrosis transmembrane conductance regulator. *J Biol Chem* **269**: 12784-12788.

Pitonzo D, Yang Z, Matsumura Y, Johnson AE, Skach WR. 2009. Sequence-specific retention and regulated integration of a nascent membrane protein by the endoplasmic reticulum Sec61 translocon. *Molecular biology of the cell* **20**: 685-698.

Pollet JF, Van Geffel J, Van Stevens E, Van Geffel R, Beauwens R, Bollen A, Jacobs P. 2000. Expression and intracellular processing of chimeric and mutant CFTR molecules. *Biochim Biophys Acta* **1500**: 59-69.

Poolman EM, Galvani AP. 2007. Evaluating candidate agents of selective pressure for cystic fibrosis. *J R Soc Interface* **4**: 91-98.

Popov M, Tam LY, Li J, Reithmeier RA. 1997. Mapping the ends of transmembrane segments in a polytopic membrane protein. Scanning N-glycosylation mutagenesis of extracytosolic loops in the anion exchanger, band 3. *J Biol Chem* **272**: 18325-18332.

PressRelease. [Accessed 4 April 2011]. Press Release, Vertex Pharmaceuticals, Inc. http://investors.vrtx.com/releasedetail.cfm?ReleaseID=560382.

Qu BH, Strickland EH, Thomas PJ. 1997. Localization and suppression of a kinetic defect in cystic fibrosis transmembrane conductance regulator folding. *J Biol Chem* **272**: 15739-15744.

Qu BH, Thomas PJ. 1996. Alteration of the cystic fibrosis transmembrane conductance regulator folding pathway. *J Biol Chem* **271**: 7261-7264.

Quinton PM. 1990. Cystic fibrosis: a disease in electrolyte transport. *Faseb J* **4**: 2709-2717.

-. 2007. Cystic fibrosis: lessons from the sweat gland. *Physiology (Bethesda)* **22**: 212-225.

-. 2008. Cystic fibrosis: impaired bicarbonate secretion and mucoviscidosis. *Lancet* **372**: 415-417.

-. 2010. Role of epithelial HCO3 transport in mucin secretion: lessons from cystic fibrosis. *Am J Physiol Cell Physiol* **299**: C1222-1233.

Rees DC, Johnson E, Lewinson O. 2009. ABC transporters: the power to change. *Nat Rev Mol Cell Biol* **10**: 218-227.

Rich DP, Gregory RJ, Anderson MP, Manavalan P, Smith AE, Welsh MJ. 1991. Effect of deleting the R domain on CFTR-generated chloride channels. *Science* **253**: 205-207.

Riordan JR. 2008. CFTR function and prospects for therapy. *Annu Rev Biochem* **77**: 701-726.

Riordan JR, Rommens JM, Kerem B, Alon N, Rozmahel R, Grzelczak Z, Zielenski J, Lok S, Plavsic N, Chou JL et al. 1989. Identification of the cystic fibrosis gene: cloning and characterization of complementary DNA. *Science* **245**: 1066-1073.

Rogers CS, Stoltz DA, Meyerholz DK, Ostedgaard LS, Rokhlina T, Taft PJ, Rogan MP, Pezzulo AA, Karp PH, Itani OA et al. 2008. Disruption of the CFTR gene produces a model of cystic fibrosis in newborn pigs. *Science* **321**: 1837-1841.

Romeo G, Devoto M, Galietta LJ. 1989. Why is the cystic fibrosis gene so frequent? *Hum Genet* **84**: 1-5.

Rommens JM, Iannuzzi MC, Kerem B, Drumm ML, Melmer G, Dean M, Rozmahel R, Cole JL, Kennedy D, Hidaka N et al. 1989. Identification of the cystic fibrosis gene: chromosome walking and jumping. *Science* **245**: 1059-1065.

Rosenberg MF, Kamis AB, Aleksandrov LA, Ford RC, Riordan JR. 2004. Purification and crystallization of the cystic fibrosis transmembrane conductance regulator (CFTR). *J Biol Chem* **279**: 39051-39057.

Rosser MF, Grove DE, Chen L, Cyr DM. 2008. Assembly and misassembly of cystic fibrosis transmembrane conductance regulator: folding defects caused by deletion of F508 occur before and after the calnexin-dependent association of membrane spanning domain (MSD) 1 and MSD2. *Mol Biol Cell* **19**: 4570-4579.

Rost B, Sander C. 1993. Prediction of protein secondary structure at better than 70% accuracy. *J Mol Biol* **232**: 584-599.

-. 1994. Combining evolutionary information and neural networks to predict protein secondary structure. *Proteins* **19**: 55-72.

Rowe SM, Miller S, Sorscher EJ. 2005. Cystic fibrosis. *N Engl J Med* **352**: 1992-2001.

Rudiger S, Buchberger A, Bukau B. 1997. Interaction of Hsp70 chaperones with substrates. *Nat Struct Biol* **4**: 342-349.

Sambrook J, Fritsch, E.F., and Maniatis, T. 1989. Molecular Cloning: A laboratory Manual. Cold Spring Harbor Laboratory Press, New York.

Sampson HM, Robert R, Liao J, Matthes E, Carlile GW, Hanrahan JW, Thomas DY. 2011. Identification of a NBD1-binding pharmacological chaperone that corrects the trafficking defect of F508del-CFTR. *Chem Biol* **18**: 231-242.

Sato S, Ward CL, Krouse ME, Wine JJ, Kopito RR. 1996. Glycerol reverses the misfolding phenotype of the most common cystic fibrosis mutation. *J Biol Chem* **271**: 635-638.

Seibert FS, Jia Y, Mathews CJ, Hanrahan JW, Riordan JR, Loo TW, Clarke DM. 1997. Disease-associated mutations in cytoplasmic loops 1 and 2 of cystic fibrosis transmembrane conductance regulator impede processing or opening of the channel. *Biochemistry* **36**: 11966-11974.

Seibert FS, Linsdell P, Loo TW, Hanrahan JW, Clarke DM, Riordan JR. 1996a. Disease-associated mutations in the fourth cytoplasmic loop of cystic fibrosis transmembrane conductance regulator compromise biosynthetic processing and chloride channel activity. *J Biol Chem* **271**: 15139-15145.

Seibert FS, Linsdell P, Loo TW, Hanrahan JW, Riordan JR, Clarke DM. 1996b. Cytoplasmic loop three of cystic fibrosis transmembrane conductance regulator contributes to regulation of chloride channel activity. *J Biol Chem* **271**: 27493-27499.

Serohijos AW, Hegedus T, Aleksandrov AA, He L, Cui L, Dokholyan NV, Riordan JR. 2008. Phenylalanine-508 mediates a cytoplasmic-membrane domain contact in the CFTR 3D structure crucial to assembly and channel function. *Proc Natl Acad Sci U S A* **105**: 3256-3261.

Sheppard DN. 2011. Cystic fibrosis: CFTR correctors to the rescue. *Chem Biol* **18**: 145-147.

Sheppard DN, Ostedgaard LS, Rich DP, Welsh MJ. 1994. The amino-terminal portion of CFTR forms a regulated Cl- channel. *Cell* **76**: 1091-1098.

Sheppard DN, Rich DP, Ostedgaard LS, Gregory RJ, Smith AE, Welsh MJ. 1993. Mutations in CFTR associated with mild-disease-form Cl- channels with altered pore properties. *Nature* **362**: 160-164.

Sinn PL, Anthony R, McCray PB, Jr. Genetic Therapies for Cystic Fibrosis Lung Disease. *Hum Mol Genet*.

Skach WR. 2009. Cellular mechanisms of membrane protein folding. *Nature structural & molecular biology* **16**: 606-612.

Sloane PA, Rowe SM. 2010. Cystic fibrosis transmembrane conductance regulator protein repair as a therapeutic strategy in cystic fibrosis. *Curr Opin Pulm Med* **16**: 591-597.

Smith PC, Karpowich N, Millen L, Moody JE, Rosen J, Thomas PJ, Hunt JF. 2002. ATP binding to the motor domain from an ABC transporter drives formation of a nucleotide sandwich dimer. *Mol Cell* **10**: 139-149.

Stecenko AA, Moran A. 2010. Update on cystic fibrosis-related diabetes. *Curr Opin Pulm Med* **16**: 611-615.

Stoltz DA, Meyerholz DK, Pezzulo AA, Ramachandran S, Rogan MP, Davis GJ, Hanfland RA, Wohlford-Lenane C, Dohrn CL, Bartlett JA et al. 2010. Cystic fibrosis pigs develop lung disease and exhibit defective bacterial eradication at birth. *Science translational medicine* **2**: 29ra31.

Stutts MJ, Canessa CM, Olsen JC, Hamrick M, Cohn JA, Rossier BC, Boucher RC. 1995. CFTR as a cAMP-dependent regulator of sodium channels. *Science* **269**: 847-850.

Sun F, Zhang R, Gong X, Geng X, Drain PF, Frizzell RA. 2006. Derlin-1 promotes the efficient degradation of the cystic fibrosis transmembrane conductance regulator (CFTR) and CFTR folding mutants. *J Biol Chem* **281**: 36856-36863.

Sun X, Sui H, Fisher JT, Yan Z, Liu X, Cho HJ, Joo NS, Zhang Y, Zhou W, Yi Y et al. 2010. Disease phenotype of a ferret CFTR-knockout model of cystic fibrosis. *J Clin Invest* **120**: 3149-3160.

Sun X, Yan Z, Yi Y, Li Z, Lei D, Rogers CS, Chen J, Zhang Y, Welsh MJ, Leno GH et al. 2008. Adeno-associated virus-targeted disruption of the CFTR gene in cloned ferrets. *J Clin Invest* **118**: 1578-1583.

Tector M, Hartl FU. 1999. An unstable transmembrane segment in the cystic fibrosis transmembrane conductance regulator. *Embo J* **18**: 6290-6298.

Teem JL, Berger HA, Ostedgaard LS, Rich DP, Tsui LC, Welsh MJ. 1993. Identification of revertants for the cystic fibrosis delta F508 mutation using STE6-CFTR chimeras in yeast. *Cell* **73**: 335-346.

Therien AG, Grant FE, Deber CM. 2001. Interhelical hydrogen bonds in the CFTR membrane domain. *Nat Struct Biol* **8**: 597-601.

Thibodeau PH, Brautigam CA, Machius M, Thomas PJ. 2005. Side chain and backbone contributions of Phe508 to CFTR folding. *Nat Struct Mol Biol* **12**: 10-16.

Thibodeau PH, Richardson JM, 3rd, Wang W, Millen L, Watson J, Mendoza JL, Du K, Fischman S, Senderowitz H, Lukacs GL et al. 2010. The cystic fibrosis-causing mutation deltaF508 affects multiple steps in cystic fibrosis transmembrane conductance regulator biogenesis. *J Biol Chem* **285**: 35825-35835.

Thomas PJ, Shenbagamurthi P, Sondek J, Hullihen JM, Pedersen PL. 1992. The cystic fibrosis transmembrane conductance regulator. Effects of the most common cystic fibrosis-causing mutation on the secondary structure and stability of a synthetic peptide. *J Biol Chem* **267**: 5727-5730.

Van Goor F, Straley KS, Cao D, Gonzalez J, Hadida S, Hazlewood A, Joubran J, Knapp T, Makings LR, Miller M et al. 2006. Rescue of DeltaF508-CFTR trafficking and gating in human cystic fibrosis airway primary cultures by small molecules. *Am J Physiol Lung Cell Mol Physiol* **290**: L1117-1130.

von Heijne G. 1989. Control of topology and mode of assembly of a polytopic membrane protein by positively charged residues. *Nature* **341**: 456-458.

-. 1992. Membrane protein structure prediction. Hydrophobicity analysis and the positive-inside rule. *J Mol Biol* **225**: 487-494.

Walter P, Blobel G. 1983a. Preparation of microsomal membranes for cotranslational protein translocation. *Methods Enzymol* **96**: 84-93.

-. 1983b. Signal recognition particle: a ribonucleoprotein required for cotranslational translocation of proteins, isolation and properties. *Methods Enzymol* **96**: 682-691.

Wang B, Heath-Engel H, Zhang D, Nguyen N, Thomas DY, Hanrahan JW, Shore GC. 2008a. BAP31 interacts with Sec61 translocons and promotes retrotranslocation of CFTRDeltaF508 via the derlin-1 complex. *Cell* **133**: 1080-1092.

Wang X, Koulov AV, Kellner WA, Riordan JR, Balch WE. 2008b. Chemical and biological folding contribute to temperature-sensitive DeltaF508 CFTR trafficking. *Traffic* **9**: 1878-1893.

Wang X, Matteson J, An Y, Moyer B, Yoo JS, Bannykh S, Wilson IA, Riordan JR, Balch WE. 2004. COPII-dependent export of cystic fibrosis transmembrane conductance regulator from the ER uses a di-acidic exit code. *J Cell Biol* **167**: 65-74.

Wang X, Venable J, LaPointe P, Hutt DM, Koulov AV, Coppinger J, Gurkan C, Kellner W, Matteson J, Plutner H et al. 2006. Hsp90 cochaperone Aha1 downregulation rescues misfolding of CFTR in cystic fibrosis. *Cell* **127**: 803-815.

Ward A, Reyes CL, Yu J, Roth CB, Chang G. 2007. Flexibility in the ABC transporter MsbA: Alternating access with a twist. *Proceedings of the National Academy of Sciences of the United States of America* **104**: 19005-19010.

Ward CL, Omura S, Kopito RR. 1995. Degradation of CFTR by the ubiquitin-proteasome pathway. *Cell* **83**: 121-127.

Welsh MJ, Smith AE. 1993. Molecular mechanisms of CFTR chloride channel dysfunction in cystic fibrosis. *Cell* **73**: 1251-1254.

Widdicombe JH. 2010. Transgenic animals may help resolve a sticky situation in cystic fibrosis. *J Clin Invest* **120**: 3093-3096.

Wigley WC, Vijayakumar S, Jones JD, Slaughter C, Thomas PJ. 1998. Transmembrane domain of cystic fibrosis transmembrane conductance regulator: design, characterization, and secondary structure of synthetic peptides m1-m6. *Biochemistry* **37**: 844-853.

Wilschanski M, Durie PR. 2007. Patterns of GI disease in adulthood associated with mutations in the CFTR gene. *Gut* **56**: 1153-1163.

Wilschanski M, Miller LL, Shoseyov D, Blau H, Rivlin J, Aviram M, Cohen M, Armoni S, Yaakov Y, Pugatch T et al. 2011. Chronic ataluren (PTC124) treatment of nonsense mutation cystic fibrosis. *Eur Respir J*.

Woolhead CA, McCormick PJ, Johnson AE. 2004. Nascent membrane and secretory proteins differ in FRET-detected folding far inside the ribosome and in their exposure to ribosomal proteins. *Cell* **116**: 725-736.

Xie J, Drumm ML, Ma J, Davis PB. 1995. Intracellular loop between transmembrane segments IV and V of cystic fibrosis transmembrane conductance regulator is involved in regulation of chloride channel conductance state. *J Biol Chem* **270**: 28084-28091.

Xiong X, Bragin A, Widdicombe JH, Cohn J, Skach WR. 1997. Structural cues involved in endoplasmic reticulum degradation of G85E and G91R mutant cystic fibrosis transmembrane conductance regulator. *J Clin Invest* **100**: 1079-1088.

Yang H, Shelat AA, Guy RK, Gopinath VS, Ma T, Du K, Lukacs GL, Taddei A, Folli C, Pedemonte N et al. 2003. Nanomolar affinity small molecule correctors of defective Delta F508-CFTR chloride channel gating. *J Biol Chem* **278**: 35079-35085.

Ye Y, Shibata Y, Yun C, Ron D, Rapoport TA. 2004. A membrane protein complex mediates retro-translocation from the ER lumen into the cytosol. *Nature* **429**: 841-847.

Yoo JS, Moyer BD, Bannykh S, Yoo HM, Riordan JR, Balch WE. 2002. Non-conventional trafficking of the cystic fibrosis transmembrane conductance regulator through the early secretory pathway. *J Biol Chem* **277**: 11401-11409.

Younger JM, Chen L, Ren HY, Rosser MF, Turnbull EL, Fan CY, Patterson C, Cyr DM. 2006. Sequential quality-control checkpoints triage misfolded cystic fibrosis transmembrane conductance regulator. *Cell* **126**: 571-582.

Younger JM, Ren HY, Chen L, Fan CY, Fields A, Patterson C, Cyr DM. 2004. A foldable CFTR{Delta}F508 biogenic intermediate accumulates upon inhibition of the Hsc70-CHIP E3 ubiquitin ligase. *J Cell Biol* **167**: 1075-1085.

Zhang F, Kartner N, Lukacs GL. 1998. Limited proteolysis as a probe for arrested conformational maturation of delta F508 CFTR. *Nat Struct Biol* **5**: 180-183.

Zhang L, Aleksandrov LA, Riordan JR, Ford RC. 2011. Domain location within the cystic fibrosis transmembrane conductance regulator protein investigated by electron microscopy and gold labelling. *Biochim Biophys Acta* **1808**: 399-404.

Zhang L, Aleksandrov LA, Zhao Z, Birtley JR, Riordan JR, Ford RC. 2009. Architecture of the cystic fibrosis transmembrane conductance regulator protein and structural changes associated with phosphorylation and nucleotide binding. *J Struct Biol* **167**: 242-251.

Zielenski J. 2000. Genotype and phenotype in cystic fibrosis. *Respiration* **67**: 117-133.

Zielenski J, Tsui LC. 1995. Cystic fibrosis: genotypic and phenotypic variations. *Annu Rev Genet* **29**: 777-807.